DENSITY FUNCTIONAL THEORY AND TOPOLOGICAL ANALYSIS OF BIOLOGICALLY ACTIVE COMPLEXES OF PLATINUM METAL WITH L-CYSTEINE AND 2-MERCAPTOPYRIMIDINE

by

HASAN CAN YAZICI

THESIS SUBMITTED TO
THE GRADUATE SCHOOL OF NATURAL AND APPLIED SCIENCES
OF
THE ABANT İZZET BAYSAL UNIVERSITY
IN PARTIAL FULFILLMENT OF THE REQUIREMENTS FOR THE DEGREE
OF MASTER OF SCIENCE
IN DEPARTMENT OF CHEMISTRY

FEBRUARY 2015

Approval of the Graduate School of Natural and Applied Sciences

_____

Prof. Dr. Duran Karakaş
Director

I certify that this thesis satisfies all the requirements as a thesis for the degree of Master of Science.

_____

Prof. Dr. Nedime DÜRÜST
Head of the Department

This is to certify that we have read this thesis and that in our opinion it is fully adequate, in scope and quality, as a thesis for the degree of Master of Science.

_____

Prof. Dr. İzzet MORKAN
Supervisor

Examining Committee Members

1- Prof. Dr. İzzet MORKAN _____

2- Prof. Dr. Ayşe MORKAN _____

3- Assist. Prof. Dr. Bahadır ALTINTAŞ _____

4- Assist. Prof. Dr. Gürcan YILDIRIM _____

5- Assist. Prof. Dr. Sevim DEMİRÖZÜ ŞENOL _____

ABSTRACT

DENSITY FUNCTIONAL THEORY AND TOPOLOGICAL ANALYSIS OF BIOLOGICALLY ACTIVE COMPLEXES OF PLATINIUM METAL WITH L-CYSTEINE AND 2-MERCAPTOPYRIMIDINE

Hasan Can YAZICI

M.Sc., Department of Chemistry

Supervisor: Prof. Dr. İzzet Amour MORKAN

FEBRUARY 2015, 101 pages

Biological events are the most important states to be investigated. As the days pass, biological events which take part in different areas in our life with their different aspects are being subjects of many scientific researches. In todays world, many fatal diseases that lead to illnesses and in need of solutions are threatening the mankind. Especially, the deformations and defects in the structure of DNA may turn into diseases threatening the human life. The reason of this deformation is caused by formation of intermolecular interactions (hydrogen bonding, ionic interactions, etc.) by nucleic acid bases found in DNA which are Adenine, Cytosine, Thymine and Guanine between

themselves, aminoacids or some organic molecules. This situation has become interesting and investigated widely by strong theoretical studies. In addition, the complexes of these bases, aminoacids and some biologically active organic molecules, with transition metals which are used in applications of medical treatments is interesting in the same aspect. So, the formation of potential application areas of usage in drugs is predicted and it has started to be a very important research and investigation subject.

Firstly in this project, all complexes having intermolecular interactions (hydrogen bonding), possibly be formed between L-cysteine between 2-mercaptopyrimidine which is a biologically active virus preventive and bacteria inhibitor productive, will be subjected to detalied quantum analysis. By using DFT method, all structural parameters will be perfectly calculated. In addition, by doing the Quantum theory calculations (QTAIM) with Bond analysis (NBO) for all the atoms in the molecule, all energy-density relations will be revealed; and with structural parameters, the strength of hydrogen bonds and the deformations caused by those will be predicted. The structures will be tested with suitable correlation graphs and will be discussed complexes of most stable and highly deformations.

In the second stage, the L-cysteine mentioned above will be exposed to proper metal bindings that may form a potential application because of their biological roles. For this bindings, Platinum metal will be used.

Structures of L-cysteine and 2-mercaptopyrimidine and from different atom positions in their structures will be bound to metal from different points and all possible complexes formed will be analyzed structurally by six DFT (B3LYP, BHANDH, HCTH, MPW1PW91, PBEPBE, and TPSSKCIS) method. Center structures of cisplatin is used for metal bounds. Especially, Natural bond Orbital Analysis (NBO), HOMO-LUMO and Investigation of other molecular orbitals, the Energy Profiles, Harmonic Vibration Frequency and Detalied Orbital Analysis to achieve the best results for all these complexes will be examined in vacuum.

As a result, it is predicted from these studies that the deformations caused by intermolecular interactions between L-cysteine and 2-mercaptopyrimidine happening in cell, and the complexes that may form between these structures and transition metals may find potential treatment application fields in medicine and these two studies will have an important place both in science and technology.

Keywords: L-cysteine, 2-mercaptopyrimidine, Natural Bond Orbital, DFT calculations, HOMO-LUMO, cisplatin, hydrogen bonding

ÖZET

L-SİSTEİN VE 2-MERKAPTOPİRİMİDİN İLE PLATİN METALİ'NİN BİYOLOJİK AKTİF KOMPLEKSLERİNİN YOĞUNLUK FONKSİYONEL TEORİ VE TOPOLOJİK ANALİZİ

Hasan Can YAZICI
Yüksek Lisans, Kimya Bölümü
Tez Yöneticisi: Prof. Dr. İzzet Amour MORKAN
ŞUBAT 2015, 101 sayfa

Biyolojik olaylar, araştırılması gereken en önemli meselelerdendir. Gün geçtikçe farklı boyutlarıyla birçok alanda hayatımızda yer alan bu biyolojik olayların derinlemesine incelenmesi pek çok bilimsel araştırmaya konu olmaktadır. Hastalıklara neden olan ve çözüm ihtiyacı duyulan birçok ölümcül hastalık günümüzde insanlık için tehdit unsuru oluşturmaktadır. Özellikle DNA'daki deformasyonlar ve yapısındaki aksaklıklar insan hayatını tehdit eden hastalıklara dönüşebilmektedir. Bu deformasyonların sebebi, DNA yapısında bulunan Adenin, Sitozin, Timin ve Guanin nükleikasit bazlarının kendi aralarında, aminoasitlerle veya bazı organik moleküllerle, moleküllerarası etkileşimler (hidrojen bağı, iyonik etkileşimler v.b.)

oluşturmasından kaynaklanmaktadır. Bu durum son zamanlarda, güçlü teorik çalışmalarla geniş çapta incelenen, son derece ilgi çekici bir konu haline dönüşmüştür. Ayrıca bu bazlar, aminoasitler ve biyolojik aktifliğe sahip bazı organik moleküllerin, geçiş metalleri ile oluşturdukları, tıpta tedavi amaçlı kullanılan kompleksleri de aynı şekilde ilgi çekmektedir. Dolayısıyla ilaç kullanımına ait potansiyel uygulama alanları oluşabileceği tahmin edilmiş ve bu konu çok önemli bir araştırma ve inceleme konusu olmaya başlamıştır.

Bu projede, ilk olarak L-sistein biyolojik aktifliği olan virüs önleyici ve bakteri inhibitör geliştirici olarak testedilmiş 2-merkaptopirimidin arasında oluşabilecek tüm moleküllerarası etkileşimlere (hidrojen bağı) sahip kompleksler kuantumsal olarak ayrıntılı bir şekilde analize tabii tutulacaktır. DFT yöntemi kullanılarak, yapısal tüm parametreler en doğru şekilde bulunacaktır. Ayrıca, moleküldeki tüm atomlar için kuantum teori hesaplamaları (QTAIM), bağ analizi (NBO) ile birlikte yapılarak tüm enerji yoğunluk ilişkileri ortaya çıkarılacak ve yapısal parametreler ile birlikte hidrojen bağlarının kuvveti ve yapılarda oluşturduğu deformasyonlar tahmin edilecektir. Aynı zamanda, yapılar, gerekli korelasyon grafikleri ile estedilecektir ve komplekslerden en kararlı ve deformasyonu en yüksek kompleksler tartışılacaktır.

İkinci aşamada ise, yukarıda adı geçen DNA nükleikasit bazları, biyolojik rollerinden dolayı potansiyel bir uygulama oluşturabilecek uygun metal bağlanmalarına maruz bırakılacaktır. Bu bağlanmalar için platin

metali kullanılacaktır. L-sistein ile 2-merkaptopirimidin yapıları ve bunların yapısındaki farklı atom pozisyonlarından Platin metali ile farklı şekillerde bağlanarak oluşabilecek tüm kompleksler, altı adet DFT (B3LYP, BHANDH, HCTH, MPW1PW91, PBEPBE, ve TPSSKCIS) yöntemi ile yapısal olarak analiz edilecektir. Metal bağlanmaları için sisplatin merkez yapısı kullanılacaktır. Vakum ortamında özellikle, doğal orbital analizi (NBO), HOMO-LUMO ve diğer moleküler orbitallerin incelenmesi, reaktivitenin belirlenmesi, enerji profil diyagramları, yapı analizi ve çözümü için harmonik titreşim frekansları ve ve tüm bu kompleksler için en doğru sonuçların meydana getirilmesi için detaylı orbital analizi (NBO) yapılacaktır.

Sonuç olarak bu çalışmalardan, öncelikle, L-sistein ile 2-merkaptopirimidin arasındaki moleküllerarası etkileşimlerden doğan deformasyonların ve oluşturulması planlanan komplekslerin, potansiyel tedavi amaçlı uygulama alanları olabileceği düşünülmektedir ve bu iki tür çalışma bilim ve teknoloji açısından önemli bir yer edinecektir.

Keywords: L-sistein, 2-merkaptopirimidin, Doğal bağ orbital, DFT hesaplamaları, HOMO-LUMO, sisplatin, hidrojen bağı

to my wife

ACKNOWLEDGMENTS

I am heartily thankful to my supervisor, Prof. Dr. İzzet MORKAN and Prof. Dr. Ayşe UZTETİK MORKAN, whose encouragement, guidance and support from the initial to the final level enabled met to develop an understanding of the subject and also moral support and motivation. I would like to thank my wife, SÜLHİYE YAZICI. The constant inspiration and guidance kept me focused and motivated by my wife. I have served as scholarship master student in the TÜBİTAK 1001 project of **113Z302** number. So, i am thank to Prof. Dr. Ayşe UZTETİK MORKAN and TÜBİTAK.

TABLE OF CONTENTS

LIST OF FIGURES

LIST OF TABLES

LIST OF ABBREVIATIONS

ABBREVIATION	NOMENCLATURE
DNA	Deoxyribonucleic Acid
DFT	Density Functional Theory
L-cys	L-cysteine
2-mpym	2-mercaptopyrimidine
QTAIM	Quantum Theory Atoms in Molecules
NBO	Natural Bond Orbital
CON	Conformer
BCP	Bond Critical Point
RCP	Ring Critical Point
BSSE	Basis Set Superposition Error
CP	Counterpoise
ZPVE	Zero Point Vibrational Energy
H-bond	Hydrogen Bond
R_{X---H}	The Bond Length of Donor Group
ΔR_{X---H}	Bond Elongation
R_{X---H}^{Mon}	The Bond Length of Donor Group in Monomers
$R_{H- \ - \ -Y}$	The Length of Hydrogen Bond

$\delta R_{Y- - - H}$	The Hydrogen Bonding Parameter
$\angle X\text{-}Y- - -H$	The Angle of Hydrogen Bond
R_H^{VDW}	The van der Waals Radii of Hydrogen Atom
R_Y^{VDW}	The van der Waals Radii of Acceptor Atom
ρ_b	Electron Density on Hydrogen Bond
$\nabla^2_{\rho b}$	The Laplacian Electron Density on H-Bond
H_b	The Electron Energy Density of H-Bond
V_b	Electron Potential Energy Density of H-Bond
G_b	The Electron Kinetic Energy Density of H-Bond
$\ln\nabla^2_{\rho b}$	Logaritmic Laplacian Electron Density
$\ln\rho_b$	Logaritmic Electron Density
E(2)	The Stabilization Energy
CT	Charge Transfer
NCT	Non-Charge Transfer
ΔE	Binding Energy
ΔE_{int}	Interaction Energy
ΔE_{prep}	Preparation Energy
ΔE_{CT}	Charge Transfer Energy
ΔE_{NCT}	Non-Charge Transfer Energy
Δv	The Gap Between the Streching Frequency of Hydrogen Bonding and the Streching Frequency of Monomer
v_{X---H}	The Streching Frequency of Hydrogen Bond
I	Intensity

S	Symmetry Type
Pt	Platinum
HOMO	Highest Occupied Molecular Orbital
LUMO	Lowest Unoccupied Molecular Orbital
HF	Hartee Fock Theory
MP2	Møller-Plesset Perturbation Theory
B3LYP	Becke, Three-Parameter, Lee-Yang-Parr
BHANDH	Becke’s Half And Half Functional
HCTH	Handy’s Family of Functional
MPW1PW91	Perdew-Wang Exchange as Modified by Adamo and Barone
PBEPBE	The 1996 Pure Functional of Perdew, Burke and Ernzerhof
TPSSKCIS	Combination of The exchange functional of Tao, Perdew, Staroverov, and Scuseria and The Krieger-Chen-Iafrate-Savin correlation functional
ECP	Effective Core Potential
SDD	Stuttgart/Dresden Basis Set
HSAB	Hard and Soft of Acids and Bases
μ	Electronic Chemical Potentials
ω	Electrophilicity
η	Chemical Hardness
AO	Atomic Orbital
NAO	Natural Atomic Orbital
NHO	Natural Hybrid Orbital

NPA	Natural Population Analysis
NLMO	Natural Localized Molecular Orbital
MO	Molecular Orbital
NLS	Natural Lewis Structure
NMB	Natural Minimal Basis Set
LP	Lone Pair
KE	Kinetic Energy
EE	Electron-Electron Repulsion Energy
PE	Potential Energy
NN	Nuclear Repulsion Energy
MEP	Molecular Electrostatic Potential
PMH	Principle of Maximum Hardness
C_v	Heat Capacity
ΔS	Entropy
ΔH	Entalpy Change
ΔG	Gibbs Free Energy
PED	Potential Energy Distribution
v	Stretching
δ	In-Plane Bending
γ	Out-of-Plane Bending
τ	Torsion
coor	Coordination

CHAPTER 1

INTRODUCTION

Hydrogen bonding interactions between 2-mercaptopyrimidine and L-cysteine have been investigated in part 1 of this work. Hydrogen bonding interactions among amino acids and nucleic acid bases create the most significant interactions accountable for the specificity of protein binding [1-3]. Furthermore, some reviews concerning the evolution of the genetic code [4, 5] have emphaized the involvement of specific interactions between amino acids and their codon or anticodon nucleotides. Thus, quantitative labours on these interactions are very profitable for the explication of a number of biological operations in physicochemical terms. but, suchlike biological systems are very large that no current quantum chemical method is within achieve for the study of them even with the most powerful computing capabilities. An alternative approach is quantitative studies on simplified model systems at a currently viable computational level. Some theoretical researches on nucleobase and amino acid complexes have been reported for uracil (or thymine) with glycine, alanine leucine, or cysteine [6–14] and with the hydrophilic side chains of asparagines [15]. These studies may provide some basic information about intrinsic affinities for hydrogen bonds in the

complexes, which are essential for understanding its biological function. Even in such simplified model systems, the hydrogen bonding interactions are also very complex because more than one proton donor and acceptor sites can be found in almost all nucleobase or amino acid molecule. Besides, it is sensible to ascribe the fundamental nature of hydrogen bonding interactions, hydrogen bonding complexes must be considered carefully using a reliable theoretical model. MP2 method is deemed to be a reliable method for description of hydrogen bonding interactions. However, MP2 approach is not a cost-effective approach for the computation of such biomolecular systems even with a medium-size basis set. Density functional theory (DFT) has been accepted by the ab initio quantum chemistry community as a cost-effective approach for description of hydrogen bonding interactions. Many studies have shown that molecular structures and vibrational frequencies calculated by DFT methods are more reliable than MP2 methods [14,16–18].

Generally, the formation of H-bond can be estimated by the structural parameters (e.g., hydrogen bond length and bond angle), and the strength of hydrogen bond also can be determined by the enlarging or shortening of H-bond length. However, the structural parameters cannot provide sufficient information to accurately describe the nature of hydrogen bonding interactions in biological system. Therefore, a scientific method for description of hydrogen bonding interactions is highly desirable. The quantum theory of atoms in molecules (QTAIM) and natural bond orbital (NBO) analysis have proved to be very useful tools in describing electron

densities in various systems and in extending the understanding of H-bond [19–21]. According to QTAIM, the presence of a bond critical point (BCP) between two atoms is a universal indicator of bonded interactions and the electron density $\boldsymbol{\rho_b}$ at BCP point is related to the bond strength or bond order. Therefore, the existence of BCP and the topological properties of electron density $\boldsymbol{\rho_b}$ can be used to study the nature of H-bond. Especially, according to QTAIM, Koch and Popelier [22] proposed a set of criteria for the existence of H-bonds. The criteria provide a basis to distinguish these interactions from van der Waals interactions and have been proved to be valid for standard and nonconventional H-bonds.

The formation of H-bond implies that a certain amount of electronic charge is transferred from the H-acceptor to the H-donor, and a rearrangement of electron density within each part of molecule is occurred. Electron delocalization or charge transfer **(CT)** effects can be identified from the presence of off-diagonal elements of the Fock matrix in the NBO basis [23]. The interaction between filled and lone pair electrons and anti-bonding orbitals represents the deviation of the molecule from the lewis structure and can beused as a measure of delocalization because of H-bond in this work. The strength of these delocalization interactions, **E(2),** is estimated by second-order perturbation theory:

$$E(2) = -n_\sigma \frac{\langle \sigma | F | \sigma^* \rangle^2}{\varepsilon_{\sigma^*} - \varepsilon_\sigma} = -n_\sigma \frac{F_{ij}^2}{\Delta\varepsilon}$$

where $\mathbf{F_{(ij)}}$ is the Fock matrix element between the **i (σ)** and **j** (**σ***), $\boldsymbol{\varepsilon_{\sigma}}$, $\boldsymbol{\varepsilon_{\sigma^*}}$ are the energies of both donor and acceptor groups, $\mathbf{n_{\sigma}}$ is the population (a lone pair in the H-bond) [23].

In this part 1, we mainly discuss the structures and hydrogen bonding interactions of the L-cysteine & 2-mercaptopyrimidine complexes (Cys-2mpym) by DFT with counterpoise method, QTAIM, NBO Energy, and Vibrational analysis are carried out to study the nature of H-bonds.

Designs of novel potential cisplatin complexes with L-cysteine and 2-mercaptopyrimidine molecules have been investigated in part 2 of this work. The interest in platinum-based antitumor drugs has its origin in the 1960s, with the serendipitous discovery by Rosenberg of the inhibition of cell division by platinum complexes [24]. *cis-diamminedichloroplatinum(II) (cis-$[PtCl_2(NH_3)_2]$**(1)**)* and *cis-diamminetetrachloroplatinum(IV) (cis-$[PtCl_4(NH_3)_2]$**(2)**)* were identified as the platinum compounds responsible for the phenomenon [25, 26]. Deducing that Ptlatinum compounds would have uses in cancer treatment, Rosenberg and coworkers performed experiments with Sarcoma 180 and Leukemia L1210 bearing mice [25, 27-30]. This eventually led to *cis-diamminedichloroplatinum(II) (cisplatin **(1)**)* entering phase I clinical trials in 1971. Approval of cisplatin for the treatment of testicular and ovarian cancer was given in 1978 [31]. Today, *cisplatin* is one of the three most widely utilized antitumor drugs in the world and has annual sales of approximately $500 million (U.S.) [32, 33]. It is highly effective in

treating testicular and ovarian cancers, and it contributes to the treatment of oropharyngeal carcinoma, bronchogenic carcinoma, cervical carcinoma, lymphoma, osteosarcoma, melanoma, bladder carcinoma, and neuroblastoma [32].

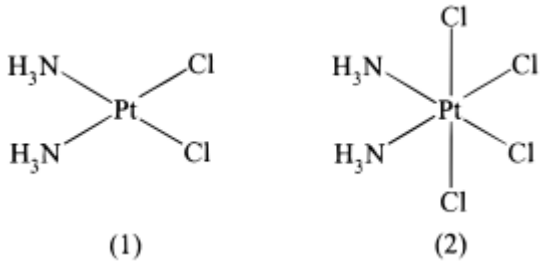

Figure 1.1. cis-Diamminedichloroplatinum(II) (cis-$[PtCl_2(NH_3)_2]$(1)) and cis-diamminetetrachloroplatinum(IV) (cis-$[PtCl_4(NH_3)_2]$(2))

Despite its success, *cisplatin* has several disadvantages that include severe toxicity such as nephrotoxicity, neurotoxicity, and emetogensis. The toxic side effects of *cisplatin* limit the dose that can be given to patients; typical doses are 100 mg/day for up to five consecutive days [34]. To help alleviate nephrotoxicity, intravenous hydration and diuresis have been employed [32], though they pose an inconvenience to treatment on an outpatient basis. The use of serotonin receptor antagonists have helped reduce nausea and vomiting in some patients [35-38]. A number of protecting or rescue agents such as mesna, WR-2721, diethyldithiocarbamate, and thiosulfate have also been used to control *cisplatin* toxicity; however, the exact role of these agents is not well understood, and they are as of yet not routinely used in Pt chemotherapy [39-41 *Cisplatin* is used in the treatment of a number of cancers, but its applicability is still limited to a relatively narrow range of tumors. Some tumors have natural resistance to *cisplatin*, while

others develop resistance after the initial treatment. *Cisplatin* also has limited solubility in aqueous solution and is administered intravenously, another inconvenience to outpatient treatment. These drawbacks coupled with *cisplatin* toxicity have been the impetus for the development of an improved platinum antitumor drug.

Since the introduction of *cisplatin*, thousands of platinum compounds have been synthesized and evaluated as potential antitumor agents. Over 28 have entered human clinical trials, [32-42]. But only *diammine[1,1-cyclobutanedicarboxylato(2-)]-O,O'-platinum(II)(carboplatin(**3**))* received worldwide approval and achieved routine clinical use. *Carboplatin* is less toxic than *cisplatin* and can be given at a much higher dose than *cisplatin* (up to 2000 mg/dose) [34]. The lower toxicity of *carboplatin* in comparison to *cisplatin* has been the advantage that enabled it to achieve worldwide approval and use. Unfortunately, *carboplatin* is still only active in the same range of tumors as cisplatin and is still administered intravenously. In recent years, two other Platnum compounds have received limited approval for use

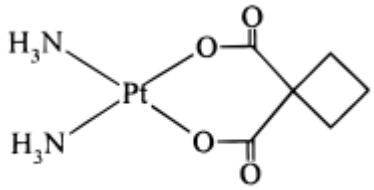

(3)

Figure 1.2. diammine[1,1-cyclobutanedicarboxylato(2-)]-O,O' platinum(II) (carboplatin(3))

in some countries. *(trans-L-Diaminocyclohexane)oxalatoplatinum(II) (oxaliplatin or LOHP(**4**))* has been approved for the secondary treatment of metastatic colorectal cancer in France and other European countries. *Cis-diammine-glycoloato-O,O'-platinum(II) (nedaplatin or 254-S (**5**))* [42] has received approval for use in Japan [42]. The search continues for an improved Pt antitumor agent, motivated by the desire to design a less toxic, orally active compound that is non-cross-resistant with *cisplatin and carboplatin*.

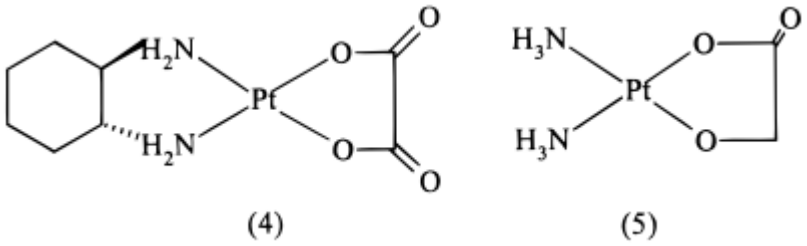

(4) (5)

Figure 1.3. (trans-L-Diaminocyclohexane)oxalatoplatinum(II) (oxaliplatin or LOHP(**4**)). cis-Diammine-glycoloato-O,O'-platinum(II) (nedaplatin or 254-S (**5**)).

In the years following the introduction of *cisplatin*, the design of new platinum antitumor drugs concentrated mainly on direct *cisplatin* analogues, which adhered to the set of structure-activity relationships summarized by Cleare and Hoeschele in 1973 [43, 44]. More recently, there have been efforts to rationally design new platinum complexes based on an improved understanding of the mechanisms of platinum drug resistance. Specific chemical and structural features can be incorporated into new platinum compounds such that they are able to circumvent a specific drug resistance

mechanism. There have also been efforts directed at the design of unconventional complexes that violate the original structure-activity relationships, such as trans Platinum compounds and binuclear platinum complexes. As the in vivo behavior and mechanism of actions for these complexes are expected to be different from those of *cisplatin* or *carboplatin*, it is hoped that they will overcome platinum drug resistance in tumors and be applicable to a broader range of cancers. There has also been interest in Pt(IV) complexes for their potential as orally active agents. Since the original discovery by Rosenberg, the volume of research into platinum antitumor drugs has been staggering. Thousands of platinum compounds have been synthesized and evaluated. Review articles have appeared regularly over the years dealing with the synthesis, preclinical screening, mechanism of actions, [34, 41, 45-55] and clinical trials of platinum drugs [32, 42, 48, 56].

Of the thousands of platinum compounds evaluated for antitumor activity, the majority of them adhered to the set of structure-activity relationships summarized by Cleare and Hoeschele [43, 44]. These relationships state that for a platinum complex to show antitumor activity, the Pt(II) or Pt(IV) complex should have a cis geometry with the general formulas of *cis-*$[PtX_2(Am)_2]$ or *cis-*$[PtX_2Y_2(Am)_2]$, where X is the leaving group and Am is an inert amine with at least one N-H moiety. The leaving group, X, should be an anion with intermediate binding strength to platinum and have a weak trans effect to avoid labilizing the amine. Complexes with labile leaving groups such as ClO_4^- or NO_3^- are highly toxic, while complexes with inert

leaving groups are generally inactive. The structure-activity relationships dominated Pt drug design for over 30 years and remained valid until relatively recently. This is reflected in the fact that all platinum compounds that have entered clinical trials so far adhere to this set of guidelines. A number of researchers have taken a completely different approach to platinum drug design and have prepared compounds that violate the structure-activity relationships but yet show antitumor activities. Efforts have also been directed toward the rational design of compounds with specific characteristics that could allow them to be administered orally or to circumvent known mechanisms of platinum drug resistance.

Sulfur-containing biomolecules such as cysteine (Cys), methionine (Met), glutathione (GSH), metallothionein (MT) and albumin play significant roles in platinum anticancer chemotherapy because of their high affinity to platinum(II) compounds [41, 57, 58]. Sulfur is involved in the entire metabolic process of platinum drugs, including reactions prior to cell uptake, deactivation prior to DNA binding, and formation of DNA-adduct, etc [59]. The nature of the final products for most of these reactions has been clarified [59-61]. The platinum-sulfur interactions can be used to produce favorable effects in the clinical application of platinum-based drugs. It is possible now to employ sulfur-containing compounds as chemoprotectants to mitigate the severe toxic side effects of platinum drugs and some of them have been registered in a number of European countries [62-64]. Moreover, the design

of new generations of platinum-based drugs can be benefited from the understanding of these interactions.

Platinum(II) has a high affinity for sulphur, so after administrating Pt(II) complex in the human body there is a strong possibility for binding with sulphur-donor bio-molecules. Sulphur-donor biomolecules are present in large amounts in the form of peptides, proteins and enzymes. Binding of platinum complexes with sulphur-donor biomolecules are responsible for the occurrence of toxic effects. [65-67]. However, a certain amount of platinum complexes being bound to nitrogen-donor bio-molecules (amino acids or DNA). Today, it is generally accepted that the anti-tumor activity of platinum drugs can be ascribed to interactions between the metal complex and DNA, primarily with the genetic DNA, which is located in the nucleus. The interactions with mitochondrial DNA are less responsible for the antitumor activity of the platinum complexes [68]. When the Pt(II) complexes reach the DNA, the possibilities for coordination are different. Binding of Pt(II) complexes to DNA primarily occurs through the N7 atoms of guanine, while a binding to N7 and N1 of adenine and N3 of cytosine occurs in small amount [54-56]. Since the DNA molecule containing a different sequence of purine and pyrimidine bases, it was found that with 60% represented the coordination of the type 1,2-(GPG), i.e., the coordination realizes *via* two molecules of guanosine-5’-monophosphate (5’-GMP), which are located on opposite strands of DNA. About 25% is represented by coordination of the type 1,2-(APG), i.e. coordination with adenosine-5'monophosphate (5’-AMP)

and 5’-GMP placed on opposite DNA strands. Other ways of coordinations (monofunctional binding of the type 1,3-(GPG), coordination via guanosine located on the same chain of DNA, etc.) are less frequent. On the **Figure 1.4.** is shown the varied ways of coordination of cisplatin to DNA [69, 70].

However, as noted above, the cells contain other biomolecules which can also react with platinum complexes. High affinities for the platinum complexes show the biomolecules that contain sulphur, as the thiols and the thioethars. Namely, Pt(II) as "soft" acid forms very stable compounds with sulphur donor ("soft" bases). The resulting compounds are responsible for the occurrence of toxicity (nephrotoxicity, neurotoxicity, resistance, etc.).

Since the concentration of thiols, including glutathione (GSH) and L-cysteine, in intracellular liquid is about 10 mM, it is assumed that most of the platinum complex bound to sulphur before it comes to the molecules of DNA [65-67, 69, 71]. Binding of platinum complexes to sulphur from thioethers are the kinetically favored process.

The resulting Pt-S (thioether) bond may be terminated in the presence of DNA, i.e. N7 atom of 5’-GMP can substitute the molecule of thioether [67, 72]. For these reasons the compounds of the type Pt-S (thioethers) are believe to be the reservoirs of “platinum complexes’’ in the body, i.e. they are suitable intermediates in the reaction of Pt(II) complexes and DNA.

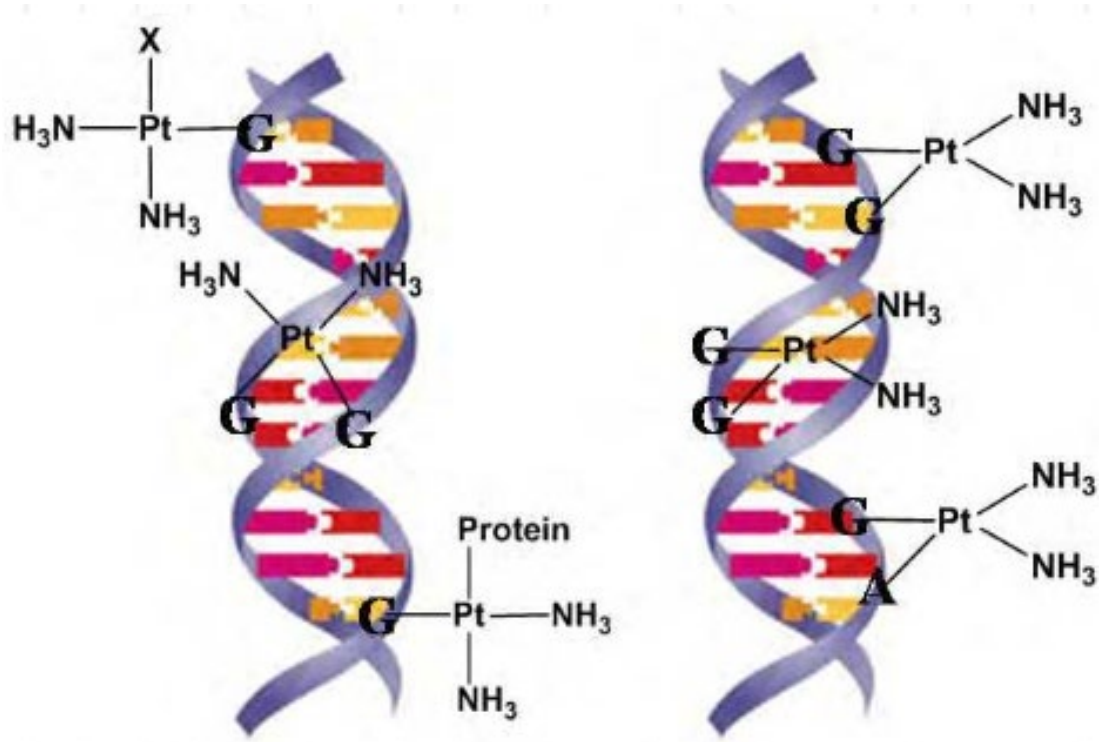

Figure 1.4. The different ways of coordinations of cisplatin to DNA.

Pt-S (thioethers) bond can be terminated in the presence of thiol molecules. The product of this substitution is thermodynamically stable. Also, Pt(II) complex can direct bind to sulphur from thiol molecules and the resulting Pt-S(thiol) bond is very stable and can not be easy broken. It is believed that compounds of the type Pt-S (thiol) are responsible for the occurrence of toxic effects during the use of Pt(II) complexes as anticancer reagents. The Pt-S (thiol) bond can be terminated in the presents of compounds known as "rescue agents", which are compounds with sulphur and they are very strong nucleophiles (diethyldithiocarbamate, thiourea, thiosulfate, glutathione, cysteine, biotin, etc.) [68, 69, 72].

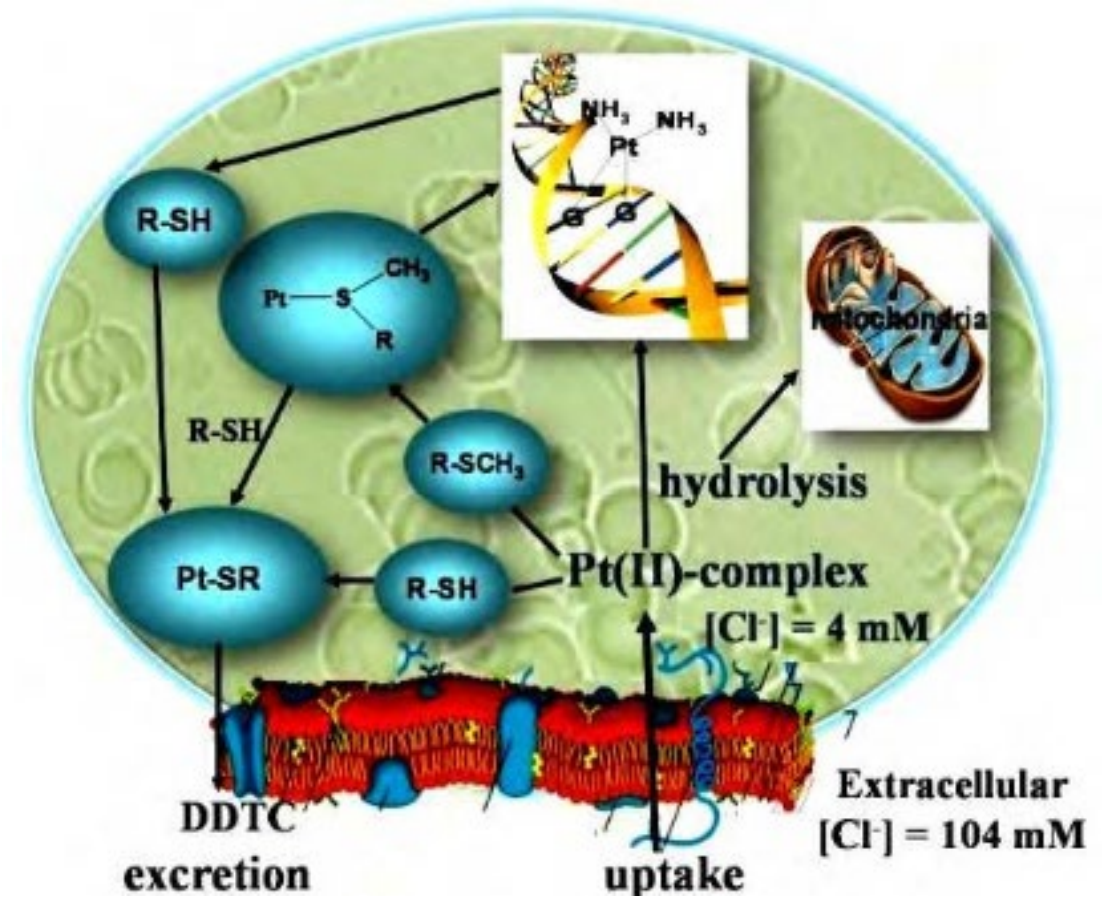

Figure 1.5. Schematic presentation of the levels of action of cisplatin in the cell and possible biological consequences.

In recent years a much attention has given to studies of the anti-tumor activity of polynuclear Pt(II) complexes structurally similar to cisplatin [73]. The bridge ligand can be diamine ligands of the type $NH_2(CH_2)nNH_2$ (n = 6) [63]. In the reaction with DNA primarily is obtained compound in which complex is bound simultaneously to both spirale [74, 75]. It was found that the presence of the hydrophobic part of the molecule enhances the absorption of these compounds on the cell membrane, where their activity decrease. Also, the polynuclear Pt(II) complexes with heterocyclic nitrogen compounds as bridge ligands were synthesized [76]. Pt(IV) complexes are

also very interesting. They react more slowly than the corresponding Pt(II) complexes [77]. It assumed that first Pt(IV) complexes by reduction translate to Pt(II) complexes and then the mechanism of action is the same as in the case of Pt(II) complexes [78]. For the reduction of Pt(IV) complexes can serve glutathione, L-cysteine, L-methionine, DL-penicilamin [79] or ascorbic acid [80].

Besides the already mentioned complexes of Pt(II), there are other platinum compounds such as *trans-[$PtCl_2(NH_3)_2$]* which does not show anti-tumor activity [81]. These complexes were also intensively studied, [82] as well as some dinuclear complexes of trans-geometry [83]. Special attention in recent years were given to the investigation of dinuclear complexes of platinum and paladium [84].

Informations presented here, could contribute to a better understanding of the precise biochemical mechanism of some Pt(II) complexes. Moreover, the results of the substitution reactions with biologically relevant ligands could help to get more information on the possible interaction modes of Pt(II) complexes with in vivo targets and their representative application in the study of their anti-tumour properties. Detailed knowledge of the interactions between transition metal ions complexes with biomolecules and stability of final products under varying experimental conditions is fundamental for future investigations of new pharmacological agents and discovery of the alternative tumor treatment.

Connecting theoretical calculations, chemistry, biochemistry and cellular biology and establishement of the structure-activity relationship Pt(II) complexes will help to solve some of the questions and will finally result in more tailored drug design. Numerous data imply that interactions of Pt(II) complexes and investigation of the mechanism of their reaction with DNA fragments (purine and pyrimidine bases, as well as oligonucleotides) are important for anti-tumor activity of Pt(II). Investigations of the interaction of Pt(II) complexes with S-donor biomolecules can help us to get better insights in the destiny of anti-tumor drugs in the cells after their uptake, as well as to obtain more information about the inner cellular processes, which are affected by therapy. Further research in this area will be based on the synthesis and investigation of the substitution reactions of the transition metals complexes especially Pt(II) complexes. This complexes are investigated in order to find compounds that would demonstrate greater anti-tumour activity and less toxicity and resistance compared to cisplatin.

CHAPTER 2

RESULTS AND DISCUSSION

PART 1: Hydrogen Bonding Interactions Between 2-mercaptopyrimidine and L-cysteine

2.1.1. Computational Details

In this process of first part, we mainly discuss the structures and hydrogen bonding interactions of the cysteine and 2-mercaptopyrimidine complexes (Cys-2mpym) by DFT, and QTAIM and NBO analysis are carried out to study the nature of H-bonds. The three-parameter hybrid functional according to Becke with additional correlation corrections because of Lee et al. [85, 86] was used (B3LYP) with 6-311G basis set [87, 88]. First, the structures of cysteine and 2-mercaptopyrimidine monomers were fully optimized. The Cys-2mpym complexes were constructed starting from the most stable cysteine and 2-mercaptopyrimidine monomers. All complexes were also fully optimized at the same level. To take into account the effects of the basis set superposition error, the counterpoise method [89] was implemented in each step of the iterative process of geometry optimization in an integrated way to ensure that complex and monomer are being computed

with a consistent basis set. The harmonic vibrational frequencies were calculated with analytic second derivatives at the same level confirmed the structures as minima. All frequencies were unscaled. The interaction energies were calculated based on the basis set superposition error correction. Finally, QTAIM and NBO analysis were carried out to investigate the nature of hydrogen bonding interactions in complexes.

All optimization and frequency calculations have done with Gaussian package. Multiwfn and NBOPro programs have been used for the calculation and display of QTAIM analysis. All energies have been calculated by NBOPro software.

2.1.2. Structures

Recently, conformers of cysteine have been studied by different research groups [90–93]. In this work, the properties of L-cysteine and 2-mercaptopyrimidine were well reproduced at the B3LYP/6-311G level. The optimized conformers of L-cysteine **(A)** and 2-mercaptopyrimidine **(B)** were presented in **Figure 2.1.2.1.**. L-cysteine and 2-mercaptopyrimidine molecules can offer several possible donor and acceptor sites to form used as H-acceptor. 2-mercaptopyrimidine, another monomer, could offer N3 as H-acceptor, whereas thiol group (SH, S4) and (CH, C5) group as H-donor. 27 kinds of H-bonds complexes can be found from the most stable monomers. All optimized complexes were presented in **Figure 2.1.2.2.**, and the structural parameters of H-bonds were listed in **Table 2.1.2.1.**.

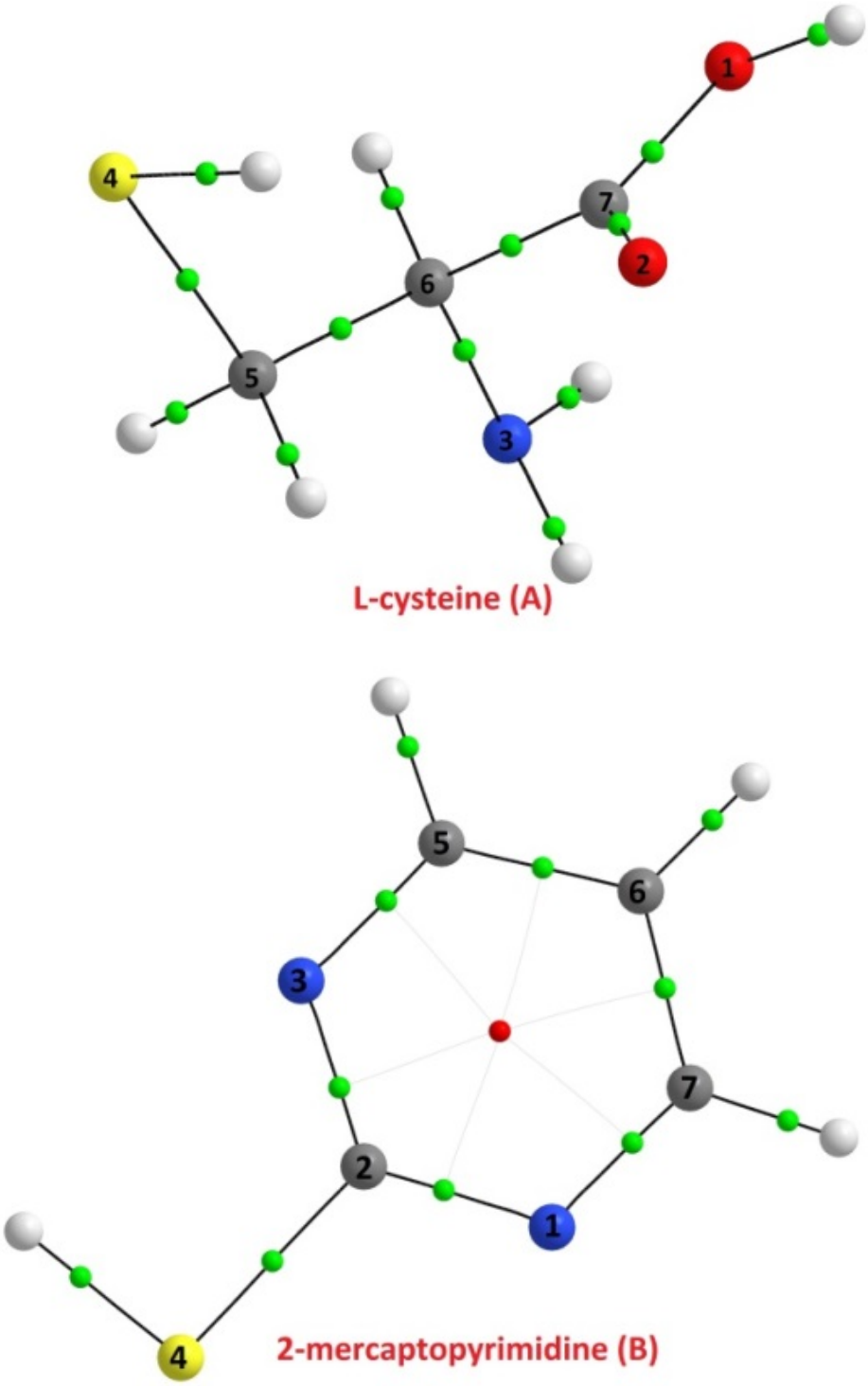

Figure 2.1.2.1. Molecular graphs of free cysteine and 2-mercaptopyrimidine monomers. Large circles correspond to attractors attributed to atomic positions: white, H; blue, N; gray, C; red, O; yellow, S. Small circles are attributed to critical points: green, BCP; red, RCP.

The vibrational frequency calculations approved that all optimized complexes have no imaginary frequencies and are stable structures. The presence of Hydrogen bonding can be defined by BCP between the donor (X-H) and acceptor groups (Y). The coexistences of several H-bonds may be result in the formation of ring structures characterized by ring critical point (RCP). Also, the heterocyclic structure of 2-mercaptopyrimidine fragment characterized by a RCP has no relationship with H-bond. The distance between BCP and corresponding RCP can also be used as a standard to prediction the structural stability of the H-bond. The unity between these two critical points represents bond division and sequent ring opening [94]. As

Figure 2.1.2.2. (Continued)

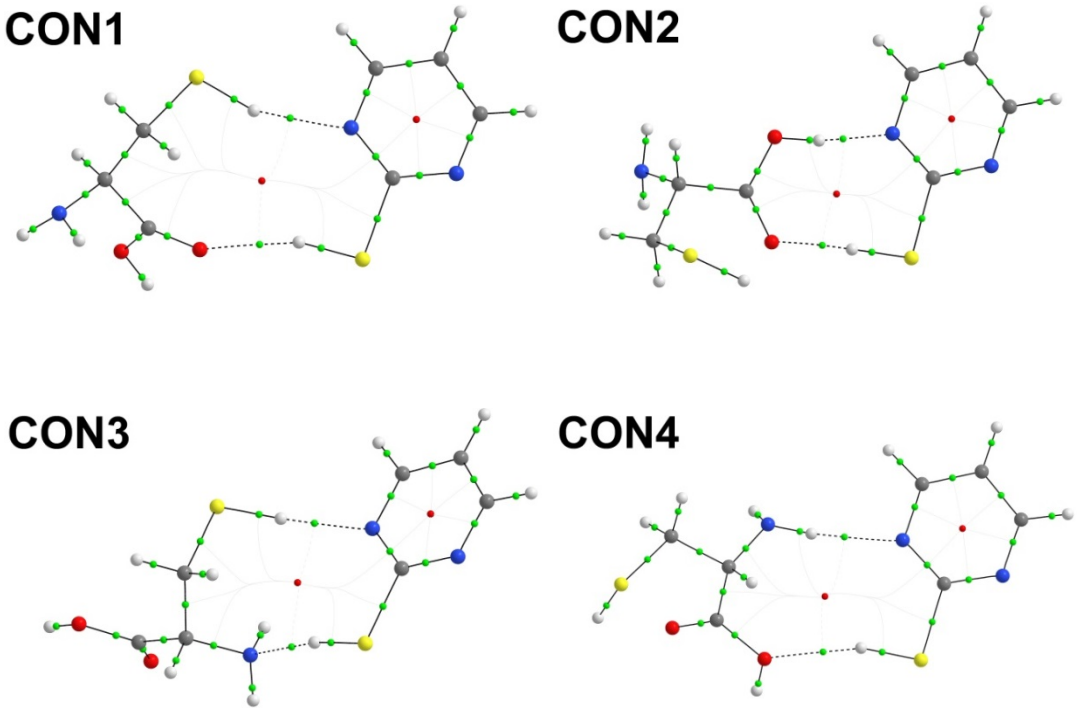

Figure 2.1.2.2. (Continued)

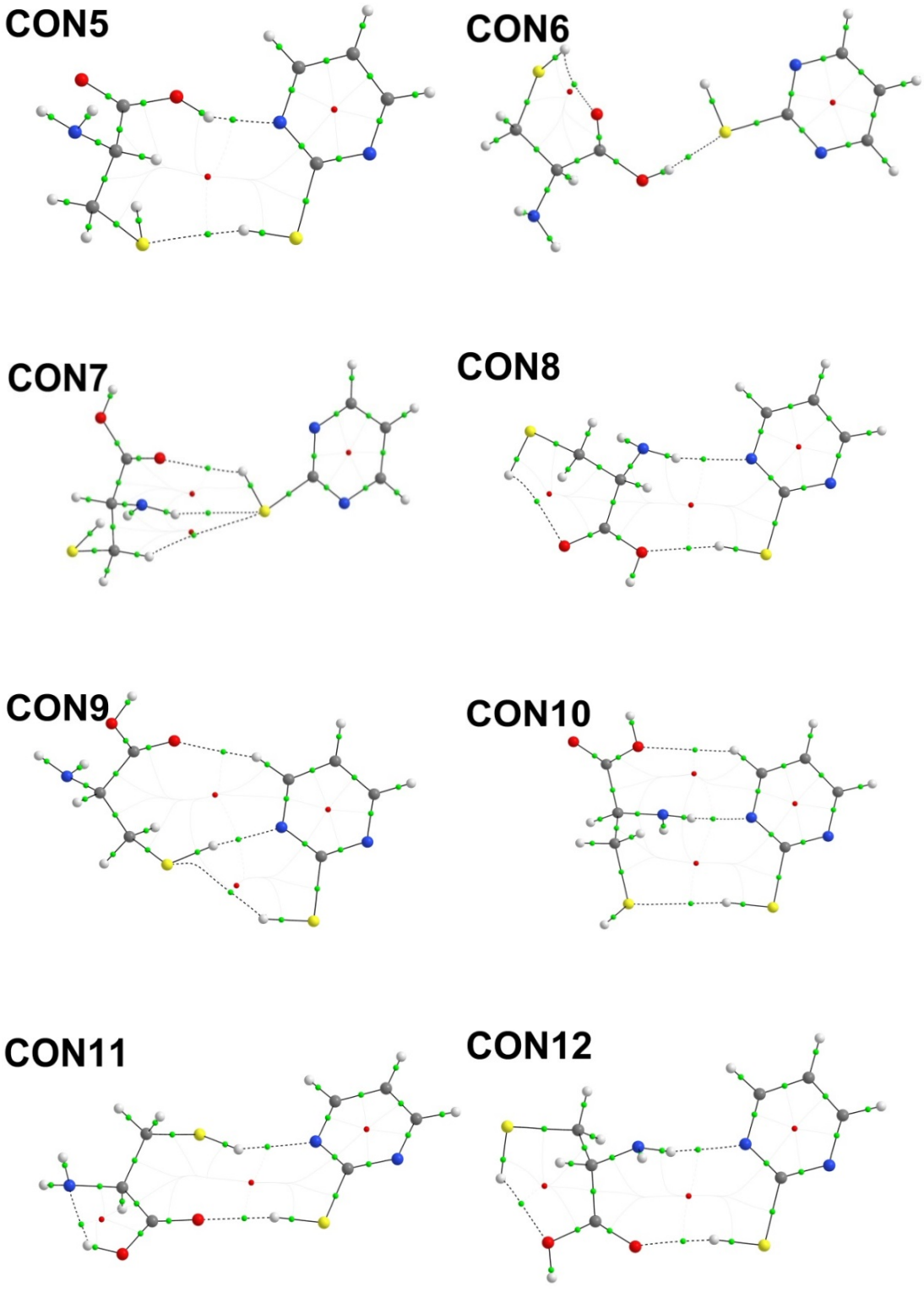

Figure 2.1.2.2. (Continued)

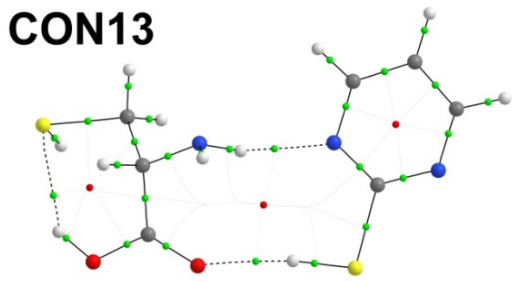

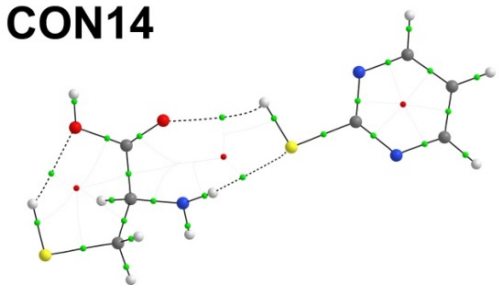

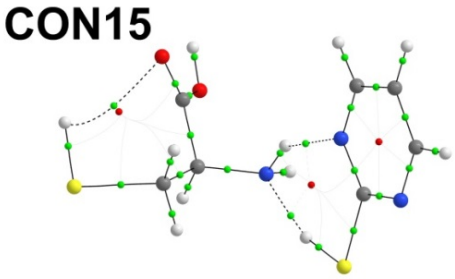

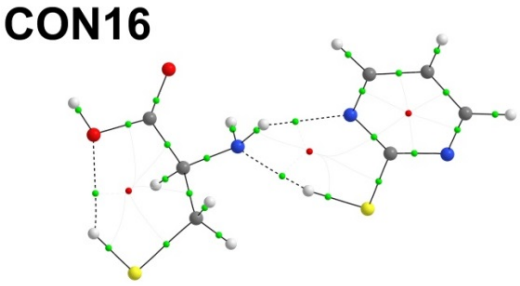

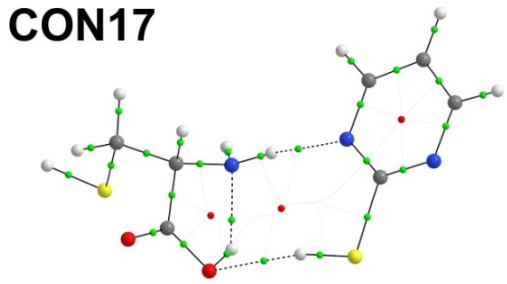

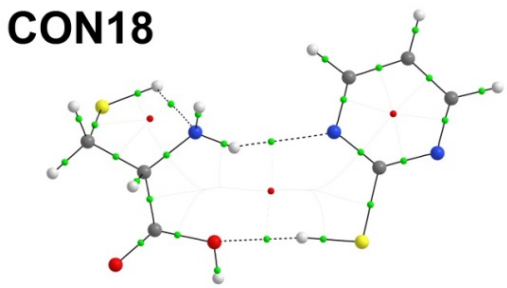

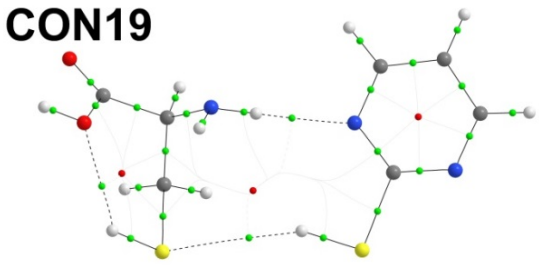

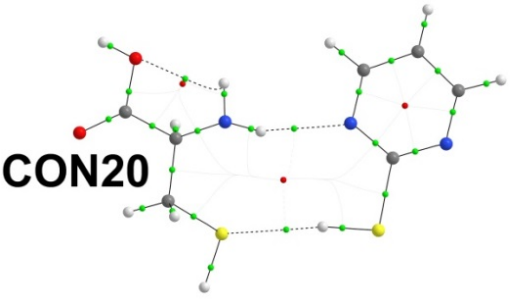

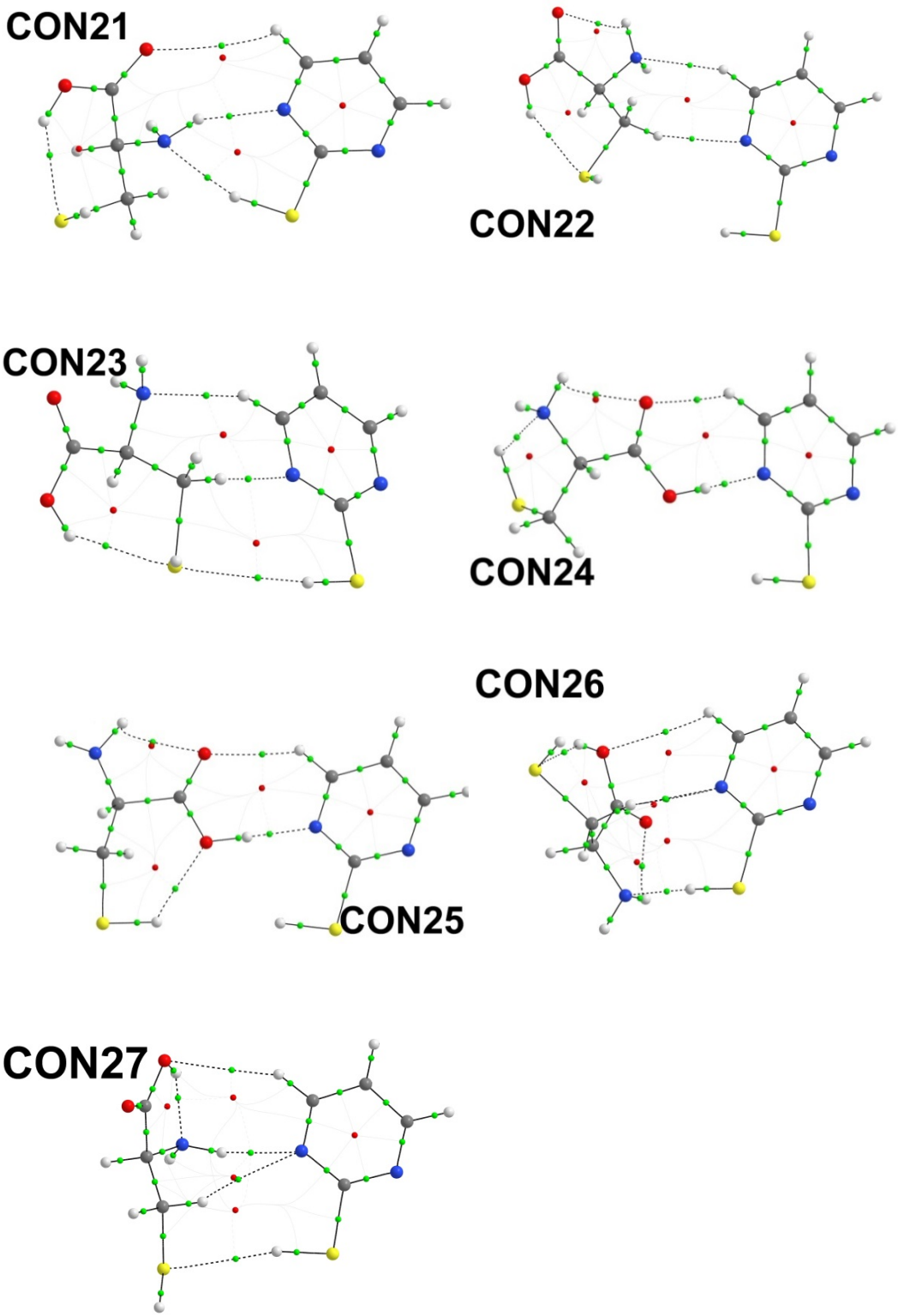

Figure 2.1.2.2. Molecular graphs of Cys-2-mpym complexes. Large circles correspond to attractors attributed to atomic positions: white, H; blue, N; gray, C; red, O; yellow, S. Small circles are attributed to critical points: green, BCP; red, RCP.

shown in **Figure 2.1.2.1.** and **2.1.2.2.**, Some intra-molecular H-bonds can be found in Cys-2mpym complexes. For example, the intra-molecular hydrogen bonding of $O1^{A}H---N3^{A}$ is involved in **CON11, CON17,** and **CON27**, respectively, and other intra-molecular H-bond $S4^{A}H$ with interaction of $O1^{A}$ and $O2^{A}$ exists in **CON6, CON10, CON12, CON14, CON15, CON16, CON19** and **CON25**, respectively, whereas intra-molecular $O_1{}^{A}H---S^{A}$ H-bond forms **CON13, CON21, CON22,** and **CON26**. Finally, H-bonds of $S^{A}H---N^{A}$ complexes are in **CON18** and **CON24,** respectively.

Besides above intra-molecular H-bonds, different intra-molecular H-bonds can be found in complexes. There are multiple intra-molecular H-bonds in different complexes. For example, **CON22, CON24**, **CON25,** and **CON26** have two intra-molecular H-bond in L-cysteine part of complexes. In addition, conformers of **CON6, CON10, CON11, CON12, CON13, CON14, CON15, CON16, CON17, CON18, CON19, CON20, CON21, CON23,** and **CON27** have one intra-molecular H-bond. **CON1, CON2, CON3, CON4, CON5, CON7, CON8,** and **CON9** have no intra-molecular H-bond in complexes, too.

Consequently, the most important part of this work is to understand inter-molecular H-bonds in complexes. For example, in addition, some molecules have only three inter-molecular H-bonds in complexes of **CON7, CON8,** and **CON9,** respectively. Next, complexes of **CON10, CON11, CON12, CON13, CON14, CON15, CON16, CON17, CON18, CON19,** and

CON20 exist two inter-molecular and one intra-molecular H-bonds also **CON1, CON2, CON3, CON4,** and **CON5** complexes have only two inter-molecular H-Bond. In summary, other complexes of **CON21** and **CON27** form interactions of both inter-molecular and intra-molecular H-bonds.

Table 2.1.2.1. The structural parameters of inter-molecular and intra-molecular H-bonds in Cys-2mpym complexes calculated at B3LYP/6-311G level.

COMPLEXES	H-BOND	R_{X---H}	R_{X---H}^{Mon}	ΔR_{X---H}	R_{Y---H}	δR_{Y---H}	∠X-Y---H
CON1	**$S4^{A}H---N3^{B}$**	1.39929	1.38314	0.01615	2.11632	0.63368	159.34
	$S4^{B}H---O2^{A}$	1.38560	1.38182	0.00378	2.08190	0.63810	160.65
CON2	**$O1^{A}H---N3^{B}$**	1.02662	0.97741	0.04921	1.66649	1.08351	170.32
	$S4^{B}H---O2^{A}$	1.40819	1.38182	0.02637	1.86594	0.85406	177.21
CON3	**$S4^{A}H---N3^{B}$**	1.40847	1.38314	0.02533	2.01990	0.73010	174.09
	$S4^{B}H---N3^{A}$	1.43962	1.38182	0.05780	1.85459	0.89541	170.85
CON4	**$N3^{A}H---N3^{B}$**	1.01667	1.00967	0.00700	2.09570	0.65430	167.26
	$S4^{B}H---O1^{A}$	1.38688	1.38182	0.00506	2.21204	0.50796	161.11
CON5	**$O1^{A}H---N3^{B}$**	1.00359	0.97741	0.02618	1.78272	0.96728	154.15
	$S4^{B}H---S4^{A}$	1.39272	1.38182	0.01090	2.60592	0.39408	164.45
CON6	**$O1^{A}H---S4^{B}$**	0.98566	0.97741	0.00825	2.43705	0.56295	169.94
	$S4^{A}H---O2^{A}$	1.38302	1.38314	-0.00012	2.63472	0.08528	114.40
CON7	**$C5^{A}H---S4^{B}$**	1.08636	1.08461	0.00175	3.54603	-0.79603	138.11
	$N3^{A}H---S4^{B}$	1.00848	1.00967	-0.00119	3.02347	-0.27347	150.17
	$S4^{B}H---O2^{A}$	1.38142	1.38182	-0.00040	2.41553	0.33447	129.03
CON8	**$S4^{A}H---N3^{B}$**	1.40486	1.38314	0.02172	2.03163	0.71837	171.25
	$S4^{B}H---S4^{A}$	1.38424	1.38182	0.00242	3.08243	-0.08243	152.56
	$C5^{B}H---O2^{A}$	1.08021	1.08041	-0.00020	2.24991	0.47009	156.02
CON9	**$N3^{A}H---N3^{B}$**	1.01357	1.01118	0.00239	2.13672	0.61328	172.70
	$S4^{B}H---S4^{A}$	1.38773	1.38182	0.00591	2.80463	0.19537	169.75
	$C5^{B}H---O1^{A}$	1.08015	1.08041	-0.00026	2.73807	-0.01807	136.71
CON10	**$N3^{A}H---N3^{B}$**	1.01479	1.00967	0.00512	2.12498	0.62502	162.59
	$S4^{B}H---O1^{A}$	1.38600	1.38182	0.00418	2.21944	0.50056	165.18
	$S4^{A}H---O2^{A}$	1.38255	1.38314	-0.00059	2.51843	0.20157	114.51

Table 2.1.2.1. (Continued)

CON11	**S4^{A}H---N3^{B}**	1.39816	1.38314	0.01502	2.15313	0.59687	149.41
	S4^{B}H---O2^{A}	1.38566	1.38182	0.00384	2.03419	0.68581	167.59
	O1^{A}H---N3^{A}	0.99600	0.97741	0.01859	1.89154	0.85846	122.65
CON12	**N3^{A}H---N3^{B}**	1.01843	1.01118	0.00725	2.12513	0.62487	165.19
	S4^{B}H---O2^{A}	1.38826	1.38314	0.00512	2.07984	0.64016	166.11
	S4^{A}H---O1^{A}	1.38241	1.38182	0.00059	2.35907	0.36093	123.30
CON13	**N3^{A}H---N3^{B}**	1.01976	1.01118	0.00858	2.11197	0.63803	164.29
	S4^{B}H---O2^{A}	1.38969	1.38314	0.00655	2.02203	0.69797	168.31
	O1^{A}H---S4^{A}	0.98334	0.97741	0.00593	2.37257	0.62743	137.27
CON14	**N3^{A}H---S4^{B}**	1.00940	1.00967	-0.00027	2.91674	0.08326	170.80
	S4^{B}H---O2^{A}	1.37911	1.38182	-0.00271	2.62458	0.09542	112.00
	S4^{A}H---O1^{A}	1.38271	1.38314	-0.00043	2.41487	0.30513	124.46
CON15	**N3^{A}H---N3^{B}**	1.02260	1.01118	0.01142	2.12401	0.62599	147.44
	S4^{B}H---N3^{A}	1.42380	1.38314	0.04066	1.92391	0.82609	161.52
	S4^{A}H---O2^{A}	1.38311	1.38182	0.00129	2.64364	0.07636	113.52
CON16	**N3^{A}H---N3^{B}**	1.02271	1.01118	0.01153	2.13460	0.61540	145.60
	S4^{B}H---N3^{A}	1.42508	1.38314	0.04194	1.91970	0.83030	161.99
	S4^{A}H---O1^{A}	1.38240	1.38182	0.00058	2.33243	0.38757	123.55
CON17	**N3^{A}H---N3^{B}**	1.01847	1.00967	0.00880	2.12587	0.62413	166.40
	S4^{B}H---O1^{A}	1.38485	1.38182	0.00303	2.31082	0.40918	168.98
	O1^{A}H---N3^{A}	1.00545	0.97741	0.02804	1.82420	0.92580	125.58
CON18	**N3^{A}H---N3^{B}**	1.01239	1.00967	0.00272	2.27095	0.47905	147.25
	S4^{B}H---O1^{A}	1.38540	1.38182	0.00358	2.27745	0.44255	159.56
	S4^{A}H---N3^{A}	1.39406	1.38314	0.01092	2.26918	0.48082	115.43
CON19	**N3^{A}H---N3^{B}**	1.01598	1.01118	0.00480	2.14225	0.60775	175.43
	S4^{B}H---S4^{A}	1.38475	1.38182	0.00293	3.03682	-0.03682	149.78
	S4^{A}H---O1^{A}	1.38310	1.38314	-0.00004	2.39858	0.32142	124.43
CON20	**N3^{A}H---N3^{B}**	1.01392	1.01118	0.00274	2.26574	0.48426	158.50
	S4^{B}H---S4^{A}	1.38878	1.38182	0.00696	2.71140	0.28860	163.82
	N3^{A}H---O1^{A}	1.00871	1.00967	-0.00096	2.23043	0.48957	153.68
CON21	**N3^{A}H---N3^{B}**	1.02425	1.01118	0.01307	2.04271	0.70729	153.78
	S4^{B}H---N3^{A}	1.40775	1.38182	0.02593	2.10148	0.64852	158.83
	C5^{B}H---O2^{A}	1.08057	1.08041	0.00016	3.03482	-0.31482	123.02
	O1^{A}H---S4^{A}	0.98356	0.97741	0.00615	2.35182	0.64818	139.13
CON22	**C5^{A}H---N3^{B}**	1.08377	1.08461	-0.00084	2.44667	0.30333	156.78
	C5^{B}H---N3^{A}	1.08283	1.08041	0.00242	2.51929	0.23071	149.79
	O1^{A}H---S4^{A}	0.98686	0.97741	0.00945	2.25818	0.74182	148.51
	N3^{A}H---O2^{A}	1.01349	1.00967	0.00382	2.15700	0.56300	111.10

Table 2.1.2.1. (Continued)

CON23	**$C5^{A}H---N3^{B}$**	1.08443	1.08461	-0.00018	2.30189	0.44811	174.49
	$S4^{B}H---S4^{A}$	1.38300	1.38182	0.00118	3.44653	-0.44653	170.16
	$C5^{B}H---N3^{A}$	1.08294	1.08041	0.00253	2.52671	0.22329	152.94
	$O1^{A}H---S4^{A}$	0.98290	0.97741	0.00549	2.39478	0.60522	136.24
CON24	**$O1^{A}H---N3^{B}$**	1.02199	0.97741	0.04458	1.67592	1.07408	178.63
	$C5^{B}H---O2^{A}$	1.08126	1.08041	0.00085	2.33859	0.38141	137.33
	$N3^{A}H---O2^{A}$	1.01072	1.01118	-0.00046	2.20722	0.51278	108.54
	$S4^{A}H---N3^{A}$	1.39186	1.38314	0.00872	2.32651	0.42349	114.13
CON25	**$O1^{A}H---N3^{B}$**	1.02337	0.97741	0.04596	1.68092	1.06908	178.93
	$C5^{B}H---O2^{A}$	1.08114	1.08041	0.00073	2.31748	0.40252	137.33
	$N3^{A}H---O2^{A}$	1.00894	1.01118	-0.00224	2.19746	0.52254	108.56
	$S4^{A}H---O1^{A}$	1.38112	1.38314	-0.00202	2.29619	0.42381	123.80
CON26	**$C5^{A}H---N3^{B}$**	1.08507	1.08659	-0.00152	2.40489	0.34511	145.10
	$S4^{B}H---N3^{A}$	1.42058	1.38182	0.03876	1.99246	0.75754	174.38
	$C5^{B}H---O1^{A}$	1.08081	1.08041	0.00040	2.91322	-0.19322	124.51
	$O1^{A}H---S4^{A}$	0.98663	0.97741	0.00922	2.23647	0.76353	150.58
	$N3^{A}H---O1^{A}$	1.01618	1.01118	0.00500	2.16316	0.55684	110.09
CON27	**$C5^{A}H---N3^{B}$**	1.08599	1.08461	0.00138	3.06101	-0.31101	126.14
	$N3^{A}H---N3^{B}$	1.02165	1.01118	0.01047	2.11962	0.63038	162.00
	$S4^{B}H---S4^{A}$	1.38708	1.38000	0.00708	2.85863	0.14137	165.73
	$C5^{B}H---O1^{A}$	1.08092	1.08041	0.00051	2.82039	-0.10039	146.98
	$O1^{A}H---N3^{A}$	1.00369	0.97741	0.02628	1.83183	0.91817	125.34

During the process of the formation of X-H---Y H-bond, electrons transfer happened between X-H donor and Y acceptor group result in the shortening of H---Y bond length. The shorter H---Y bond length is, the stronger the interaction is, and vice versa. H---Y bond length $O1^{A}H---N3^{B}$ (1.66649 A°, **CON2**), $O1^{A}H---N3^{B}$ (1.67592 A°, **CON24**), $O1^{A}H---N3^{B}$ (1.68092 A°, **CON25**), respectively. In addition, the complexes of **CON3**, **CON5**, **CON15**, **CON16**, and **CON26** have lower the length of hydrogen bonding. H-bonds are the shortest ones, which indicate that the strength of

H-bonds should be the strongest. The corresponding $\Delta R_{X\text{---}H}$ and $\delta R_{Y\text{- - -}H}$ have high values in these complexes, as well.

2.1.3. QTAIM Analysis

The QTAIM was used here to deepen the nature of the hydrogen bonding interactions. The electronic topological properties at H---Y BCPs of inter-molecular H-bonds including electron density ρ_b, the Laplacian of the electron density $\nabla^2_{\rho b}$, and the electron energy density H_b of all complexes were listed in **Table 2.1.3.1.**.

2.1.3.1. Electron Density

It has been indicated very often that the electron density at the H---Y BCP ρ_b is a good measure of H-bond strength. The shorter H---Y distance corresponds to the stronger H-bond and in consequence is characterized by the greater electron density at the corresponding H---Y BCP. Two quantitative criteria proposed by Koch and Popelier usually are used to characterize the strength of a H-bond, ρ_b and its Laplacian $\nabla^2_{\rho b}$, in the range of 0.002–0.035 and 0.024–0.139 a.u. [22], respectively, which is markedly lower than for a covalent bond. As shown in **Table 2.1.3.1.**, for all complexes, most of ρ_b values are within this range. The ρ_b values of $O1^AH\text{---}N3^B$ (0.05955, **CON2**), $O1^AH\text{---}N3^B$ (0.05812, **CON24**), $O1^AH\text{---}N3^B$ (0.05752, **CON25**), respectively. The ccomplexes of **CON3**, **CON5**, **CON15**,

Table 2.1.3.1. The densities of inter-molecular and intra-molecular H-bonds in Cys-2mpym complexes.

COMPLEXES	H-BOND	ρ_b	V_b	G_b	H_b	$\nabla^2_{\rho b}$
CON1	**S4^{A}H---N3^B**	0.02476	-0.01631	0.01761	0.00131	0.07569
	S4^{B}H---O2^A	0.01928	-0.01443	0.01687	0.00244	0.07722
CON2	**O1^{A}H---N3^B**	0.05955	-0.05731	0.04415	-0.01316	0.12397
	S4^{B}H---O2^A	0.03565	-0.02891	0.02893	0.00002	0.11579
CON3	**S4^{A}H---N3^B**	0.03043	-0.02137	0.02178	0.00042	0.08880
	S4^{B}H---N3^A	0.04576	-0.03585	0.03041	-0.00544	0.09988
CON4	**N3^{A}H---N3^B**	0.02278	-0.01584	0.01785	0.00202	0.07947
	S4^{B}H---O1^A	0.01675	-0.01182	0.01304	0.00122	0.05702
CON5	**O1^{A}H---N3^B**	0.04528	-0.04134	0.03581	-0.00553	0.12110
	S4^{B}H---S4^A	0.01520	-0.00798	0.00876	0.00078	0.03818
CON6	**O1^{A}H---S4^B**	0.01761	-0.01035	0.01119	0.00085	0.04816
	S4^{A}H---O2^A	0.00859	-0.00576	0.00656	0.00080	0.02945
CON7	**C5^{A}H---S4^B**	0.00175	-0.00066	0.00112	0.00046	0.00632
	N3^{A}H---S4^B	0.00525	-0.00225	0.00321	0.00096	0.01666
	S4^{B}H---O2^A	0.01035	-0.00700	0.00828	0.00127	0.03818
CON8	**S4^{A}H---N3^B**	0.02995	-0.02096	0.02149	0.00053	0.08808
	S4^{B}H---S4^A	0.00548	-0.00278	0.00387	0.00109	0.01985
	C5^{B}H---O2^A	0.01280	-0.00871	0.01077	0.00206	0.05133
CON9	**N3^{A}H---N3^B**	0.02049	-0.01378	0.01589	0.00212	0.07204
	S4^{B}H---S4^A	0.00989	-0.00479	0.00579	0.00100	0.02716
	C5^{B}H---O1^A	0.00545	-0.00335	0.00408	0.00073	0.01925
CON10	**N3^{A}H---N3^B**	0.02139	-0.01458	0.01670	0.00212	0.07530
	S4^{B}H---O1^A	0.01623	-0.01143	0.01266	0.00124	0.05558
	S4^{A}H---O2^A	0.01039	-0.00711	0.00808	0.00097	0.03620
CON11	**S4^{A}H---N3^B**	0.02298	-0.01470	0.01615	0.00145	0.07040
	S4^{B}H---O2^A	0.02056	-0.01598	0.01888	0.00290	0.08714
	O1^{A}H---N3^A	0.03960	-0.03475	0.03255	-0.00220	0.12142
CON12	**N3^{A}H---N3^B**	0.02159	-0.01467	0.01670	0.00203	0.07490
	S4^{B}H---O2^A	0.02035	-0.01495	0.01707	0.00212	0.07675
	S4^{A}H---O1^A	0.01363	-0.00951	0.01069	0.00118	0.04749
CON13	**N3^{A}H---N3^B**	0.02221	-0.01523	0.01722	0.00199	0.07682
	S4^{B}H---O2^A	0.02268	-0.01725	0.01957	0.00232	0.08755
	O1^{A}H---S4^A	0.02155	-0.01413	0.01435	0.00022	0.05830
CON14	**N3^{A}H---S4^B**	0.00596	-0.00269	0.00378	0.00109	0.01948
	S4^{B}H---O2^A	0.00696	-0.00465	0.00587	0.00122	0.02834
	S4^{A}H---O1^A	0.01235	-0.00846	0.00944	0.00098	0.04166

Table 2.1.3.1. (Continued)

CON15	**N3^{A}H---N3^{B}**	0.02250	-0.01539	0.01739	0.00200	0.07754
	S4^{B}H---N3^{A}	0.03879	-0.02938	0.02674	-0.00264	0.09638
	S4^{A}H---O2^{A}	0.00845	-0.00569	0.00651	0.00083	0.02936
CON16	**N3^{A}H---N3^{B}**	0.02194	-0.01488	0.01697	0.00209	0.07624
	S4^{B}H---N3^{A}	0.03899	-0.02947	0.02687	-0.00260	0.09709
	S4^{A}H---O1^{A}	0.01428	-0.01004	0.01131	0.00128	0.05037
CON17	**N3^{A}H---N3^{B}**	0.02162	-0.01454	0.01655	0.00201	0.07423
	S4^{B}H---O1^{A}	0.01442	-0.00966	0.01032	0.00066	0.04393
	O1^{A}H---N3^{A}	0.04599	-0.04195	0.03670	-0.00525	0.12581
CON18	**N3^{A}H---N3^{B}**	0.01586	-0.00964	0.01176	0.00212	0.05554
	S4^{B}H---O1^{A}	0.01470	-0.01019	0.01121	0.00102	0.04892
	S4^{A}H---N3^{A}	0.02205	-0.01438	0.01510	0.00072	0.06325
CON19	**N3^{A}H---N3^{B}**	0.02085	-0.01398	0.01605	0.00207	0.07244
	S4^{B}H---S4^{A}	0.00587	-0.00266	0.00355	0.00088	0.01772
	S4^{A}H---O1^{A}	0.01259	-0.00865	0.00971	0.00106	0.04311
CON20	**N3^{A}H---N3^{B}**	0.01603	-0.00973	0.01174	0.00201	0.05500
	S4^{B}H---S4^{A}	0.01205	-0.00607	0.00705	0.00098	0.03211
	N3^{A}H---O1^{A}	0.01617	-0.01283	0.01624	0.00341	0.07857
CON21	**N3^{A}H---N3^{B}**	0.02623	-0.01930	0.02099	0.00170	0.09077
	S4^{B}H---N3^{A}	0.02668	-0.01769	0.01811	0.00043	0.07416
	C5^{B}H---O2^{A}	0.00261	-0.00156	0.00217	0.00061	0.01114
	O1^{A}H---S4^{A}	0.02250	-0.01495	0.01496	0.00001	0.05988
CON22	**C5^{A}H---N3^{B}**	0.01175	-0.00642	0.00775	0.00134	0.03637
	C5^{B}H---N3^{A}	0.01181	-0.00656	0.00733	0.00077	0.03238
	O1^{A}H---S4^{A}	0.02699	-0.01895	0.01772	-0.00123	0.06594
	N3^{A}H---O2^{A}	0.02048	-0.01602	0.01891	0.00289	0.08718
CON23	**C5^{A}H---N3^{B}**	0.01549	-0.00902	0.01091	0.00189	0.05120
	S4^{B}H---S4^{A}	0.00257	-0.00096	0.00152	0.00055	0.00827
	C5^{B}H---N3^{A}	0.01176	-0.00649	0.00727	0.00077	0.03216
	O1^{A}H---S4^{A}	0.02063	-0.01334	0.01373	0.00039	0.05648
CON24	**O1^{A}H---N3^{B}**	0.05812	-0.05586	0.04366	-0.01220	0.12583
	C5^{B}H---O2^{A}	0.01282	-0.00818	0.00964	0.00146	0.04441
	N3^{A}H---O2^{A}	0.01878	-0.01502	0.01786	0.00284	0.08278
	S4^{A}H---N3^{A}	0.01975	-0.01266	0.01349	0.00083	0.05726
CON25	**O1^{A}H---N3^{B}**	0.05752	-0.05494	0.04306	-0.01188	0.12471
	C5^{B}H---O2^{A}	0.01336	-0.00859	0.01014	0.00155	0.04678
	N3^{A}H---O2^{A}	0.01927	-0.01559	0.01852	0.00293	0.08577
	S4^{A}H---O1^{A}	0.01553	-0.01106	0.01239	0.00133	0.05487

Table 2.1.3.1. (Continued)

CON26	**$C5^{A}H---N3^{B}$**	0.01334	-0.00745	0.00899	0.00154	0.04210
	$S4^{B}H---N3^{A}$	0.03496	-0.02488	0.02321	-0.00168	0.08611
	$C5^{B}H---O1^{A}$	0.00393	-0.00243	0.00311	0.00068	0.01514
	$O1^{A}H---S4^{A}$	0.02802	-0.02001	0.01843	-0.00158	0.06743
	$N3^{A}H---O1^{A}$	0.02008	-0.01569	0.01868	0.00299	0.08668
CON27	**$C5^{A}H---N3^{B}$**	0.00405	-0.00216	0.00275	0.00059	0.01335
	$N3^{A}H---N3^{B}$	0.02203	-0.01492	0.01684	0.00192	0.07506
	$S4^{B}H---S4^{A}$	0.00909	-0.00429	0.00526	0.00097	0.02496
	$C5^{B}H---O1^{A}$	0.00458	-0.00269	0.00333	0.00064	0.01588
	$O1^{A}H---N3^{A}$	0.04502	-0.04084	0.03613	-0.00471	0.12569

CON16, and **CON26** provide the same criterias according to table. H-bonds are excess of the range, which indicates that a partial covalent character is attributed to the H-bonds. Generally, the $\boldsymbol{\rho_b}$ decreases as a result of the lengthening of the corresponding bond. The opposite occurs when the bond length shorten. As pointed out by Galvez et al. [95], the linear behavior between the density and the H-bond length is only held in the neighborhood of equilibrium, whereas the density $\boldsymbol{\rho_b}$ decays exponentially in the long range. Because of different atoms as H-acceptor in different H-bonds, H---Y bond distance cannot be used directly, so a H-bond parameter, $\boldsymbol{\delta R_{Y\cdots H}}$ [96], is defined as

$$\boldsymbol{\delta R_{Y\cdots H} = R_H^{vDW} + R_Y^{vDW} - R_{H\cdots Y}} \qquad \textbf{(1)}$$

where $\boldsymbol{R_H^{vDW}}$ and $\boldsymbol{R_Y^{vDW}}$ are van der Waals radii of H and Y atoms given by Bondi [97], respectively.

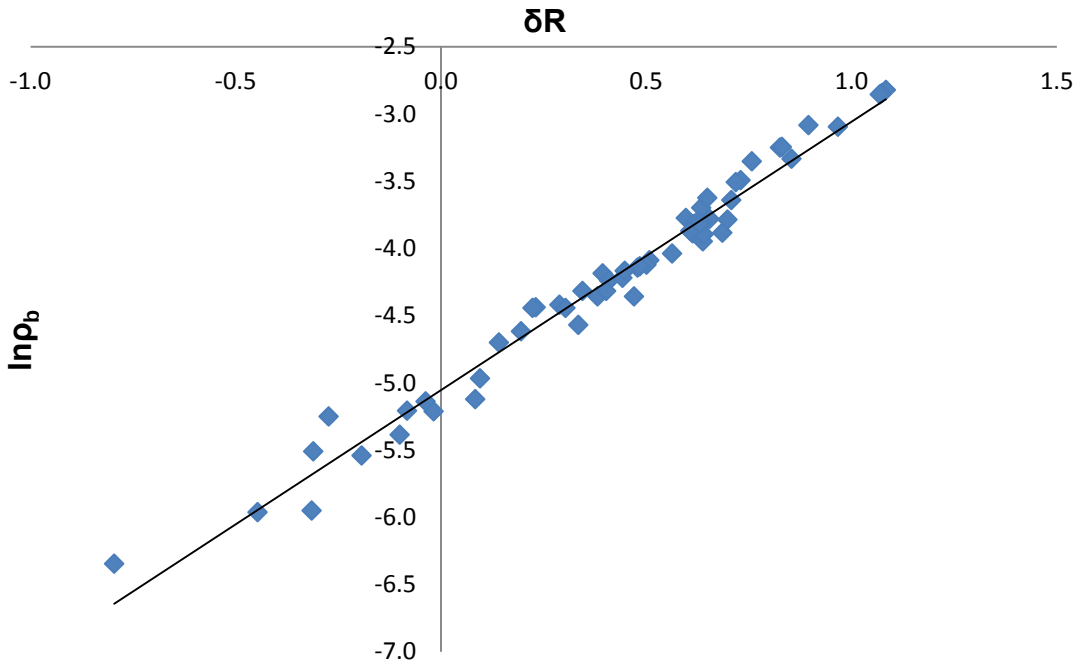

Figure 2.1.3.1.1. Correlation between the electron density ρ_b at the BCPs in the logarithmic value $\ln\rho_b$ and the H-bond parameter **δR.**

To understand the nature of H-bond with the density properties at BCPs, a linear regression analysis between the logarithmic plot $\ln\rho_b$ and $\delta R_{Y\cdots H}$ was carried out, the fitted curve was shown in **Figure 2.1.3.1.1.**, and a good linear relationship can be expressed as

$$\ln\rho_b = 1.9971\delta R - 5.0523 \qquad R = 0.9755 \qquad (2)$$

2.1.3.2. Electron Energy Density

The Laplacian of the electron density $\nabla^2_{\rho b}$ another important topological property which can be used to estimate H-bonds. According to QTAIM, the closed shell interactions (e.g., ionic bonds, H-bonds, and van der

Waals interactions) correspond to a positive value at BCP, $\nabla^2_{\rho b}$ whereas for covalent bonds, the $\nabla^2_{\rho b}$ has a negative value [19, 20]. There is a well-known relationship resulting from the virial theorem between $\nabla^2_{\rho b}$ and energetic properties of BCP:

$$¼\,\nabla^2_{\rho b} = 2G_b + V_b \quad (3)$$

$$H_b = G_b + V_b \quad (4)$$

where G_b (always positive) and V_b (always negative) are the kinetic and potential energy densities, respectively, and H_b is the total energy density. The sign of H_b will depend on which contribution, potential or kinetic, will locally prevail on the BCP. $H_b < 0$ reflects a prevalence of the potential energy, which is a consequence of the stabilization of the accumulated electron charge, a typical feature of covalent interactions [98, 99]. In this way, a partial covalent character is attributed to the H-bonds exhibiting $H_b < 0$ Moreover, the $\nabla^2_{\rho b}$ at BCP is low and positive, which is typical of closed shell interactions. Therefore, $\nabla^2_{\rho b}$ and H_b at H---Y BCP can be used as criteria to characterize H-bonds. Koch and Popelier [22] proposed for weak and medium H-bonds that both $\nabla^2_{\rho b}$ and $H_b > 0$; for strong H-bonds it is: $\nabla^2_{\rho b} > 0$ and $H_b < 0$, whereas for very strong ones both $\nabla^2_{\rho b}$ and $H_b < 0$. The latter are usually classified as covalent in nature. This classification shows that weak H-bonds eventually merge with (weaker) van der Waals interactions, whereas strong H-bonds merge, at the other end of the continuum, with covalent and polar bonds. According to the criteria of H-bonds proposed by

Koch and Popelier [20], all H-bonds have positive $\nabla^2_{\rho b}$ values and fall within the 0.024–0.139 a.u. range. As shown in **Table 2.1.3.1.**, the values of $\nabla^2_{\rho b}$ (0.12397, 0.12583, 0.12471) of $O1^AH\text{---}N3^B$ H-bonds in **CON2, CON24, CON25** are the biggest ones among complexes, and there are the smallest values of $\mathbf{H_b}$ (-0.01316, -0.01220, -0.01188) of $O1^AH\text{---}N3^B$ H-bonds in **CON2, CON24, CON25**, respectively.The complexes of **CON3**, **CON5**, **CON15**, **CON16**, and **CON26** have similar stronger H-bons. In addition, other H-bonds of these complexes have positive $\mathbf{H_b}$ values. According to **Table 2.1.3.1.**, other inter-molecular H-bonds in complexes have highly positive and low negative or fully positive of the $\mathbf{H_b}$ values and are weak H-bonds according to above criteria. Because both the bond distance and electron energy density are relate to the strength of H-bond, the relationship between $\nabla^2_{\rho b}$ and $R_{H\text{-}\cdots\text{-}Y}$ was also investigated. Because of different atoms as H-acceptor in different H-bonds, **δR** defined in Equation (2) was used to replace $R_{H\text{-}\cdots\text{-}Y}$ for regression analysis, a linear relationship between the logarithmic $\nabla^2_{\rho b}$ and **δR** can be expressed as follows:

$$\ln\nabla^2_{\rho b} = 1.8227\delta R - 3.8209 \qquad R = 0.9748 \qquad (5)$$

The fitted curve was shown in **Figure 2.1.3.2.1.**. Thus, the estimate results of the strength of H-bonds by QTAIM are consistent with those by bond lengths analysis.

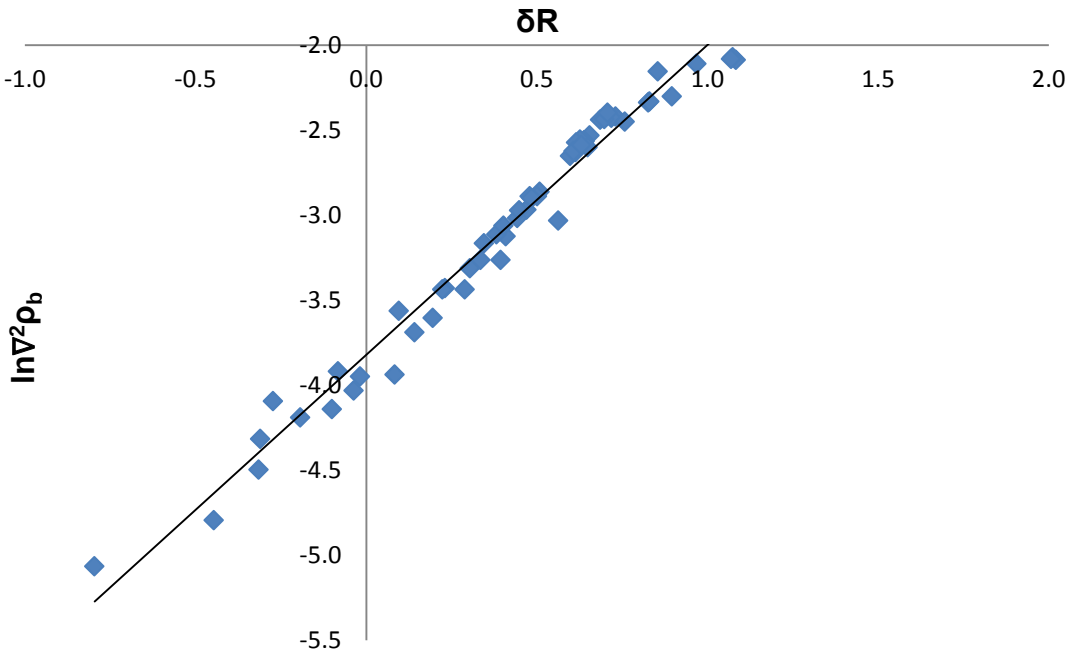

Figure 2.1.3.2.1. Correlation between the logarithmic Laplacian of the electron density at the BCPs of H-bonds $\mathbf{ln\nabla^2_{\rho b}}$ and H-bond parameter **δR**.

2.1.4. NBO Analysis and Energy

The NBO analysis was also performed here to deepen the nature of H-bonds. The results of NBO analysis were shown in **Table 2.1.4.1.**. As shown in **Table 2.1.4.1.**, the O (and S) atom involved in H-bond has two branches: one has sp hybrid characteristics, and the other one has more p hybrid characteristics; they correspond to two **E(2)** values, respectively. In contrast to the O (S) atoms, the N atom shows p characteristics in H-bonds. Thereby, the O (S) atoms exhibit more flexibility (less anisotropic) than the N atom in H-bond. The three largest **E(2)** value of **38.24, 36.81,** and **36.58** kcal/mol are found for the $O1^{A}H\text{---}N3^{B}$ H-bond in **CON2**, **CON24**, and **CON25**, respectively, which indicates the strongest charge-transfer effect

happened to them. The sum of **E(2)** values of both S(sp) and S(p) branch for **$N3^{A}H$---$S4^{B}$** inter-molecular H-bond in **CON7** and **CON14** are **0.70** and **1.06** kcal/mol ,respectively, which are bigger than other H-bonds. In addition, the relationship between **E(2)** and **ρ_b** was also investigated because **E(2)** is responsible for the strength of H-bond, and the **E(2) ~ ρ_b** correlation was plotted in **Figure 2.1.4.1.**. As shown in **Figure 2.1.4.1.**, **E(2)** linearly depend on **ρ_b** as well, and the regression equations for the H-bonds involving O, N and S atom as H-acceptor, respectively, are expressed as

$E(2) = 400.37\rho_b - 2.7540$ **R = 0.9351** **(6)**

$E(2) = 750.83\rho_b - 8.9365$ **R = 0.9726** **(7)**

$E(2) = 615.15\rho_b - 2.7299$ **R = 0.9756** **(8)**

Figure 2.1.4.1. (Continued)

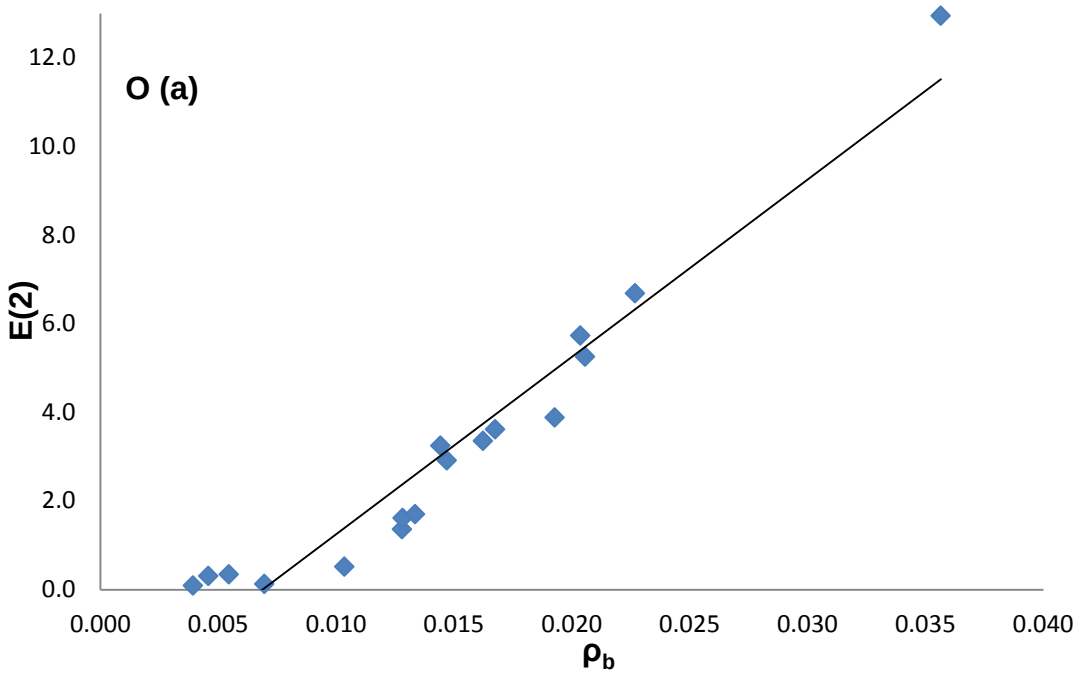

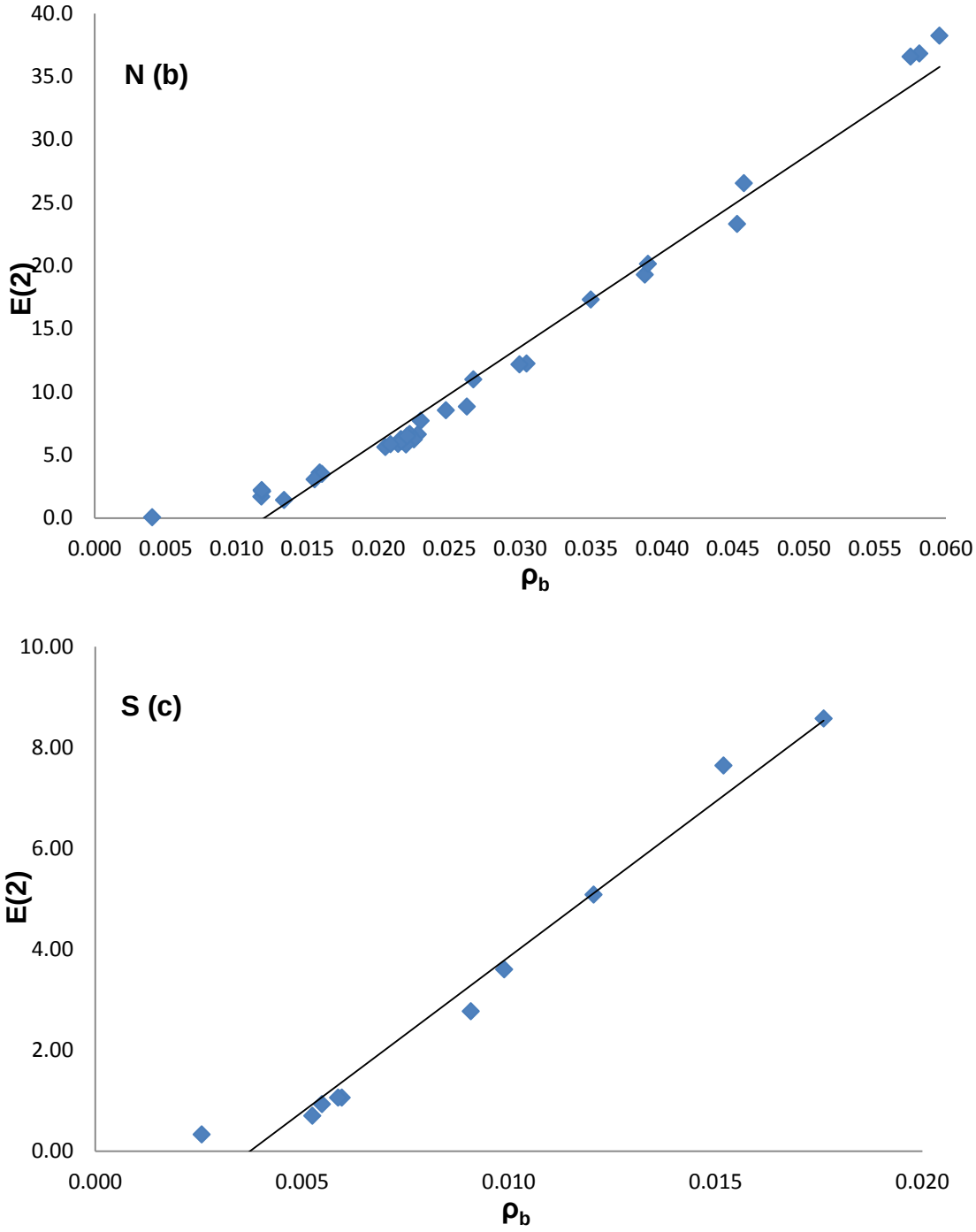

Figure 2.1.4.1. Correlation between the sum of second perturbation energies **E(2)** (the sum of sp and p branch, in kcal/mol for O and S atoms) and the electron density ρb at BCPs of H-bonds. **(a)** O atom, **(c)** N atom, and **(b)** S atom as H-acceptor.

Table 2.1.4.1. Natural bond orbital analysis of hydrogen bonds. (E(2): kcal/mol)[a].

COMPLEXES	H-BOND	H Acceptor		E(2)	COMPLEXES	H-BOND	H Acceptor		E(2)
	Bond---L.Pair	S	P			Bond---L.Pair	S	P	
CON1	$S4^{A}H---N3^{B}$	28.53	71.47	**8.53**	CON14	$N3^{A}H---S4^{B}$	71.23	28.77	**0.18**
	$S4^{B}H---O2^{A}$	61.85	38.15	**3.68**			0.00	100.00	**0.88**
		0.05	99.95	**0.20**		$S4^{B}H---O2^{A}$	61.87	38.13	**0.12**
CON2	$O1^{A}H---N3^{B}$	27.60	72.40	**38.24**		$S4^{A}H---O1^{A}$	0.04	99.96	**0.75**
	$S4^{B}H---O2^{A}$	2.40	97.60	**12.94**	CON15	$N3^{A}H---N3^{B}$	28.26	71.74	**6.22**
CON3	$S4^{A}H---N3^{B}$	28.43	71.57	**12.25**		$S4^{B}H---N3^{A}$	13.59	86.41	**19.29**
	$S4^{B}H---N3^{A}$	17.30	82.70	**26.53**	CON16	$N3^{A}H---N3^{B}$	28.27	71.73	**5.83**
CON4	$N3^{A}H---N3^{B}$	28.36	71.64	**6.63**		$S4^{B}H---N3^{A}$	14.37	85.63	**20.14**
	$S4^{B}H---O1^{A}$	45.93	54.07	**3.15**		$S4^{A}H---O1^{A}$	45.88	54.12	**0.95**
		0.02	99.98	**0.46**	CON17	$N3^{A}H---N3^{B}$	28.40	71.60	**6.09**
CON5	$O1^{A}H---N3^{B}$	27.93	72.07	**23.31**		$S4^{B}H---O1^{A}$	45.99	54.01	**0.39**
	$S4^{B}H---S4^{A}$	70.60	29.40	**0.79**			0.33	99.67	**2.85**
		3.20	96.80	**6.85**		$O1^{A}H---N3^{A}$	10.40	89.60	**17.08**
CON6	$O1^{A}H---S4^{B}$	71.45	28.55	**1.44**	CON18	$N3^{A}H---N3^{B}$	28.60	71.40	**3.60**
		0.31	99.69	**7.13**		$S4^{B}H---O1^{A}$	45.77	54.23	**2.13**
CON7	$N3^{A}H---S4^{B}$	0.00	100.00	**0.70**			0.18	99.82	**0.78**
	$S4^{B}H---O2^{A}$	62.17	37.83	**0.51**		$S4^{A}H---N3^{A}$	8.32	91.68	**4.68**
CON8	$S4^{A}H---N3^{B}$	28.31	71.69	**12.18**	CON19	$N3^{A}H---N3^{B}$	28.37	71.63	**5.85**
	$S4^{B}H---S4^{A}$	0.70	99.30	**0.93**		$S4^{B}H---S4^{A}$	73.09	26.91	**0.24**
	$C5^{B}H---O2^{A}$	61.73	38.27	**1.36**			0.38	99.62	**0.82**
CON9	$N3^{A}H---N3^{B}$	28.39	71.61	**5.62**		$S4^{A}H---O1^{A}$	45.84	54.16	**0.63**
	$S4^{B}H---S4^{A}$	72.73	27.27	**0.36**			0.11	99.89	**0.62**
		2.21	97.79	**3.24**	CON20	$N3^{A}H---N3^{B}$	28.63	71.37	**3.48**
	$C5^{B}H---O1^{A}$	46.20	53.80	**0.15**		$S4^{B}H---S4^{A}$	70.84	29.16	**0.48**
		0.00	100.00	**0.19**			3.72	96.28	**4.60**
CON10	$N3^{A}H---N3^{B}$	28.39	71.61	**5.86**	CON21	$N3^{A}H---N3^{B}$	28.07	71.93	**8.84**
	$S4^{B}H---O1^{A}$	46.08	53.92	**3.35**		$S4^{B}H---N3^{A}$	13.71	86.29	**10.99**
CON11	$S4^{A}H---N3^{B}$	28.59	71.41	**7.71**		$O1^{A}H---S4^{A}$	73.25	26.75	**0.51**
	$S4^{B}H---O2^{A}$	61.54	38.46	**5.25**			1.22	98.78	**9.36**
	$O1^{A}H---N3^{A}$	13.44	86.56	**12.38**	CON22	$C5^{A}H---N3^{B}$	28.65	71.35	**1.70**
CON12	$N3^{A}H---N3^{B}$	28.39	71.61	**6.25**		$C5^{B}H---N3^{A}$	12.48	87.52	**2.12**
	$S4^{B}H---O2^{A}$	61.82	38.18	**3.35**		$O1^{A}H---S4^{A}$	70.11	29.89	**0.62**
		0.20	99.80	**2.38**			4.35	95.65	**13.60**
	$S4^{A}H---O1^{A}$	45.71	54.29	**0.74**		$N3^{A}H---O2^{A}$	0.05	99.95	**1.63**
		0.03	99.97	**0.59**	CON23	$C5^{A}H---N3^{B}$	28.50	71.50	**3.06**
CON13	$N3^{A}H---N3^{B}$	28.38	71.62	**6.65**		$S4^{B}H---S4^{A}$	73.45	26.55	**0.06**
	$S4^{B}H---O2^{A}$	61.32	38.68	**4.42**			0.86	99.14	**0.27**
		0.37	99.63	**2.26**		$C5^{B}H---N3^{A}$	16.26	83.74	**2.21**
	$O1^{A}H---S4^{A}$	0.91	99.09	**8.55**		$O1^{A}H---S4^{A}$	0.86	99.14	**7.82**

Table 2.1.4.1. (Continued)

COMPLEXES	H-BOND	H Acceptor		E(2)	COMPLEXES	H-BOND	H Acceptor		E(2)
	Bond---L.Pair	S	P			Bond---L.Pair	S	P	
CON24	**$O1^{A}H---N3^{B}$**	27.53	72.47	**36.81**	CON26	**$C5^{A}H---N3^{B}$**	28.53	71.47	**1.42**
	$C5^{B}H---O2^{A}$	62.61	37.39	**0.53**		**$S4^{B}H---N3^{A}$**	14.70	85.30	**17.32**
		0.00	1.00	**1.08**		**$C5^{B}H---O1^{A}$**	0.01	99.99	**0.09**
	$N3^{A}H---O2^{A}$	0.00	1.00	**1.15**		$O1^{A}H---S4^{A}$	69.69	30.31	**0.64**
	$S4^{A}H---N3^{A}$	10.00	90.00	**3.75**			4.81	95.19	**14.19**
CON25	**$O1^{A}H---N3^{B}$**	27.58	72.42	**36.58**		$N3^{A}H---O1^{A}$	0.05	99.95	**1.57**
	$C5^{B}H---O2^{A}$	62.71	37.29	**0.59**	CON27	**$C5^{A}H---N3^{B}$**	28.36	71.64	**0.06**
		0.00	1.00	**1.11**		**$N3^{A}H---N3^{B}$**			**6.49**
	$N3^{A}H---O2^{A}$	0.00	1.00	**1.15**		**$S4^{B}H---S4^{A}$**	1.16	98.84	**2.77**
	$S4^{A}H---O1^{A}$	39.05	60.95	**1.48**		**$C5^{B}H---O1^{A}$**	0.01	99.99	**0.30**
						$O1^{A}H---N3^{A}$	11.93	88.07	**16.53**

[a]*The values are O (or S) sp hybrid branch to form the Hbond; those in the H acceptor are O (or S) p hybrid branch. The lone pair of N atom is mainly of p character. See discussion in the text.*

Based on the NBO analysis, the binding energies $\Delta\mathbf{E}$ of Cys-2mpym complexes were decomposed into several terms and were summarized **Table 2.1.4.2.**. $\Delta\mathbf{E}$ can be decomposed as follows:

$$\Delta\mathbf{E} = \Delta\mathbf{E}_{\mathbf{prep}} + \Delta\mathbf{E}_{\mathbf{int}} \qquad \mathbf{(9)}$$

where the preparation energy $\Delta\mathbf{E}_{\mathbf{prep}}$ is the amount of energy required to deform the separate bases from their free monomer structure to the geometry that they acquire in the pair complex; the interaction energy $\Delta\mathbf{E}_{\mathbf{int}}$ represents the actual energy change when the prepared bases are combined to form the pair complex. In general, $\Delta\mathbf{E}_{\mathbf{prep}}$ is positive because the structural deformation brings the molecular energy to a higher energy level, whereas $\Delta\mathbf{E}_{\mathbf{int}}$ is a negative value unless the complex is unstable. According to NBO

theory [23], $\Delta \mathbf{E_{int}}$ is decomposed into the charge-transfer **(CT)** and noncharge-transfer **(NCT)** parts

$$\Delta \mathbf{E_{int}} = \Delta \mathbf{E_{NCT}} + \Delta \mathbf{E_{CT}} \quad \textbf{(10)}$$

where $\Delta \mathbf{E_{CT}}$ account for the orbital interaction and polarization interactions, $\Delta \mathbf{E_{NCT}}$ consists of the classical electrostatic interaction and the Pauli steric repulsion interaction. The $\Delta \mathbf{E_{CT}}$ term can be closely tracked by **E(2)** formula in introduction part of this working as proposed by Reed et al. [100]. To estimate the total **CT** effects between L-cysteine and 2-mercaptopyrimidine moiety in complexes, the $\Delta \mathbf{E_{CT}}$ terms were obtained by summarizing E(2) for inter-molecular H-bonds listed in **Table 2.1.4.1.**. In the NBO scheme, $\Delta \mathbf{E_{CT}}$ is negative because it is evaluated as the variational energy lowering because of expanding the variational space on each monomer to include unfilled orbitals on the other monomer. Thereby, $\Delta \mathbf{E_{NCT}}$ can be further calculated with Equation (10) and is positive as shown in **Table 2.1.4.2.**. As shown in **Table 2.1.4.2.**, the absolute values of $\Delta \mathbf{E_{CT}}$ in **CON2**, **CON24**, **CON3**, **CON25**, **CON5**, **CON16**, **CON15**, and **CON26** are the best values, respectively. The values of -13.85, -13.51, -11.15, -7.69, -6.58, and -4.92 kcal/mol in **CON24**, **CON2**, **CON25**, **CON3**, **CON15**, and **CON16**, have better binding energy, respectively and interaction energy of $\Delta \mathbf{E_{int}}$ in **CON2**, **CON25**, **CON24**, **CON5**, **CON3**, **CON15**, **CON16**, and **CON26** have good values. Between these complexes because of the higher $\Delta \mathbf{E_{prep}}$ (8.39, and 6.50 kcal/mol) in **CON5** and **CON26** indicating the serious structural deformation to form the complexes. Therefore, the $\Delta \mathbf{E_{prep}}$ is an important factor for the stability of

Table 2.1.4.2. Preparation energies ΔE_{prep}, interaction energies ΔE_{int}, binding energies ΔE, charge-transfer ΔE_{CT}, and noncharge-transfer energies ΔE_{NCT} in kcal/mol, also counterpoise corrected energy in hartrees of the L-cys-2mpym complexes.

COMPLEXES	ΔE_{prep}	ΔE_{int}	ΔE	ΔE_{CT}	ΔE_{NCT}	CP Corrected
CON1	0.80	-5.21	-4.41	-19.71	14.50	-1384.39740
CON2	2.79	-16.30	-13.51	-61.54	45.24	-1384.41190
CON3	1.71	-9.41	-7.69	-46.66	37.25	-1384.40263
CON4	0.34	-5.55	-5.20	-14.50	8.95	-1384.39866
CON5	8.39	-12.33	-3.94	-37.66	25.33	-1384.39665
CON6	0.16	-4.06	-3.90	-11.70	7.64	-1384.39658
CON7	1.42	-2.43	-1.00	-4.89	2.47	-1384.39196
CON8	2.44	-7.24	-4.80	-24.05	16.82	-1384.39802
CON9	0.92	-5.15	-4.23	-15.75	10.60	-1384.39711
CON10	3.21	-5.03	-1.82	-10.49	5.45	-1384.39327
CON11	0.24	-5.35	-5.11	-19.99	14.64	-1384.39852
CON12	1.67	-6.02	-4.34	-16.50	10.49	-1384.39729
CON13	5.89	-6.63	-0.74	-18.84	12.22	-1384.39154
CON14	2.06	-2.10	-0.04	-3.63	1.52	-1384.39043
CON15	0.77	-7.35	-6.58	-30.95	23.60	-1384.40085
CON16	2.16	-7.07	-4.92	-31.74	24.67	-1384.39821
CON17	2.08	-5.71	-3.63	-12.99	7.28	-1384.39615
CON18	1.05	-3.37	-2.32	-9.82	6.45	-1384.39407
CON19	3.27	-4.34	-1.08	-10.63	6.29	-1384.39209
CON20	3.10	-3.43	-0.33	-11.58	8.15	-1384.39089
CON21	5.69	-6.76	-1.07	-25.51	18.76	-1384.39207
CON22	5.12	-3.15	1.97	-7.02	3.88	-1384.38723
CON23	5.60	-3.71	1.89	-8.96	5.26	-1384.38735
CON24	0.52	-14.36	-13.85	-45.08	30.72	-1384.41243
CON25	3.24	-14.38	-11.15	-45.04	30.66	-1384.40813
CON26	6.50	-7.00	-0.50	-26.76	19.76	-1384.39116
CON27	0.42	-6.67	-7.09	-14.30	7.63	-1384.40167

complexes except for H-bonds. Additionally, the binding energy of **CON22** is much smaller than other complexes, which means the weakest hydrogen bonding interactions exist in **CON22**.

2.1.5. Vibrational Frequencies

The harmonic vibration frequencies of all inter-molecular H-bonds in complexes and monomers calculated at the B3LYP/6-311G level were given in **Table 2.1.5.1.**. Because of the concurrence of several inter- and intra-molecular H-bonds in one complex, the mixture of vibrational modes is unavoidable, so more than one X-H vibrational modes can be found for some H-bonds. **Table 2.1.5.1.** list one $\Delta\mathbf{v}$ value for the change of O-H in L-cysteine also one S-H in Both L-cysteine and 2-mercaptopyrimidine as stretching vibrational mode. As to N-H and C-H group, symmetric and asymmetric stretching vibration were found and listed in **Table 2.1.5.1.**, respectively.

The change of the stretching frequency is usually used to estimate the strength of H-bond. Compared with free monomer, most of stretching frequencies associated with H-bond in complexes shift to lower frequencies.

The $O_1{}^AH$ stretching frequency of $O_1{}^AH\text{---}N^B$ H-bond in **CON2, CON24,** and **CON25** have the largest shift values with 971.44, 894.01, and 912.74 cm^{-1}, respectively, which indicate that the $O_1{}^AH\text{---}N^B$ H-bond in **CON2,**

Table 2.1.5.1. The ν_{X---H} stretching frequency , I intensity, and S kind of symmetry of inter-molecular H-bonds in complexes and monomers (frequency in cm^{-1} and intensity in km/mol).

COMPLEXES	H-BOND	ν_{X---H}	I	Δν	S	COMPLEXES	H-BOND	ν_{X---H}	I	Δν	S
CON1	**$S4^AH---N3^B$**	2272.58	384.71	-190.12		CON14	**$N3^AH---S4^B$**	3677.18	36.97	33.64	A
	$S4^BH---O2^A$	2436.40	154.12	-41.76				3545.26	75.99	24.54	S
CON2	**$O1^AH---N3^B$**	2662.05	2787.33	-971.44			**$S4^BH---O2^A$**	2500.01	4.13	21.85	
	$S4^BH---O2^A$	2187.68	535.56	-290.48			$S4^AH---O1^A$	2464.75	5.87	2.05	
CON3	**$S4^AH---N3^B$**	2177.07	718.07	-285.63		CON15	**$N3^AH---N3^B$**	3567.33	30.24	-76.21	A
	$S4^BH---N3^A$	1890.30	1177.24	-587.86				3362.08	195.66	-158.64	S
CON4	**$N3^AH---N3^B$**	3605.04	66.42	-38.50	A		**$S4^BH---N3^A$**	2023.66	978.44	-454.50	
		3425.24	388.72	-95.48	S		$S4^AH---O2^A$	2463.02	7.95	0.32	
	$S4^BH---O1^A$	2424.08	86.38	-54.08		CON16	**$N3^AH---N3^B$**	3554.10	26.50	-89.44	A
CON5	**$O1^AH---N3^B$**	3069.75	1128.47	-563.74				3371.23	188.78	-149.49	S
	$S4^BH---S4^A$	2343.79	232.99	-134.37			**$S4^BH---N3^A$**	2012.55	981.66	-465.61	
CON6	**$O1^AH---S4^B$**	3454.85	759.29	-178.64			$S4^AH---O1^A$	2466.73	2.02	4.03	
	$S4^AH---O2^A$	2462.98	8.71	0.28		CON17	**$N3^AH---N3^B$**	3614.55	67.79	-28.99	A
CON7	**$C5^AH---S4^B$**	3155.47	5.71	-9.54	A			3416.08	337.90	-104.64	S
		3086.74	9.99	-2.31	S		**$S4^BH---O1^A$**	2443.03	55.45	-35.13	
	$N3^AH---S4^B$	3699.51	30.67	55.97	A		$O1^AH---N3^A$	3136.09	217.78	-497.40	
		3556.33	39.60	35.61	S	CON18	**$N3^AH---N3^B$**	3641.80	77.91	-1.74	A
	$S4^BH---O2^A$	2480.00	17.11	1.84				3511.25	200.61	-9.47	S
CON8	**$S4^AH---N3^B$**	2204.25	559.35	-258.45			**$S4^BH---O1^A$**	2438.81	50.81	-39.35	
	$S4^BH---S4^A$	2449.37	10.27	-28.79			$S4^AH---N3^A$	2369.69	30.27	-93.01	
	$C5^BH---O2^A$	3188.87	19.55	-2.88	A	CON19	**$N3^AH---N3^B$**	3612.25	55.81	-31.29	A
		3163.38	2.81	-23.40	S			3447.76	269.16	-72.96	S
CON9	**$N3^AH---N3^B$**	3676.34	56.57	32.80	A		**$S4^BH---S4^A$**	2443.25	22.79	-34.91	
		3476.20	260.98	-44.52	S		$S4^AH---O1^A$	2459.93	4.16	-2.77	
	$S4^BH---S4^A$	2407.50	76.85	-70.66		CON20	**$N3^AH---N3^B$**	3632.63	50.79	-10.91	A
	$C5^BH---O1^A$	3198.50	4.99	6.75	A			3487.06	149.26	-33.66	S
		3188.23	13.45	1.45	S		**$S4^BH---S4^A$**	2391.80	142.45	-86.36	
CON10	**$N3^AH---N3^B$**	3612.65	90.24	-30.89	A		$N3^AH---O1^A$	3632.63	61.37	-10.91	A
		3453.98	288.81	-66.74	S			3487.06	149.26	-33.66	S
	$S4^BH---O1^A$	2423.83	85.25	-54.33		CON21	**$N3^AH---N3^B$**	3568.74	26.18	-74.80	A
	$S4^AH---O2^A$	2467.89	4.72	5.19				3334.42	316.77	-186.30	S
CON11	**$S4^AH---N3^B$**	2293.01	374.42	-169.69			**$S4^BH---N3^A$**	2190.98	466.91	-287.18	
	$S4^BH---O2^A$	2439.83	219.16	-38.33			**$C5^BH---O2^A$**	3194.27	7.24	2.52	A
	$O1^AH---N3^A$	3292.95	216.13	-340.54				3186.78	14.07	0.00	S
CON12	**$N3^AH---N3^B$**	3599.21	43.82	-44.33	A		$O1^AH---S4^A$	3465.67	221.65	-167.82	
		3417.92	293.70	-102.80	S	CON22	**$C5^AH---N3^B$**	3165.14	37.95	0.13	A
	$S4^BH---O2^A$	2407.47	185.52	-70.69				3085.26	9.16	-3.79	S
	$S4^AH---O1^A$	2466.94	4.11	-11.22			**$C5^BH---N3^A$**	3189.82	11.77	-1.93	A
CON13	**$N3^AH---N3^B$**	3593.22	39.04	-50.32	A			3159.07	12.56	-27.71	S
		3401.44	334.95	-119.28	S		$O1^AH---S4^A$	3392.74	357.37	-240.75	
	$S4^BH---O2^A$	2392.19	240.96	-85.97			$N3^AH---O2^A$	3628.50	15.47	-15.04	A
	$O1^AH---S4^A$	3473.30	215.28	-160.19				3502.56	27.18	-18.16	S

Table 2.1.5.1. (Continued)

COMPLEXES	H-BOND	$\nu_{X\cdots H}$	I	Δv	S	COMPLEXES	H-BOND	$\nu_{X\cdots H}$	I	Δv	S
CON23	**$C5^AH\cdots N3^B$**	3156.63	34.81	-11.82	A	CON26	**$C5^AH\cdots N3^B$**	3173.45	12.78	8.44	A
		3078.91	44.76	-15.53	S			3095.45	11.27	6.40	S
	$S4^BH\cdots S4^A$	2466.03	0.44	3.33			**$S4^BH\cdots N3^A$**	2068.60	760.49	-409.56	
	$C5^BH\cdots N3^A$	3188.73	11.74	23.72	A		**$C5^BH\cdots O1^A$**	3188.78	14.93	-2.97	A
		3159.41	47.73.86	70.36	S			3183.87	9.74	-2.91	S
	$O1^AH\cdots S4^A$	3483.85	163.74	-149.64			$O1^AH\cdots S4^A$	3391.63	399.21	-241.86	
CON24	**$O1^AH\cdots N3^B$**	2739.48	2596.85	-894.01			$N3^AH\cdots O1^A$	3598.32	13.60	-45.22	A
	$C5^BH\cdots O2^A$	3196.46	4.04	4.71	A			3474.09	19.63	-46.63	S
		3190.27	26.40	3.49	S	CON27	**$C5^AH\cdots N3^B$**	3168.45	11.58	3.44	A
	$N3^AH\cdots O2^A$	3660.87	16.44	17.33	A			3094.44	7.08	5.39	S
		3533.73	15.15	13.01	S		**$N3^AH\cdots N3^B$**	3607.76	39.83	-35.78	A
	$S4^AH\cdots N3^A$	2388.60	18.30	-74.10				3380.73	279.78	-139.99	S
CON25	**$O1^AH\cdots N3^B$**	2720.75	2605.57	-912.74			**$S4^BH\cdots S4^A$**	2415.18	51.68	-62.98	
	$C5^BH\cdots O2^A$	3197.22	3.15	5.47	A		**$C5^BH\cdots O1^A$**	3193.74	13.60	1.99	A
		3191.37	27.87	4.59	S			3187.10	2.37	0.32	S
	$N3^AH\cdots O2^A$	3681.02	16.37	37.48	A		$O1^AH\cdots N3^A$	3160.21	231.06	-473.28	
		3551.60	12.71	30.88	S	A - CYS	O1H	3633.49	33.97		
	$S4^AH\cdots O1^A$	2473.31	0.66	10.61			C5H	3165.01	2.44		A
B - 2-MPYM	S4H	2478.16	4.43					3089.05	3.92		S
	C5H	3191.75	21.98		A		S4H	2462.70	9.17		
		3186.78	6.94		S		N3H	3643.54	4.84		A
								3520.72	1.91		S

CON24 and **CON25** should be the strongest H-bonds among these complexes. The shift values of $S^BH\cdots N^A$ (**CON26, CON5, CON16, CON15,** and **CON3)** are between 250 and 600 cm^{-1}**,** and they can be considered as the stronger H-bonds, which is consistent with the analysis of the geometry. The H-accept ability of N^A atom in L-cysteine is weaker than N^B atom in 2-mercaptopyrimidine, so the H-bonds involving N^A atom in L-cysteine as H-acceptor have smaller shift than above involving N^B atom in 2-mercaptopyrimidine as H-acceptor. The shift values of $S^BH\cdots S^A$ **(CON8, CON9, CON19, CON20, CON23 and CON27)** are between 0 and 140 cm^{-1}. Again, N^A is the strongest H-bond shift values than S^A with S^BH bond coordination. The shift of H-bonds involving C atom is small. For example,

the shift of the H-bond C^BH---$O1^A$ in **CON9, CON26** and **CON27** is between 0 and 7 cm^{-1} and the shift of the H-bond C^AH---N^B in **CON22, CON23, and CON27** is between 0 and 20 cm^{-1}.

Because the change of both H-bond length $\Delta\mathbf{R_{X\cdots H}}$ and vibrational frequency shifts $\Delta\mathbf{v}$ canbe used to estimate the strength of H-bond, the correlation should exist between them. To study the relationship between of $\Delta\mathbf{v}$ and $\Delta\mathbf{R_{X\cdots H}}$, a linear correlation analysis was carried out, a linear correlation was shown in **Figure 2.1.5.1.**, and the fitted equation is

$$\Delta\mathbf{v} = -14800\Delta\mathbf{R_{X\cdots H}} + 7.0347 \qquad \mathbf{R = 0.8648} \qquad \mathbf{(11)}$$

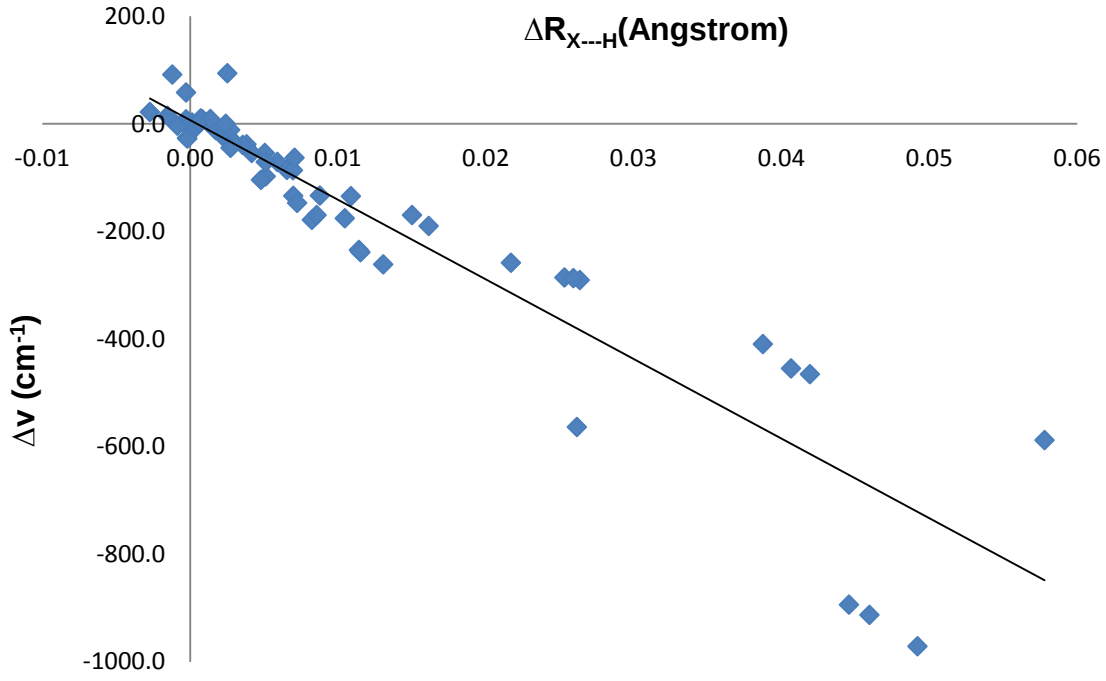

Figure 2.1.5.1. Correlation between the frequency shifts $\Delta\mathbf{v}$ and the bond elongation $\Delta\mathbf{R_{X\cdots H}}$.

On the basis of harmonic vibrational approximation, it is easy to understand this linear correlation if these frequencies represent the localized X-H stretching and almost do not depend on the proton acceptors.

PART 2: Designs of Novel Potential Cisplatin Complexes with 2-mercaptopyrimidine and L-cysteine Molecules

2.2.1. Computational Details

The design of complexes have been prepared as **Figure 2.2.1.1.** and **2.2.1.2.**. Complexes have position of cis- both chlorines and ligands (2-mercaptopyrimidine and L-cysteine). The complex 1 in **Figure 2.2.1.1.,** platinum is bounded to two ligands from their nitrogen atoms using square planar molecular geomerty. The complex 2 in **Figure 2.2.1.2.**, platinum is bounded to L-cystein ligand from its sulphur atom and 2-mercaptopyrimidine ligand from its nitrogen atom using square planar molecular geomerty.

The main goal of this present work is to investigate the structural, electronic, and vibrational properties of complex 1 and 2 and is to determine DFT function having the most stable geometry. The calculations have been done using combination of some quantum chemical softwares as Gaussian, Gaussview, NBOPro, multiwfn, VEDA and chemcraft. All quantum chemical calculations were resulted with using six DFT functions of B3LYP (the three-parameter hybrid functional according to Becke with additional correlation

corrections because of Lee et al.) [40, 41], BHANDH (Becke's "half and half" functional, BH&H and the success of the BH&H functional is attributed to cancellation of errors between Hartree–Fock (HF) and LDA exchange energies) [101, 102], HCTH (Handy's family of functionals including gradient-corrected correlation) [103-105], MPW1PW91 (uses Perdew-Wang exchange as modified by Adamo and Barone combined with PW91 correlation) [106], PBEPBE (The 1996 pure functional of Perdew, Burke and Ernzerhof as made into a hybrid by Adamo) [107-109], and TPSSKCIS (combination of The exchange functional of Tao, Perdew, Staroverov, and Scuseria and The Krieger-Chen-Iafrate-Savin correlation functional) [110, 111] In here, In calculations, geometry optimizations have been calculated the same situation for complex 1 and 2 how have been found their minumum energy level in all DFT functions. The vibrational frequency calculations confirmed that all optimized complexs have no imaginary frequencies and are stable structures.

In summary part of calculations, B3LYP, BHANDH, HCTH, MPW1PW91, PBEPBE, and TPSSKCIS are classified as letters of A, B, C, D, E, and F, respectively. That is, for example **1B** is made of Both complex 1 and BHANDH DFT function. SDD (Stuttgart/Dresden) basis set for Pt atom with own ECP (effective core potential) [112] and 6-31G [113, 114] basis set of George Petersson and coworkers for other atoms (Cl, S, C, N, O, H) have been used during all calculations.

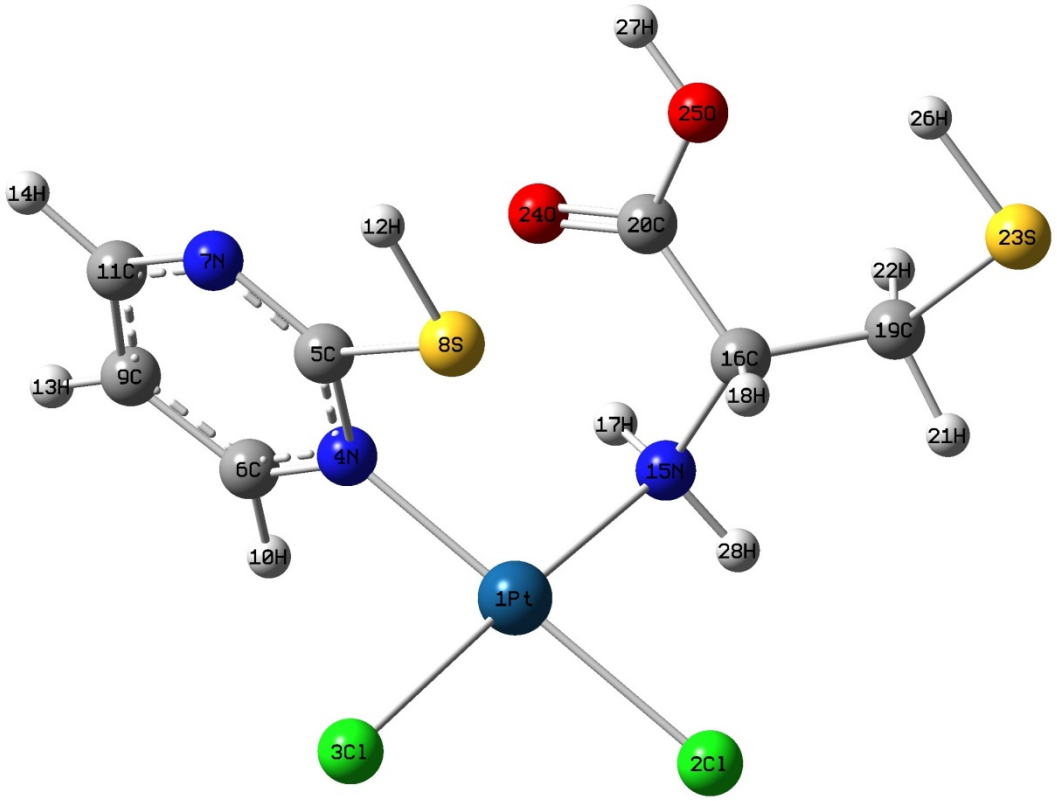

Figure 2.2.1.1. Complex 1.

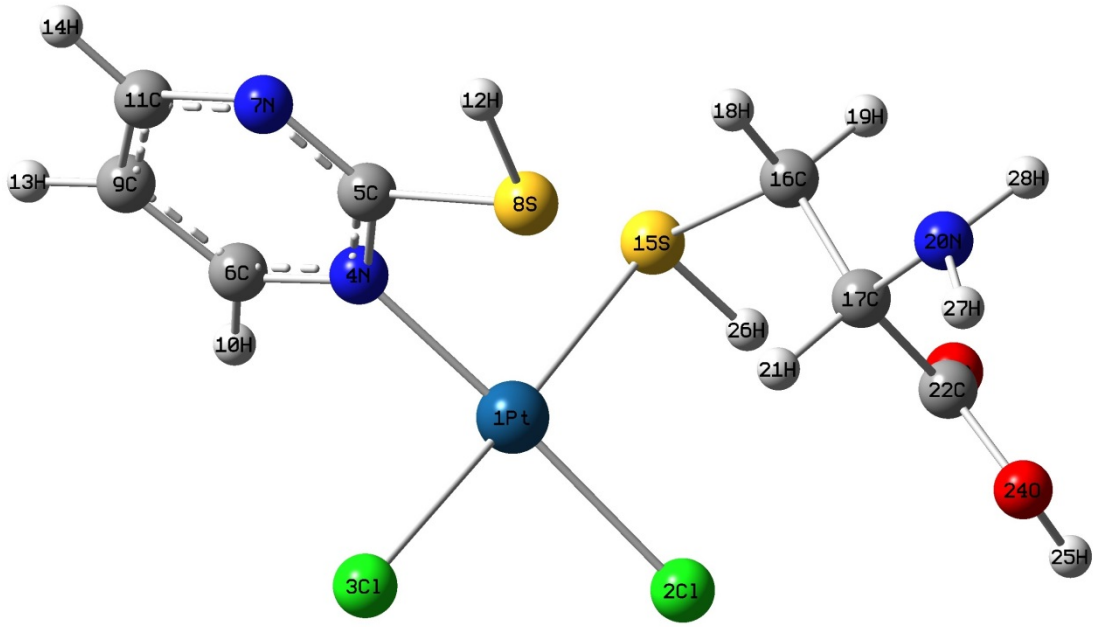

Figure 2.2.1.2. Complex 2.

Calculation results are consist of sturtural properties, detailed energy analysis and Natural orbital analysis to understand qualities and stabilies of all calculation methods. Structural properties have bond lengths and bond angles for minimum geometries of all DFT methods. Energy analysis forms specially thermodynamic properties. This thermodynamic phenomenon, referred to as two complexes influence, is also related to the hard and soft acids and bases (HSAB) principle. HSAB principle states that, ‘hard acids prefer to coordinate with hard bases and soft acids prefer to coordinate with soft bases for both their thermodynamic and kinetic properties’ [115, 116]. For this, Global chemical reactivity descriptors such as chemical hardness (η), electrophilicity (ω), and electronic chemical potentials (μ) are calculated and used to probe the relative stability and reactivity of compounds 1 and 2. The obvious preference of the structural arrangement in 1 and 2 is investigated using Parr and Pearson’s principle of maximum hardness and according to schrödinger equation, potential energy, kinetic energy, nuclear repulsion energy and electron-electron repulsion energy have been calculated from total electronic energy. Natural bond orbital analysis has importance to understand properties of all bonds for complexes. So, the system of input basis > AOs > NAOs > NHOs > NBOs > NLMOs > MOs is used for forming bonds from known atoms. In here, 3-center 4-electrons bond state has been founded between metal and ligands also,forming of 1-center (lone pair) and 2-center (bonding and anti-bonding) and quantum chemical characters of all centers have investigated with detailed tables for complete solution of all complexes.

As a results, many comparisions have been done from all these parameters with the most drawing, tables, and values.

2.2.2. Structural Properties

Optimized geometries for complex 1 and 2 were obtained using A, B3LYP; B, BHANDH; C, HCTH; D, MPW1PW91; E, PBEPBE and F, TPSSKCIS level of theory. The structural parameters were calculated and are presented in **Table 2.2.2.1.**. A significant structural difference among the complexes is the bond angle defined by the cis-chlorines and the Pt-center (∠Cl2–Pt–Cl3). The bond angles of complex 1 is 94.04 for **1A**, 94.86 for **1B**, 93.13 for **1C**, 94.10 for **1D,** 93.66 for **1E** and 93.97 for **1F;** also for complex 2 is 91.79 for **2A**, 92.27 for **2B**, 91.49 for **2C**, 91.80 for **2D,** 91.09 for **2E** and 91.54 for **2F**. BhandH functions have highest (∠Cl2–Pt–Cl3) values for both complex 1 and 2. In addition, the bond angle defined by the cis-nitrogens and the Pt center (∠N4–Pt–N15) of complex 1 is 97.09 for **1A**, 94.86 for **1B**, 96.56 for **1C**, 97.06 for **1D,** 97.29 for **1E** and 97.23 for **1F;** the bond angle defined by the cis nitrogen, sulphur and the Pt center (∠N4–Pt–S15) of complex 2 is 92.05 for **2A**, 93.05 for **2B**, 92.37 for **2C**, 92.43 for **2D,** 91.37 for **2E** and 92.26 for **2F**. Again, angle values of both complex 1 and 2 have the best values of BhandH function. The bond angles of (∠N4–Pt–Cl3) in complex 1 are the smallest value for BhandH function (85.68) and bond angles of (∠N4–Pt–Cl3) in complex 2 is the smallest value for BhandH funtion (85.31). A special structural difference between the complex es is the

bond lengh defined by the chlorines and the Pt-center (Cl2–Pt). The bond lengths of complex 1 is 2.3879 for **1A**, 2.3303 for **1B**, 2.3842 for **1C**, 2.3604 for **1D,** 2.3811 for **1E** and 2.3888 for **1F;** also for complex 2 is 2.3811 for **2A**, 2.3255 for **2B**, 2.3738 for **2C**, 2.3546 for **2D,** 2.3757 for **2E** and 2.3815 for **2F**. BhandH functions have lower and stronger bond lengths of (Cl2–Pt) values for both complex 1 and 2. In addition, there is lower and stronger bond lengths values for (Cl3–Pt) from another DFT functions in complex 1 and 2 with BhandH function. In complex 1, there is lower and stronger

Table 2.2.2.1. Calculated bond lengths and bond angles from 1A to 2F.

ATOMS	Bond Length						ATOMS	Bond Length					
	1A	1B	1C	1D	1E	1F		2A	2B	2C	2D	2E	2F
R(1-2)	2.3879	2.3303	2.3842	2.3604	2.3811	2.3888	R(1-2)	2.3811	2.3255	2.3738	2.3546	2.3757	2.3815
R(1-3)	2.3786	2.3204	2.3732	2.3515	2.3706	2.3790	R(1-3)	2.3851	2.3252	2.3814	2.3574	2.3817	2.3866
R(1-4)	2.0599	2.0064	2.0406	2.0327	2.0273	2.0428	R(1-4)	2.0635	2.0083	2.0496	2.0357	2.0314	2.0482
R(1-15)	2.1329	2.0670	2.1392	2.1020	2.1185	2.1279	R(1-15)	2.4360	2.3701	2.4203	2.3989	2.4089	2.4264
R(4-5)	1.3624	1.3349	1.3691	1.3558	1.3760	1.3752	R(4-5)	1.3618	1.3359	1.3676	1.3552	1.3748	1.3739
R(4-6)	1.3610	1.3362	1.3622	1.3545	1.3698	1.3709	R(4-6)	1.3616	1.3380	1.3621	1.3547	1.3702	1.3709
R(5-7)	1.3392	1.3171	1.3392	1.3343	1.3456	1.3464	R(5-7)	1.3401	1.3189	1.3399	1.3353	1.3467	1.3474
R(5-8)	1.8119	1.7781	1.8004	1.7960	1.8104	1.8128	R(5-8)	1.8115	1.7770	1.7999	1.7953	1.8102	1.8124
R(6-9)	1.3910	1.3753	1.3902	1.3873	1.3981	1.3967	R(6-9)	1.3910	1.3751	1.3904	1.3873	1.3982	1.3967
R(6-10)	1.0806	1.0779	1.0817	1.0796	1.0893	1.0824	R(6-10)	1.0805	1.0780	1.0815	1.0796	1.0892	1.0823
R(7-11)	1.3493	1.3289	1.3482	1.3443	1.3590	1.3598	R(7-11)	1.3494	1.3289	1.3481	1.3444	1.3589	1.3598
R(9-11)	1.3971	1.3805	1.3966	1.3932	1.4041	1.4027	R(9-11)	1.3973	1.3812	1.3968	1.3934	1.4043	1.4028
R(9-13)	1.0816	1.0770	1.0827	1.0798	1.0901	1.0837	R(9-13)	1.0815	1.0769	1.0827	1.0798	1.0900	1.0837
R(11-14)	1.0832	1.0787	1.0849	1.0814	1.0918	1.0848	R(11-14)	1.0832	1.0787	1.0849	1.0815	1.0918	1.0849
R(15-16)	1.5036	1.4656	1.4985	1.4928	1.5085	1.5177	R(16-17)	1.5326	1.5041	1.5288	1.5241	1.5443	1.5368
R(15-17)	1.0232	1.0176	1.0221	1.0217	1.0332	1.0298	R(16-18)	1.0877	1.0845	1.0889	1.0871	1.0964	1.0895
R(15-28)	1.0249	1.0212	1.0239	1.0225	1.0359	1.0305	R(16-19)	1.0926	1.0893	1.0936	1.0919	1.1026	1.0950
R(16-18)	1.0915	1.0917	1.0915	1.0915	1.1012	1.0931	R(17-20)	1.4591	1.4299	1.4560	1.4496	1.4519	1.4682
R(16-19)	1.5493	1.5193	1.5500	1.5401	1.5516	1.5535	R(17-21)	1.0959	1.0957	1.0956	1.0960	1.1117	1.0989
R(16-20)	1.5165	1.4885	1.5165	1.5089	1.5198	1.5208	R(17-22)	1.5288	1.4995	1.5290	1.5203	1.5307	1.5334
R(19-21)	1.0929	1.0896	1.0943	1.0922	1.1023	1.0951	R(20-27)	1.0113	1.0034	1.0099	1.0080	1.0177	1.0169
R(19-22)	1.0934	1.0902	1.0946	1.0925	1.1024	1.0953	R(20-28)	1.0129	1.0049	1.0116	1.0095	1.0190	1.0184
R(20-24)	1.2367	1.2189	1.2396	1.2332	1.2476	1.2478	R(22-23)	1.2395	1.2226	1.2404	1.2360	1.2561	1.2512
R(20-25)	1.3657	1.3342	1.3677	1.3562	1.3778	1.3800	R(22-24)	1.3668	1.3293	1.3725	1.3568	1.3766	1.3821
R(25-27)	0.9827	0.9715	0.9832	0.9783	0.9943	0.9919	R(24-25)	0.9821	0.9705	0.9821	0.9776	0.9947	0.9913
R(19-23)	1.8959	1.8516	1.8811	1.8756	1.8957	1.9006	R(15-16)	1.9239	1.8644	1.9145	1.8977	1.9352	1.9375
R(23-26)	1.3774	1.3681	1.3747	1.3718	1.3896	1.3795	R(15-26)	1.3820	1.3809	1.3780	1.3805	1.4187	1.3911
							R(8-12)	1.3791	1.3681	1.3772	1.3739	1.3948	1.3834

Table 2.2.2.1. (Continued)

ATOMS	Bond Angles					
	1A	1B	1C	1D	1E	1F
A(2-1-3)	94.04	94.86	93.13	94.10	93.66	93.97
A(2-1-4)	178.20	178.79	178.20	178.49	178.42	178.34
A(2-1-15)	82.74	82.87	82.89	82.98	82.47	82.44
A(3-1-4)	86.05	85.68	86.81	86.04	86.50	86.28
A(3-1-15)	175.89	177.14	174.82	176.31	175.34	175.54
A(4-1-15)	97.09	96.56	97.06	96.82	97.29	97.23
A(1-4-5)	123.37	121.83	123.81	122.67	122.34	122.76
A(1-4-6)	118.85	119.71	118.97	119.36	120.24	119.84
A(1-15-16)	117.62	115.76	119.34	116.37	117.14	116.98
A(1-15-17)	109.00	108.94	108.56	109.59	109.25	109.91
A(1-15-28)	98.98	99.62	98.15	99.86	99.25	99.60
A(5-4-6)	117.54	118.33	117.01	117.71	117.19	117.16
A(4-5-7)	124.09	123.74	124.24	124.11	124.55	124.56
A(4-5-8)	117.41	117.30	117.36	117.20	116.23	116.50
A(4-6-9)	121.22	120.86	121.53	121.11	121.15	121.16
A(4-6-10)	115.89	116.09	115.77	115.86	115.55	115.50
A(7-5-8)	118.50	118.95	118.41	118.68	119.22	118.93
A(5-7-11)	118.17	118.47	118.20	118.08	117.71	117.66
A(5-8-12)	92.98	93.04	92.84	92.83	92.06	92.38
A(9-6-10)	122.89	123.05	122.70	123.02	123.30	123.34
A(6-9-11)	117.42	117.20	117.45	117.35	117.64	117.70
A(6-9-13)	120.76	120.97	120.60	120.79	120.55	120.53
A(7-11-9)	121.53	121.36	121.53	121.58	121.69	121.69
A(7-11-14)	116.27	116.51	116.24	116.22	116.10	115.95
A(11-9-13)	121.83	121.83	121.95	121.86	121.80	121.77
A(9-11-14)	122.20	122.13	122.23	122.20	122.22	122.36
A(16-15-17)	109.63	110.23	109.47	109.46	109.25	108.89
A(16-15-28)	110.32	110.65	110.35	110.38	110.27	110.18
A(15-16-18)	108.66	109.00	108.67	108.94	108.53	108.51
A(15-16-19)	110.55	111.27	110.11	110.52	110.46	110.14
A(15-16-20)	106.43	106.26	106.88	106.16	106.06	105.81
A(17-15-28)	110.85	111.25	110.38	110.85	111.36	111.00
A(18-16-19)	109.03	109.10	108.86	108.95	109.16	109.18
A(18-16-20)	109.52	109.30	109.71	109.51	109.92	109.88
A(19-16-20)	112.57	111.83	112.53	112.66	112.59	113.19
A(16-19-21)	108.22	108.24	108.02	107.90	108.17	107.98
A(16-19-22)	111.72	111.58	111.47	111.67	111.67	111.75
A(16-19-23)	115.36	114.54	116.30	115.28	115.01	115.07
A(16-20-24)	124.48	123.86	124.58	124.23	124.50	124.58
A(16-20-25)	112.81	113.34	112.53	113.02	112.60	112.62
A(21-19-22)	108.76	108.24	108.41	108.70	108.86	109.27
A(21-19-23)	102.53	103.52	102.18	102.75	102.68	102.58
A(22-19-23)	109.69	110.22	109.82	109.98	109.92	109.67
A(24-20-25)	122.68	122.72	122.87	122.72	122.86	122.78
A(20-25-27)	111.08	113.09	109.99	111.34	109.50	109.77
A(19-23-26)	96.91	96.36	97.54	96.90	96.07	96.45

ATOMS	Bond Angles					
	2A	2B	2C	2D	2E	2F
A(2-1-3)	91.79	92.27	91.49	91.80	91.09	91.54
A(2-1-4)	176.82	177.34	176.80	176.78	176.75	176.77
A(2-1-15)	90.00	89.32	89.42	89.71	91.12	89.98
A(3-1-4)	86.03	85.31	86.54	85.93	86.29	86.07
A(3-1-15)	176.26	176.90	175.91	176.45	175.83	175.87
A(4-1-15)	92.05	93.05	92.37	92.43	91.37	92.26
A(1-4-5)	124.17	122.43	124.52	123.46	123.20	123.60
A(1-4-6)	117.98	118.76	118.11	118.45	119.28	118.88
A(1-15-16)	102.08	106.34	110.76	108.78	108.47	109.33
A(1-15-26)	109.52	100.67	100.69	101.60	103.69	101.97
A(5-4-6)	117.67	118.51	117.19	117.89	117.36	117.33
A(4-5-7)	124.01	123.51	124.19	124.00	124.46	124.48
A(4-5-8)	117.58	117.46	117.51	117.34	116.52	116.72
A(4-6-9)	121.13	120.77	121.42	121.03	121.05	121.07
A(4-6-10)	115.86	116.00	115.76	115.84	115.50	115.48
A(7-5-8)	118.40	119.03	118.30	118.66	119.01	118.80
A(5-7-11)	118.16	118.55	118.15	118.08	117.70	117.64
A(5-8-12)	93.00	93.25	92.91	92.87	92.06	92.39
A(9-6-10)	123.01	123.22	122.82	123.13	123.45	123.44
A(6-9-11)	117.43	117.21	117.44	117.35	117.64	117.69
A(6-9-13)	120.73	120.95	120.60	120.77	120.54	120.52
A(7-11-9)	121.56	121.42	121.59	121.64	121.73	121.75
A(7-11-14)	116.24	116.45	116.19	116.18	116.05	115.91
A(11-9-13)	121.84	121.85	121.96	121.88	121.82	121.79
A(9-11-14)	122.20	122.12	122.21	122.19	122.21	122.34
A(17-16-18)	109.38	109.20	109.11	109.17	109.03	109.60
A(17-16-19)	112.00	111.75	111.93	111.93	112.37	112.38
A(16-17-20)	108.41	109.71	108.25	108.79	109.04	108.17
A(16-17-21)	109.19	108.84	109.13	109.00	107.38	108.89
A(16-17-22)	111.50	110.25	111.81	111.12	111.40	111.35
A(17-16-15)	115.71	113.22	116.58	115.09	114.66	114.73
A(18-16-19)	110.39	110.54	110.25	110.29	110.17	110.78
A(18-16-15)	104.67	106.34	104.40	105.28	105.41	104.85
A(19-16-15)	104.35	105.61	104.21	104.81	104.92	104.16
A(20-17-21)	107.84	108.30	107.62	108.02	108.53	107.80
A(20-17-22)	113.72	113.27	113.04	113.64	115.44	114.18
A(17-20-27)	114.84	116.01	114.58	115.08	115.35	113.85
A(17-20-28)	115.92	117.06	115.47	116.14	116.03	114.83
A(21-17-22)	106.03	106.31	106.86	106.12	104.65	106.27
A(17-22-23)	125.82	124.62	126.12	125.56	125.78	126.16
A(17-22-24)	111.82	112.35	111.12	111.94	112.98	111.64
A(27-20-28)	112.74	114.21	112.63	113.13	112.76	111.74
A(23-22-24)	122.36	123.00	122.72	122.49	121.23	122.19
A(22-24-25)	110.86	113.04	109.89	111.18	108.97	109.47
A(16-15-26)	95.21	94.78	96.56	95.08	90.91	93.25

values of 2.0064 and 2.0670 for (N4–Pt) and (N15–Pt) bond lengths with BhandH function, respectively. In complex 2, there is lower and stronger values of 2.0083 and 2.3701 for (N4–Pt) and (S15–Pt) bond lengths with BhandH function, respectively.

Finally, structural parameters are more important values for stability and quality degrees of structure.

2.2.3. Energy Analysis

In this part, energy parameters calculated to understand stability characters of both complex 1 and 2 as values of termodynamic, structural, and chemical reactivity. Energy kinds of total, potential, kinetic, nuclear repulsion, electron-electron repulsion, zero-point, thermal, thermal enthalpy, thermal free, HOMO, LUMO, chemical hardness, chemical potential and electrophilicity index investigated for all calculation methods. All these detailed values posted for both complex 1 and 2 in **Table 2.2.3.1.**.

Total energy is related to potential, kinetic and repulsion energies. The nuclear-nuclear repulsion (NN) energy is computed before the wave function is determined, as this property is independent of the wave function and depends only on the coordinates of the nuclei. The one-electron energy is a combination of the electron kinetic energy and the potential energy between each electron and each nucleus. These two quantities are given by “KE” and “PE” in equation and the two-electron energy corresponds to the electron-electron repulsion energy (EE).

$$E_{TOT} = E_{1e} + E_{2e} + E_{NN} \quad \textbf{(1)}$$

$$E_{TOT} = KE + PE + EE + NN \quad \textbf{(2)}$$

In complex 1, total energy has the highest value of **1B**, -2415.35654 Hartrees and is the lowest value of **1C**, -2424.53405 Hartrees. Lower kinetic energy and potential energy are found as 2338.01336 and -9886.05836 Hartrees in **1B** with BhandH function how is important for stability, respecively, also bigger kinetic energy value has 2340.26786 Hartrees in **1C** with Hcth function and high potential energy is -9742.67030 Hartrees in **1F** of Tpsskcis function. In complex 2, total energy has the highest value of **2B**, -2415.33896664 Hartrees and is the lowest value of **2C**, -2424.5192943 Hartrees. Lower kinetic energy and potential energy are found as 2338.01540 and -9919.86944 Hartrees in **2B** with BhandH function, respecively. In addition, high kinetic energy value has 2340.27855 Hartrees in **2C** with Hcth function and bigger potential energy is -9753.84308 Hartrees in **2F** of Tpsskcis function.

Highest occupied molecular (HOMO) and lowest unoccupied molecular orbital (LUMO) are effective parameters for quantum chemistry. We can determine how the complex interacts with other species; thus, they are the frontier orbitals. While the energy of the HOMO is directly related to the ionization potential. LUMO energy is directly related to the electron affinity. Energy gap between HOMO and LUMO that is an important stability for structures [117]. According to the calculation levels of **1A, 1B, 1C, 1D, 1E,** and **1F**, the energy band gap between HOMO and LUMO of the complex was found in order of 3.4865, 6.1923, 1.8195, 3.9247, 1.8021, and 1.8839 eV, respectively in complex 1. Again, As the calculation levels of **2A, 2B, 2C,**

2D, 2E, and **2F**, the energy band gap between HOMO and LUMO of the complex was found in order of 3.5940, 6.2776, 1.9251, 4.0465, 1.9093, and 2.0178 eV, respectively in complex 2. **1B** in complex 1 and **2B** in complex 2 with BhandH have the best values of energy band gap for high stability of structure. In addition, **1C, 2C** with HCTH and **1E, 2E** with PBEPBE have lower the energy band gap between HOMO and LUMO in both complex 1 and 2 for least stability. BhandH DFT function causes effective resuls to understand stability rates of complexes.

The reactivity of the active site of complex 1 and 2 can be elucidated by computation using global chemical reactivity indices. The chemical reactivity descriptors calculated using DFT are; chemical hardness (η), electronic chemical potential (μ), and electrophilicity (ω).

Chemical hardness is associated with the stability and reactivity of a chemical event. In complexes, it measures the resistance to change in the electron distribution or charge transfer. On the basis of frontier molecular orbitals, chemical hardness corresponds to the gap between the Highest Occupied Molecular Orbital (HOMO) and Lowest Unoccupied Molecular Orbital (LUMO). Chemical hardness is approximated using equation 3.

$$\eta = (E_{LUMO} - E_{HOMO})/2 \quad \textbf{(3)}$$

where E_{LUMO} and E_{HOMO} are the LUMO and HOMO energies. The larger the

HOMO–LUMO energy gap, the harder and more stable/less reactive the complex [115, 116, 119–122]. **Table 2.2.3.1.** contains the computed chemical hardness values from compounds **1A** to **1F** in complex 1 and for compounds **2A** to **2F** in complex 2. The results indicate that **1B** in complex 1 with 3.0961 eV value and **2B** in complex 2 with 3.1388 eV value are harder and less reactive than others. In addition, **2B** is harder and less reactive than **1B** structure above hardness values.

Electronic chemical potential is described as the negative of electronegativity of a complex [121] and determined using equation 4.

$$\mu = (E_{LUMO} + E_{HOMO})/2 \quad \textbf{(4)}$$

Physically, μ defines the escaping inclination of electrons from an equilibrium system [115]. The values of μ for complexes 1 and 2 are presented in table **Table 2.2.3.1.**. The tendency in electronic chemical potential for the complexes is **1F > 1E > 1C > 1A >1D > 1B** in complex and **2E > 1F > 2C > 2A >1D > 2B**. The greater the electronic chemical potential, the less stable or more reactive is the complexes 1 and 2. Therefore, **1F** in complex 1 and **2E** in complex 2 are the most reactive or less stable and **1B** in complex 1 and **2B** in complex 2 are the least reactive of the all complexes. In addition, **2B** is the more stable than **1B** with values of -8.3320 and -8.1631, respectively.

Global electrophilicity index (ω), introduced by Parr, is calculated using the electronic chemical potential and chemical hardness as shown in equation 5.

$$\omega = \mu^2/2\eta \quad \textbf{(5)}$$

Electrophilicity index measures the tilt or capacity of a species to accept electrons [122, 123]. It is a measure of the stabilization in energy after a system accepts extra amount of electronic charge from the environment [124, 125]. The electrophilicity values **(Table 2.2.3.1.)** are from **1A** to **1F**; 15.8539 eV, 10.7612 eV, 26.1499 eV, 14.9296 eV, 24.8560 eV, and 23.3117 eV in complex 1, respectively and are from **2A** to **2F**; 15.7596 eV, 11.0587 eV, 25.5253 eV, 14.8859 eV, 23.3980 eV, and 22.2950 in complex 2, respectively. Between the complexes, **1B** and **2B** is the strongest nucleophile while **1C** and **2C** is the strongest electrophile. The electrophilicity values are observed to follow the hardness tilt in corruption of the minimum electrophilicity principle (MEP: for equilibrium geometries, 'more stable isomers correspond to lower electrophilicity values') [126-128]. This clear violation may be attributed to the amiss behaviour of the chemical potential.

Finally, The structural placement of **2B** seems to be thermodynamically preferred over the structural dispositions of others. This geometric choice can be clarified by the Principle of Maximum Hardness (PMH). PMH states 'there seems to be a rule of nature that molecules

arrange themselves to be as hard as possible [112, 119, 122, 128-131]. The geometric arrangement of **2B** provides for maximum hardness and hence **2B** is the thermodynamically stable cis complex. The computed energies confirms that **2B** is more stable than the isomers **1B**. **2B** with BhandH in complex 2 has the best values as **1B** in complex 1 and others structures.

Table 2.2.3.1. Energies of total (Hart.), potential (Hart.), kinetic (Hart.), nuclear (Hart.), repulsion (Hart.), $e^{-}e^{-}$ repulsion (Hart.), zero-point (Hart.), thermal (Hart.), enthalpy (Hart.), gibbs (Hartrees), ΔE_{ZPVE} (kcal/mol), ΔE (kcal/mol), ΔH (kcal/mol), ΔG (kcal/mol), ΔS (cal/mol-Kelvin), C_v (cal/mol-Kelvin), HOMO (eV), LUMO (eV), chemical hardness (eV), chemical potential (eV) and electrophilicity index (eV), also dipole moment (Debye) for complex 1 and 2 in the all DFT functions.

PARAMETRERS	MOLECULE 1					
	1A	1B	1C	1D	1E	1F
Function	B3LYP	BHANDH	HCTH	MPW1PW91	PBEPBE	TPSSKCIS
Total Energy	-2424.07787	-2415.35654	-2424.53405	-2423.96767	-2422.65759	-2424.28386
Potential Energy	-9751.89347	-9886.05836	-9743.55045	-9791.64878	-9764.95678	-9742.67030
Kinetic Energy	2338.51830	2338.01336	2340.26786	2338.70404	2337.39932	2338.53929
Nuclear Repulsion Energy	2025.30162	2093.73149	2019.15078	2045.11156	2032.45485	2020.52289
Repulsion Energy Of e^{-}-e^{-}	2963.99569	3038.95697	2959.59776	2983.86551	2972.44502	2959.32426
Zero-Point Energy	-2423.88659	-2415.15635	-2424.34441	-2423.77362	-2422.47184	-2424.09648
Thermal Energy	-2423.86618	-2415.13705	-2424.32382	-2423.75348	-2422.45118	-2424.07581
Thermal Enthalpy	-2423.86524	-2415.13611	-2424.32288	-2423.75254	-2422.45023	-2424.07487
Thermal Free Energy	-2423.94025	-2415.20733	-2424.39849	-2423.82711	-2422.52567	-2424.15038
ΔE_{ZPVE}	120.026	125.616	118.9972	121.765	116.563	117.582
ΔE	132.835	137.726	131.9195	134.403	129.526	130.549
ΔH	133.428	138.319	132.5118	134.996	130.118	131.141
ΔG	86.356	93.628	85.0614	88.203	82.782	83.757
ΔS	157.879	149.894	159.1500	156.940	158.764	158.927
C_v	70.060	67.175	70.6290	69.194	71.287	71.121
HOMO	-6.1186	-7.5062	-5.2051	-6.4114	-5.0625	-5.0460
LUMO	-2.6321	-1.3139	-3.3856	-2.4867	-3.2604	-3.1621
HOMO-LUMO	3.4865	6.1923	1.8195	3.9247	1.8021	1.8839
Chemical Hardness, η	1.7432	3.0961	0.9098	1.9624	0.9011	0.9420
Chemical Potential, μ	-7.4347	-8.1631	-6.8979	-7.6547	-6.6928	-6.6270
Electrophilicity Index, ω	15.8539	10.7612	26.1499	14.9296	24.8560	23.3117
Dipole Moment	13.4004	13.9611	12.9287	13.4055	12.6048	12.7636
RMS Gradient	0.00000325	0.00000926	0.00000690	0.00000119	0.00000371	0.00000429

Table 2.2.3.1. (Continued)

PARAMETRERS	MOLECULE 2					
	2A	2B	2C	2D	2E	2F
Function	B3LYP	BHANDH	HCTH	MPW1PW91	PBEPBE	TPSSKCIS
Total Energy	-2424.06142	-2415.33897	-2424.51929	-2423.95310	-2422.64343	-2424.26819
Potential Energy	-9753.84308	-9919.86944	-9758.57907	-9808.01655	-9748.26288	-9756.79051
Kinetic Energy	2338.52047	2338.01540	2340.27855	2338.69495	2337.37376	2338.52062
Nuclear Repulsion Energy	2025.71251	2110.03745	2026.14201	2052.76323	2023.49151	2027.04631
Repulsion Energy Of e^--e^-	2965.54868	3056.47763	2967.63921	2992.60526	2964.75418	2966.95540
Zero-Point Energy	-2423.87179	-2415.14063	-2424.33127	-2423.76073	-2422.45938	-2424.08245
Thermal Energy	-2423.85099	-2415.12092	-2424.31024	-2423.74025	-2422.43838	-2424.06141
Thermal Enthalpy	-2423.85005	-2415.11998	-2424.30929	-2423.73931	-2422.43744	-2424.06046
Thermal Free Energy	-2423.92559	-2415.19202	-2424.38553	-2423.81408	-2422.51384	-2424.13650
ΔE_{ZPVE}	118.995	124.460	117.990	120.712	115.494	116.550
ΔE	132.046	136.826	131.185	133.562	128.671	129.757
ΔH	132.639	137.418	131.777	134.155	129.264	130.349
ΔG	85.235	92.209	83.936	87.236	81.320	82.633
ΔS	158.993	151.633	160.460	157.365	160.808	160.041
C_v	71.712	68.921	72.352	70.863	72.721	72.743
HOMO	-6.2153	-7.6472	-5.3150	-6.5230	-5.0923	-5.1441
LUMO	-2.6213	-1.3696	-3.3899	-2.4765	-3.1830	-3.1263
HOMO-LUMO	3.5940	6.2776	1.9251	4.0465	1.9093	2.0178
Chemical Hardness, η	1.7970	3.1388	0.9626	2.0232	0.9546	1.0089
Chemical Potential, μ	-7.5260	-8.3320	-7.0100	-7.7612	-6.6838	-6.7072
Electrophilicity Index, ω	15.7596	11.0587	25.5253	14.8859	23.3980	22.2950
Dipole Moment	9.3000	9.6378	9.3203	9.2953	8.9654	8.7842
RMS Gradient	0.00001334	0.00000216	0.00000435	0.00001161	0.00000294	0.00000373

2.2.4. Natural Bond Orbital Analysis

The natural bond orbital [132-140] performs the analysis of a many electron molecular wavefunction in terms of localized electron-pair bonding units. The NBO system carries out the determination of natural atomic orbitals (NAOs), natural hybrid orbitals (NHOs), natural bond orbitals (NBOs), and natural localized molecular orbitals (NLMOs), and uses these to perform natural population analysis (NPA), NBO energetic (deletions) analysis.

The NBO method makes use of only the first-order reduced density matrix of the wavefunction, and hence is applicable to wavefunctions of general mathematical form. In the open-shell case, the analysis is performed in terms of “different NBOs for different spins,” based on distinct density matrices for α and ß spin.

NBO analysis is based on a method for optimally transforming a given wavefunction into localized form, corresponding to the one-center (“lone pair”) and two-center (“bond”) elements of the chemist's Lewis structure picture. The NBOs are obtained as local block eigenfunctions of the density matrix, and are hence “natural” in the sense of Löwdin, having optimal convergence properties for describing the electron density. The set of high-occupancy NBOs, each taken doubly occupied, is said to represent the “natural Lewis structure” (NLS) of the molecule. Delocalization effects appear as weak departures from this idealized localized picture. (For transition metals, a normal-valent Lewis-like structure conforms to a dodectet rule, rather than the normal octet rule for main-group elements). The various natural localized sets can be considered to result from a sequence of transformations of the input atomic orbital basis set {χ}, input basis > AOs > NAOs > NHOs > NBOs > NLMOs > MOs.

Each natural localized set forms a complete orthonormal set of one-electron functions for expanding the delocalized molecular orbitals (MOs) or forming matrix representations of one-electron operators. The overlap of

associated “pre-orthogonal” NAOs (PNAOs), lacking only the interatomic orthogonalization step of the NAO procedure, can be used to estimate the strength of orbital interactions in the usual way, based on Mulliken-type approximations.

The optimal condensation of occupancy in the natural localized orbitals leads to partitioning into high- and low-occupancy orbital types (reduction in dimensionality of the orbitals having significant occupancy), as reflected in the orbital labelling. The small set of most highly-occupied NAOs, having a close correspondence with the effective minimal basis set of semi-empirical quantum chemistry, is referred to as the “natural minimal basis” (NMB) set. The NMB (core + valence) functions are distinguished from the weakly occupied “Rydberg” (extra-valence-shell) functions that complete the span of the NAO space, but typically make little contribution to molecular properties. Similarly in the NBO space, the highly occupied NBOs of the natural Lewis structure (NLS) can be distinguished from the “non-Lewis” antibond and Rydberg orbitals that complete the span of the NBO space. Each pair of valence hybrids hA, hB in the NHO basis give rise to a bond (σAB) and antibond (σAB*) in the NBO basis, the former a Lewis (occupied) and the latter a non-Lewis (unoccupied) orbital. The antibonds

$$\sigma_{AB} = c_A h_A + c_B h_B \quad \textbf{(6)}$$

$$\sigma_{AB}^* = c_A h_A - c_B h_B \quad \textbf{(7)}$$

(valence shell non-Lewis orbitals) typically play the primary role in departures (delocalization) from the idealized Lewis structure.

The NBO also makes extensive provision for energetic analysis of NBO interactions, based on the availability of a 1-electron effective energy operator (Fock or Kohn-Sham matrix) for the system. [As noted above, the construction of NAOs and NBOs is wholly independent of any such energy operator (or geometry) information]. Estimates of energy effects are based on second-order perturbation theory, or on the effect of deleting certain orbitals or matrix elements and recalculating the total energy.

2.2.4.1. 3-Center 4-Electron Hyperbond [141]

As described in the 3-center MO picture [142, 143] a hyperbonded triad of atoms A, B, C, with strongly interacting valence hybrids h_A, h_B, h_C can give rise to two doubly occupied MOs accommodating four electrons. Such 3-c, 4-e triads are more aptly described in Coulson's picture [144] as a strong resonance hybrid of the two localized Lewis structure representations which is denoted in the result as A:-B-:C.

A-B :C <- -> A: B-C **(8)**

Table 2.2.4.1.1. 3-Center 4-Electron hyperbond analysis of molecule 1 and 2. Contributions (%); energy of bonding, LP, non- bonding (eV); and E(2) energy (Hartrees).

3-c 4e⁻ Hyperbond	1A		1B		1C		1D		1E		1F	
	BOND 1	BOND 2	BOND 1	BOND 2	BOND 1	BOND 2	BOND 1	BOND 2	BOND 1	BOND 2	BOND 1	BOND 2
Bonding Type (A-B)	Pt-Cl2	Pt-Cl3	Pt-Cl2	Pt-Cl3	Pt-Cl2	Pt-Cl3	Pt-Cl2	Pt-Cl3	Pt-Cl2	Pt-Cl3	Pt-Cl2	Pt-Cl3
LP Type (:C)	N4	N15	N4	N15	N4	N15	N4	N15	N4	N15	N4	N15
Occupancy	3.9687	3.9752	3.9659	3.9761	3.9722	3.9758	3.9676	3.9750	3.9724	3.9742	3.9727	3.9754
3-c Bond Contribution (A-B)	59.5	61.8	59.3	61.4	58.3	61.5	59.4	61.5	57.6	60.7	58.3	60.9
3-c Bond Contribution (:C)	40.5	38.2	40.7	38.6	41.7	38.5	40.6	38.5	42.4	39.3	41.7	39.1
Bonding Energy (A-B)	-11.8955	-11.5700	-14.4346	-14.0492	-10.8527	-10.5275	-12.5945	-12.2533	-10.9920	-10.6552	-10.8195	-10.4905
LP Energy (:C)	-12.0846	-10.6443	-13.3148	-11.8130	-11.2285	-9.8677	-12.3523	-10.8680	-11.0008	-9.6543	-11.1757	-9.7896
Non-Bonding Energy (A-B*)	0.4163	0.4563	2.6958	2.7092	-0.3850	-0.4054	0.9736	1.0030	-0.3184	-0.3078	-0.1595	-0.1377
E(2) Energy (:C --- A-B*)	128.59	109.95	174.62	152.32	123.92	96.60	145.80	125.94	134.32	107.26	125.02	102.75
3-c 4e⁻ Hyperbond	2A		2B		2C		2D		2E		2F	
	BOND 1	BOND 2	BOND 1	BOND 2	BOND 1	BOND 2	BOND 1	BOND 2	BOND 1	BOND 2	BOND 1	BOND 2
Bonding Type (A-B)	Pt-Cl2	Pt-Cl3	Pt-Cl2	Pt-Cl3	Pt-Cl2	Pt-Cl3	Pt-Cl2	Pt-Cl3	Pt-Cl2	Pt-Cl3	Pt-Cl2	Pt-Cl3
LP Type (:C)	N4	S15	N4	S15	N4	S15	N4	S15	N4	S15	N4	S15
Occupancy	3.9648	3.9988	3.9610	3.9923	3.9696	4.0022	3.9630	3.9961	3.9687	4.0009	3.9689	4.0006
3-c Bond Contribution (A-B)	60.2	57.3	59.9	55.7	59.3	57.2	60.0	56.6	58.1	55.6	58.9	56.5
3-c Bond Contribution (:C)	39.8	42.7	40.1	44.3	40.7	42.8	40.0	43.4	41.9	44.4	41.1	43.5
Bonding Energy (A-B)	-12.0310	-11.5665	-14.6133	-14.0531	-10.9939	-10.5542	-12.7567	-12.2549	-11.0701	-10.5646	-10.9433	-10.4952
LP Energy (:C)	-12.1183	-10.7267	-13.4432	-11.8410	-11.2593	-9.9303	-12.3959	-10.9349	-10.9640	-9.5379	-11.1801	-9.6377
Non-Bonding Energy (A-B*)	0.1891	-0.5995	2.3448	1.2694	-0.6035	-1.3100	0.7053	-0.1676	-0.4378	-1.1510	-0.3627	-1.0593
E(2) Energy (:C --- A-B*)	125.89	127.27	170.86	189.87	119.20	117.02	142.93	151.65	131.34	128.89	121.69	121.10

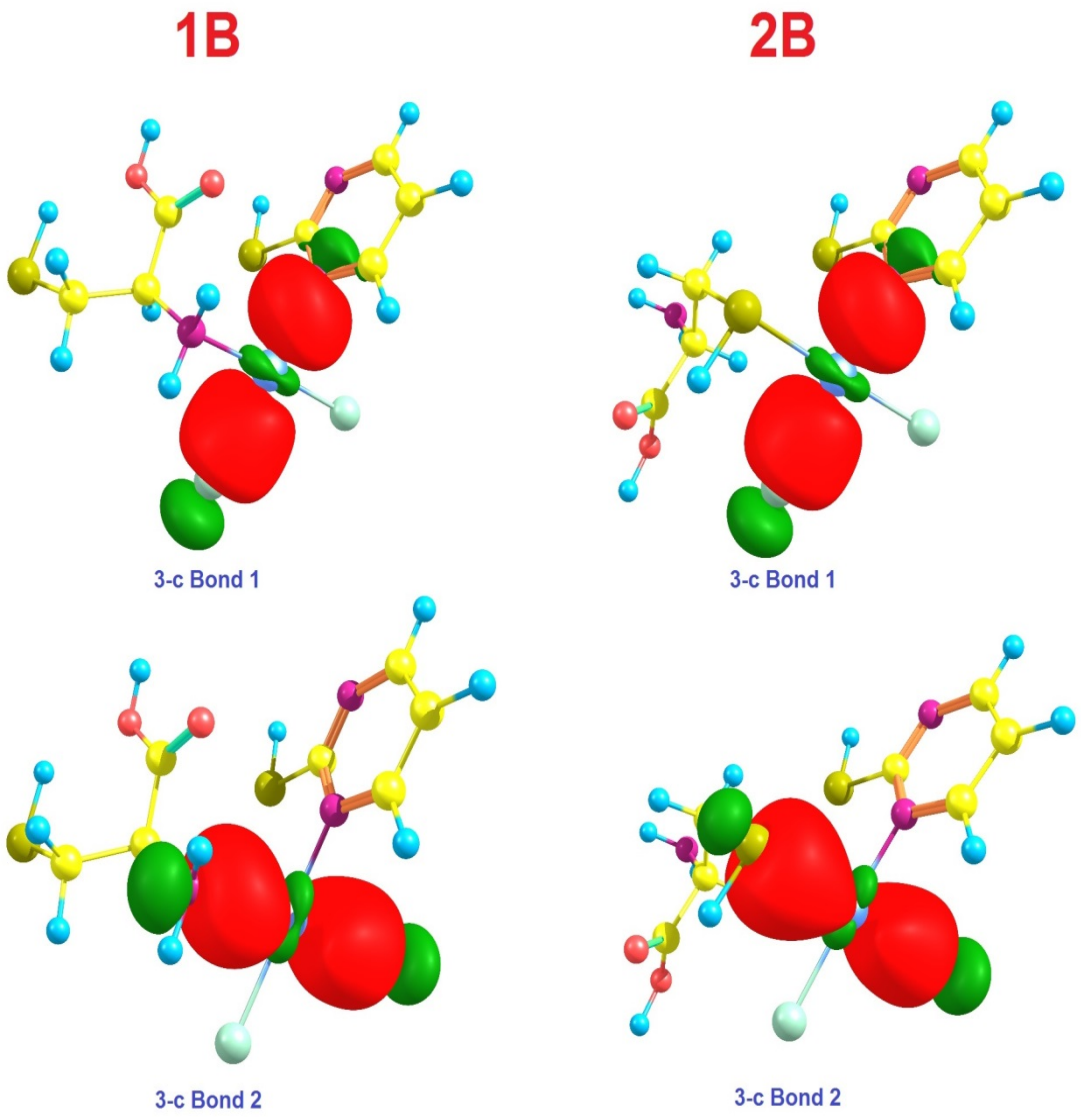

Figure 2.2.4.1.1. 3-c Bond pictures in 1B and 2B of complexes 1 and 2. Atom colours: S; dark yellow, O; red, C; purple, and H; blue. Density colours: +; red, -; green.

In NBO language, each A:-B-:C triad corresponds to strong n_C -> σ_{AB}* delocalization in the A-B :C lewis structure, or equivalently, strong n_A -> σ_{BC}* delocalization in the alternative A: B-C Lewis structure. The 3CHB search attempts to locate such A:-B-:C triads and to identify the participating NHOs and NBOs in the framework of the parent A-B :C Lewis structure.

Pictures of 3-center natural bond orbitals of **1B** and **2B** shows for complexes 1 and 2 in **Figure 2.2.4.1.1.**.

This calculation results are also seen in **Table 2.2.4.1.1.** In this table, bonding type (A-B), lone pair (C) type, occupancy, contributions percentange of bonding and lone pair in 3-c bonds and energies were calculated and investigated to understand better or worse structures. Pt-Cl2 and Pt-Cl3 formed 3-center 4-electrons with lone pairs of N4 and N15 atoms in complex 1. In addition, In complex 2, Pt-Cl2 and Pt-Cl3 formed 3-center 4-electrons with lone pairs of N4 and S15 atoms. In complexes, 2-mercaptopyrimidine complex completed quitely delocalization forming true structure. Bonding contibution (A-B) is about %60 while lone pair (C) contribution is about %40 in 3-c bonds.**1B** with BhandH function have the smallest bonding energies, -14.4346 and -14.0492 eV; lone pair energies, -13.3148 and -11.8130 eV, in complex 1, respectively and **2B** with BhandH function have the lowest bonding energies, -14.6133 and -14.0531 eV; lone pair energies, -13.4432 and -11.8410 eV in complex 2, respectively. In addition, E(2) stabilization and interaction energy have better values of both **1B** and **2B** structures than others. Lone pair of S15 atom with interaction antibonding of Pt-Cl3* is has higher E(2) stabilization energy as lone pair of N15 atom with interaction antibonding of Pt-Cl3*.

As a result, **1B** and **2B** have the smallest 3-c bond energies and highest stabilization energy E(2) for good molecular structure and **2B** is better energy values than **1B** in contrast complex 1 and complex 2.

2.2.4.2. NBO Configurations and Charges

In this part of natural bond orbital analysis shows electronic properties of atoms in bonding. Elecronic configurations of valance electrons in **Table 2.2.4.2.1.** and natural charges of atoms in **Table 2.2.4.2.2.** in complexes have investigated.

According to the NBO results, the electron configuration Pt of **1B** with BhandH in complex 1 is [core] $5d^{8.77}$ $6s^{0.57}$ and the electron configuration Pt of **2B** with BhandH in complex 2 is [core] $5d^{8.85}$ $6s^{0.59}$. Thus, **1B** in complex 1 and **2B** in complex 2 have both 68.00 core electrons, 9.34, 9.44 valence electrons (on 5d and 6s atomic orbitals) and both 0.05 Rydberg electrons (mainly on 6d and 7p orbitals) give the total of 77.39, 77.49 electrons. This is consistent with the calculated natural charge on the Pt atom in this complex, +0.61, +0.51 (corresponding to the difference between 77.39 e^-, 77.49 e^-, and the total number of electrons in the isolated Pt atom, 78 e^-), respectively. Of all the ammonia nitrogen atoms, the N15 in **1B** atom involved in hydrogen bonding in complexes have the largest negative charge (-0.91 e^-). The hydroxyl H hydrogen atom (lying in the molecular plane) has a larger positive charge (0.52 e^-) than the remaining hydrogen atoms. The two Cl2 and Cl3 atoms (bonded to Pt) in **1B** of complex 1, have significantly varied charges, -0.54 e^- and -0.52 e^-, respectively. This implies much larger accommodation of electron density on the Cl2 atom. Thus, the two chlorine atoms (bonded to Pt), show significant differences in their electronic structure.

Table 2.2.4.2.1. Electronic configurations of bonding atoms and total electron distributions in complex 1 and 2.

e^-	Electronic Configuration										Total Electrons		
	Pt		Cl2		Cl3		N4		N15		Core	Valance	Rydberg
	6s	5d	3s	3p	3s	3p	2s	2p	2s	2p			
1A	0.59	8.79	1.96	5.55	1.96	5.54	1.32	4.15	1.41	4.44	131.9866	101.6884	0.3250
1B	0.57	8.77	1.95	5.59	1.95	5.57	1.28	4.20	1.39	4.50	131.9858	101.6552	0.3591
1C	0.60	8.84	1.96	5.53	1.96	5.50	1.33	4.12	1.42	4.41	131.9862	101.6891	0.3247
1D	0.59	8.80	1.95	5.56	1.95	5.54	1.31	4.16	1.41	4.45	131.9863	101.6822	0.3315
1E	0.63	8.81	1.96	5.52	1.96	5.50	1.32	4.12	1.42	4.42	131.9859	101.6857	0.3284
1F	0.62	8.79	1.90	5.53	1.90	5.51	1.33	4.12	1.42	4.41	131.9864	101.6942	0.3194
e^-	Electronic Configuration										Total Electrons		
	Pt		Cl2		Cl3		N4		S15		Core	Valance	Rydberg
	6s	5d	3s	3p	3s	3p	2s	2p	3s	3p			
2A	0.60	8.87	1.96	5.55	1.96	5.53	1.32	4.15	1.72	4.23	131.9868	101.6972	0.3160
2B	0.59	8.85	1.95	5.58	1.95	5.57	1.28	4.20	1.69	4.25	131.9859	101.6638	0.3503
2C	0.61	8.91	1.96	5.52	1.96	5.50	1.33	4.12	1.73	4.21	131.9866	101.6969	0.3166
2D	0.60	8.88	1.95	5.55	1.96	5.53	1.31	4.16	1.71	4.23	131.9865	101.6890	0.3245
2E	0.64	8.88	1.95	5.52	1.96	5.50	1.32	4.12	1.74	4.22	131.9862	101.6987	0.3151
2F	0.63	8.87	1.96	5.53	1.96	5.50	1.33	4.12	1.73	4.21	131.9868	101.7025	0.3108

Table 2.2.4.2.2. Natural charges in complex 1 and 2.

ATOM		NBO Charge					
		1A	1B	1C	1D	1E	1F
1	Pt	0.5697	0.6079	0.5142	0.5638	0.5068	0.5370
2	Cl	-0.5133	-0.5355	-0.4879	-0.5152	-0.4798	-0.4939
3	Cl	-0.4948	-0.5224	-0.4626	-0.4963	-0.4594	-0.4723
4	N	-0.4900	-0.5059	-0.4665	-0.4936	-0.4615	-0.4760
5	C	0.2894	0.3074	0.2628	0.2874	0.2571	0.2660
6	C	0.0768	0.0835	0.0579	0.0741	0.0475	0.0644
7	N	-0.4667	-0.4878	-0.4518	-0.4710	-0.4460	-0.4522
8	S	0.0607	0.0435	0.0682	0.0587	0.0627	0.0672
9	C	-0.3094	-0.3384	-0.3089	-0.3213	-0.3122	-0.3027
10	H	0.2780	0.2957	0.2758	0.2858	0.2840	0.2750
11	C	0.0514	0.0553	0.0331	0.0479	0.0222	0.0389
12	H	0.1795	0.2020	0.1851	0.1890	0.1835	0.1748
13	H	0.2742	0.2922	0.2747	0.2826	0.2806	0.2710
14	H	0.2583	0.2761	0.2563	0.2657	0.2633	0.2544
15	N	-0.8667	-0.9087	-0.8437	-0.8767	-0.8500	-0.8494
16	C	-0.1822	-0.2060	-0.1950	-0.1967	-0.2052	-0.1847
17	H	0.4460	0.4652	0.4432	0.4553	0.4495	0.4440
18	H	0.3207	0.3433	0.3221	0.3321	0.3314	0.3202
19	C	-0.6046	-0.6598	-0.6141	-0.6331	-0.6259	-0.5990
20	C	0.7857	0.8362	0.7452	0.7926	0.7321	0.7448
21	H	0.2878	0.3084	0.2908	0.3004	0.2969	0.2886
22	H	0.2602	0.2785	0.2645	0.2697	0.2695	0.2586
23	S	-0.0568	-0.0658	-0.0573	-0.0566	-0.0633	-0.0551
24	O	-0.5863	-0.6269	-0.5632	-0.5940	-0.5525	-0.5612
25	O	-0.6988	-0.7385	-0.6694	-0.7045	-0.6687	-0.6750
26	H	0.1627	0.1851	0.1672	0.1703	0.1713	0.1593
27	H	0.5170	0.5417	0.5103	0.5238	0.5139	0.5106
28	H	0.4517	0.4738	0.4491	0.4597	0.4523	0.4468
TOTAL		0.0000	0.0000	0.0000	0.0000	0.0000	0.0000

Table 2.2.4.2.2. (Continued)

ATOM		NBO Charge					
		2A	2B	2C	2D	2E	2F
1	Pt	0.4829	0.5061	0.4288	0.4692	0.4237	0.4516
2	Cl	-0.5064	-0.5248	-0.4771	-0.5050	-0.4736	-0.4857
3	Cl	-0.4895	-0.5196	-0.4620	-0.4929	-0.4635	-0.4689
4	N	-0.4876	-0.5100	-0.4640	-0.4906	-0.4574	-0.4724
5	C	0.2883	0.3051	0.2647	0.2851	0.2583	0.2660
6	C	0.0788	0.0848	0.0609	0.0771	0.0500	0.0675
7	N	-0.4721	-0.4952	-0.4556	-0.4765	-0.4503	-0.4569
8	S	0.0590	0.0409	0.0646	0.0598	0.0596	0.0664
9	C	-0.3109	-0.3411	-0.3098	-0.3227	-0.3133	-0.3037
10	H	0.2826	0.3014	0.2800	0.2898	0.2886	0.2789
11	C	0.0542	0.0595	0.0374	0.0507	0.0243	0.0417
12	H	0.1835	0.2095	0.1892	0.1925	0.1877	0.1786
13	H	0.2753	0.2944	0.2755	0.2836	0.2812	0.2718
14	H	0.2591	0.2778	0.2572	0.2666	0.2635	0.2550
15	S	0.0326	0.0427	0.0485	0.0452	0.0318	0.0398
16	C	-0.5461	-0.6087	-0.5613	-0.5777	-0.5727	-0.5408
17	C	-0.1986	-0.2167	-0.2114	-0.2124	-0.2277	-0.2035
18	H	0.2927	0.3114	0.2942	0.3030	0.3019	0.2898
19	H	0.2643	0.2879	0.2705	0.2754	0.2674	0.2611
20	N	-0.8992	-0.9446	-0.8830	-0.9125	-0.8941	-0.8819
21	H	0.3129	0.3236	0.3119	0.3215	0.3277	0.3120
22	C	0.7834	0.8380	0.7353	0.7912	0.7401	0.7432
23	O	-0.5975	-0.6413	-0.5693	-0.6064	-0.5607	-0.5708
24	O	-0.6977	-0.7282	-0.6759	-0.7022	-0.6628	-0.6754
25	H	0.5111	0.5355	0.5058	0.5181	0.5090	0.5055
26	H	0.2362	0.2655	0.2365	0.2470	0.2404	0.2295
27	H	0.4152	0.4348	0.4144	0.4222	0.4180	0.4112
28	H	0.3934	0.4117	0.3940	0.4007	0.4031	0.3906
TOTAL		**0.0000**	**0.0000**	**0.0000**	**0.0000**	**0.0000**	**0.0000**

2.2.4.3. Bonding Orbitals Analysis

Table 2.2.4.3.1. lists the calculated occupancies (electron densities) on NBO orbitals, hybrids on atoms and polarities of bonds between atoms. According to these results, the platinum atom forms two sigma bonds with the N4 and N15 atoms in complex 1 and one sigma bonds with the N atom and one sigma bond with S15 atom. The two coordination bonds between Pt, the nitrogen and sulphur can be described as a donation of electron density from donor nitrogen and sulphur orbitals to Pt acceptor orbitals. As follows from **Table 2.2.4.3.1.**, in the **1B** of complex 1, r(Pt–Cl2) and r(Pt-Cl3) bonds

are formed from an $sd^{1.13}$ and $sd^{1.17}$ hybrids on the platinum atom (which is the mixture of s(46.64) p(0.35) d(53.01)% and s(45.98) p(0.39) d(53.62)% atomic orbitals) and $sp^{7.97}$ and $sp^{8.67}$ hybrids on the chlorine atoms (88.85% and 89.66% p contribution). The r(Pt–Cl2) and r(Pt-Cl3) bonds are strongly polarized towards the chlorine, with about 76.32% and 74.47% of electron densities concentrated on the Cl2 and Cl3 atom, respectively. Similar hybridizations and polarity of the r(Pt–Cl2) and r(Pt-Cl3) bonds are noted for **2B** in complex 2 according to **Table 2.2.4.3.1.**. In complex 1, **1B** with BhandH structure has stronger bond polarity on Chlorine atoms and smaller bond polarity on Pt atom than others (**1A, 1C, 1D, 1E,** and **1F**). Similar statements are valid for **2B** with BhandH in complex 2. The results from NBO analysis have revealed a strong electronic conjugation between the Pt–Cl2 and Pt-Cl3 bonds.

According to the NBO results, the two N4 -> Pt and N15 -> Pt in ligands (2-mpym and L-cys) bonds in complex 1 correspond to electron donations from a lone pair orbital on the nitrogen atoms and the two N4 -> Pt and S15 -> Pt in ligands (2-mpym and L-cys) bonds in complex 2 correspond to electron donations from a lone pair orbital on the nitrogen, also sulphur atoms, LP(N) and LP(S), to the acceptor Pt molecular orbitals. The **1B** in complex 1, the lone electron pair orbital, LP(N4) has 79.15% p-character and it is occupied by 1.6809 electrons (very similar electron density is noted for the LP(N4) orbital in **2B** in complex 2). The LP(N15) orbital in the title complex has 88.67% p-character and is occupied by 1.7044 electrons, which

is consistent with a lower delocalization of electrondensity (from the idealized occupancy of 2.0e), in comparison to the LP(N4) orbital.

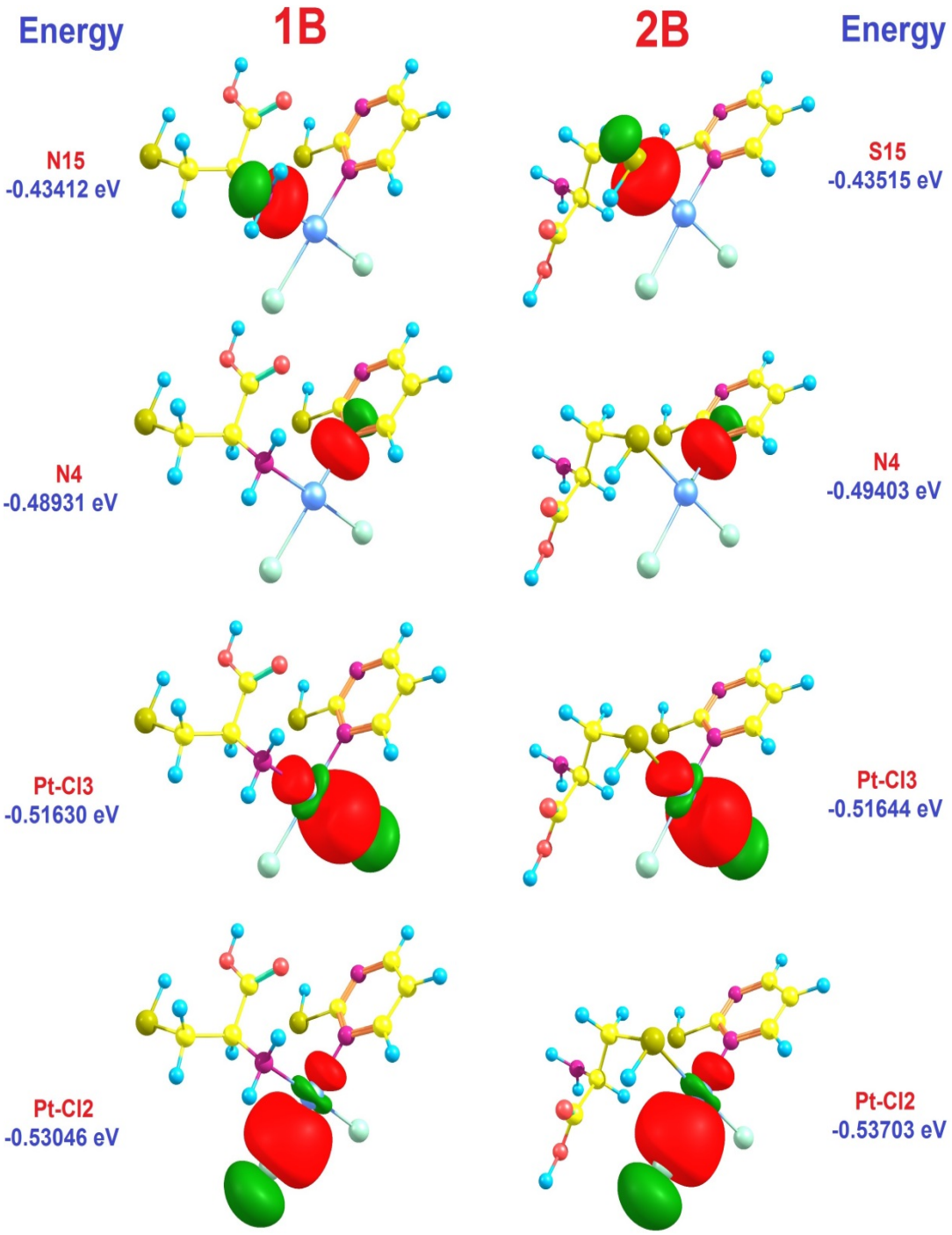

Figure 2.2.4.3.1. Natural bonding (2-center) and lone pair (1-center) orbitals and their energy levels. Atom colours: S; dark yellow, O; red, C; purple, and H; blue. Density colours: +; red, -; green.

Table 2.2.4.3.1. Occupancy (e^-), polarity (%) and atomic orbitals (%) of natural bond orbitals (NBOs) and hybrids calculated for complex 1 and 2.

Molecule	NBO Orbital[a]	Occupancy e^-	Polarity[b](%)	NBO Hybrid	AO (%)[c]
1A	σ(Pt - Cl2)	1.9682	24.85(Pt)	$sd^{1.14}$(Pt)	s(46.64) p(0.35) d(53.01)
			75.15(Cl2)	$sp^{10.81}$(Cl2)	s(8.47) p(91.53)
	σ(Pt - Cl3)	1.9645	27.04(Pt)	$sd^{1.18}$(Pt)	s(45.72) p(0.39) d(53.89)
			72.96(Cl3)	$sp^{12.01}$(Cl3)	s(7.69) p(92.31)
	LP(N4)	1.6812		$sp^{2.90}$	s(25.65) p(74.35)
	LP(N15)	1.6992		$sp^{5.57}$	s(15.21) p(84.79)
1B	σ(Pt - Cl2)	1.9726	23.68(Pt)	$sd^{1.13}$(Pt)	s(46.79) p(0.33) d(52.87)
			76.32(Cl2)	$sp^{7.97}$(Cl2)	s(11.15) p(88.85)
	σ(Pt - Cl3)	1.9693	25.53(Pt)	$sd^{1.17}$(Pt)	s(45.98) p(0.39) d(53.62)
			74.47(Cl3)	$sp^{8.67}$(Cl3)	s(10.34) p(89.66)
	LP(N4)	1.6809		$sp^{3.80}$	s(20.85) p(79.15)
	LP(N15)	1.7047		$sp^{7.82}$	s(11.33) p(88.67)
1C	σ(Pt - Cl2)	1.9613	26.12(Pt)	$sd^{1.13}$(Pt)	s(46.70) p(0.36) d(52.94)
			73.88(Cl2)	$sp^{12.28}$(Cl2)	s(7.53) p(92.47)
	σ(Pt - Cl3)	1.9564	29.00(Pt)	$sd^{1.18}$(Pt)	s(45.80) p(0.38) d(53.82)
			71.00(Cl3)	$sp^{14.14}$(Cl3)	s(6.6) p(93.39)
	LP(N4)	1.6564		$sp^{2.59}$	s(27.86) p(72.14)
	LP(N15)	1.6821		$sp^{4.88}$	s(17.00) p(83.00)
1D	σ(Pt - Cl2)	1.9685	25.01(Pt)	$sd^{1.13}$(Pt)	s(46.75) p(0.31) d(52.94)
			74.99(Cl2)	$sp^{9.82}$(Cl2)	s(9.24) p(90.76)
	σ(Pt - Cl3)	1.9648	27.08(Pt)	$sd^{1.18}$(Pt)	s(45.81) p(0.37) d(53.82)
			72.92(Cl3)	$sp^{10.82}$(Cl3)	s(8.46) p(91.54)
	LP(N4)	1.6768		$sp^{3.09}$	s(24.47) p(75.53)
	LP(N15)	1.6946		$sp^{6.17}$	s(13.95) p(86.05)
1E	σ(Pt - Cl2)	1.9639	26.46(Pt)	$sd^{1.15}$(Pt)	s(46.42) p(0.32) d(53.26)
			73.54(Cl2)	$sp^{11.40}$(Cl2)	s(8.06) p(90.94)
	σ(Pt - Cl3)	1.9590	29.21(Pt)	$sd^{1.19}$(Pt)	s(45.55) p(0.35) d(54.10)
			70.79(Cl3)	$sp^{13.02}$(Cl3)	s(7.13) p(92.87)
	LP(N4)	1.6442		$sp^{2.69}$	s(27.13) p(72.87)
	LP(N15)	1.6676		$sp^{5.21}$	s(16.10) p(83.90)
1F	σ(Pt - Cl2)	1.9655	25.85(Pt)	$sd^{1.15}$(Pt)	s(46.38) p(0.31) d(53.31)
			74.15(Cl2)	$sp^{11.69}$(Cl2)	s(7.88) p(92.12)
	σ(Pt - Cl3)	1.9610	28.41(Pt)	$sd^{1.19}$(Pt)	s(45.45) p(0.35) d(54.20)
			71.59(Cl3)	$sp^{13.25}$(Cl3)	s(7.02) p(92.98)
	LP(N4)	1.6591		$sp^{2.56}$	s(28.10) p(71.90)
	LP(N15)	1.6787		$sp^{4.79}$	s(17.28) p(82.72)

Table 2.2.4.3.1. (Continued)

Molecule	NBO Orbital[a]	Occupancy e⁻	Polarity[b](%)	NBO Hybrid	AO (%)[c]
2A	σ(Pt - Cl2)	1.9652	25.65(Pt)	$sd^{1.18}$(Pt)	s(46.62) p(0.35) d(53.03)
			74.35(Cl2)	$sp^{10.63}$(Cl2)	s(8.60) p(91.40)
	σ(Pt - Cl3)	1.9628	28.49(Pt)	$sd^{1.07}$(Pt)	s(48.16) p(0.35) d(51.49)
			71.51(Cl3)	$sp^{13.29}$(Cl3)	s(7.00) p(93.00)
	LP(N4)	1.6781		$sp^{2.89}$	s(25.72) p(74.28)
	LP(S15)	1.6463		$sp^{3.96}$	s(20.14) p(79.86)
2B	σ(Pt - Cl2)	1.9688	24.45(Pt)	$sd^{1.17}$(Pt)	s(45.85) p(0.35) d(53.81)
			75.55(Cl2)	$sp^{7.92}$(Cl2)	s(11.22) p(88.78)
	σ(Pt - Cl3)	1.9672	26.94(Pt)	$sd^{1.06}$(Pt)	s(48.34) p(0.41) d(51.25)
			73.06(Cl3)	$sp^{9.54}$(Cl3)	s(9.49) p(90.51)
	LP(N4)	1.6809		$sp^{3.76}$	s(21.01) p(78.99)
	LP(S15)	1.6334		$sp^{3.66}$	s(21.45) p(78.55)
2C	σ(Pt - Cl2)	1.9577	27.32(Pt)	$sd^{1.19}$(Pt)	s(45.45) p(0.35) d(54.20)
			72.68(Cl2)	$sp^{12.17}$(Cl2)	s(7.59) p(92.41)
	σ(Pt - Cl3)	1.9544	30.28(Pt)	$sd^{1.06}$(Pt)	s(48.49) p(0.32) d(51.18)
			69.72(Cl3)	$sp^{15.47}$(Cl3)	s(6.07) p(93.93)
	LP(N4)	1.6561		$sp^{2.58}$	s(27.89) p(72.11)
	LP(S15)	1.6302		$sp^{4.18}$	s(19.32) p(80.68)
2D	σ(Pt - Cl2)	1.9650	25.76(Pt)	$sd^{1.18}$(Pt)	s(45.76) p(0.32) d(53.92)
			74.24(Cl2)	$sp^{9.67}$(Cl2)	s(9.37) p(90.63)
	σ(Pt - Cl3)	1.9628	27.08(Pt)	$sd^{1.18}$(Pt)	s(48.21) p(0.35) d(51.44)
			72.92(Cl3)	$sp^{10.82}$(Cl3)	s(7.72) p(92.28)
	LP(N4)	1.6724		$sp^{3.08}$	s(24.49) p(75.51)
	LP(S15)	1.6331		$sp^{3.86}$	s(20.57) p(79.43)
2E	σ(Pt - Cl2)	1.9622	26.98(Pt)	$sd^{1.19}$(Pt)	s(45.58) p(0.32) d(54.10)
			73.02(Cl2)	$sp^{10.93}$(Cl2)	s(8.38) p(91.62)
	σ(Pt - Cl3)	1.9585	30.43(Pt)	$sd^{1.08}$(Pt)	s(47.91) p(0.31) d(51.78)
			69.57(Cl3)	$sp^{14.30}$(Cl3)	s(6.54) p(93.46)
	LP(N4)	1.6406		$sp^{2.68}$	s(27.19) p(72.81)
	LP(S15)	1.6018		$sp^{4.15}$	s(19.42) p(80.58)
2F	σ(Pt - Cl2)	1.9626	26.64(Pt)	$sd^{1.20}$(Pt)	s(45.34) p(0.31) d(54.35)
			73.36(Cl2)	$sp^{11.42}$(Cl2)	s(8.05) p(91.95)
	σ(Pt - Cl3)	1.9595	29.82(Pt)	$sd^{1.08}$(Pt)	s(48.03) p(0.30) d(51.66)
			70.18(Cl3)	$sp^{14.62}$(Cl3)	s(6.40) p(93.60)
	LP(N4)	1.6564		$sp^{2.56}$	s(28.13) p(71.87)
	LP(S15)	1.6235		$sp^{4.30}$	s(18.86) p(81.14)

[a] *LP(N) is a valence lone pair orbital on N atom;*
[b] *Values for the A–B sigma molecular orbital;*
[c] *Percentage contribution of atomic orbitals in NBO hybrid.*

In addition, natural bond orbital analysis showed in **Figure 2.2.4.3.1.** as pictures of bonding (2-center) and lone pair (1-center). **1B** and **2B** complexes comparised energy values in terms of their energy values. **2B** has the lower values than **1B**.

2.2.4.4. Molecular Orbital Analysis

The molecular orbital theory provides an analysis of canonical (delocalized) MOs in terms of their leading NBO contributions. Each MO φ_i can be expressed in terms of the complete orthonormal set of NBOs $\{\Omega_\alpha\}$ by the equation,

$$\varphi_i = \Sigma_\alpha \, \Omega_\alpha t_{\alpha i} \qquad \textbf{(9)}$$

the coefficients $t_{\alpha i}$ (elements of the NBOMO transformation matrix) determine the percentage contribution ($100*|t_{\alpha i}|^2$) of each NBO to the LCNBO-MO expansion of φ_i. Each coefficient $t_{\alpha i}$ can in turn be identified with an NBO Ω_α of bonding ($t_{\alpha i}^{(b)}$), nonbonding ($t_{\alpha i}^{(n)}$), or antibonding ($t_{\alpha i}^{(a)}$) character. By adding the percentage contributions of each NBO type, one obtains a convenient measure of the total bonding (b), nonbonding (n), or antibonding (a) character of each MO. These in turn can be decomposed into the contributions from individual atomic centers, leading to a detailed description of the “atom-atom bonding character” of each MO.

Table 2.2.4.4.1. Molecular orbital analysis of complexes 1 and 2 from 1A to 2F. Energy (eV), MOs (given HOMO- and LUMO+ molecular orbitals), and atomic contributions (%).

	MOs	Energy	% Atom Contributions
1A	**HOMO-4**	-6.7733	Cl2(LP)$^{50.3}$; Cl3(LP)$^{17.5}$; Pt(LP)$^{7.3}$
	HOMO-3	-6.5892	Pt(LP)$^{100.0}$
	HOMO-2	-6.4209	Pt(LP)$^{50.4}$; Cl3(LP)$^{14.2}$; Cl2(LP)$^{35.4}$
	HOMO-1	-6.3488	Cl3(LP)$^{71.9}$; Pt(LP)$^{28.1}$
	HOMO	**-6.1186**	**Cl3(LP)$^{45.3}$; Pt(LP)$^{34.8}$; Cl2(LP)$^{19.9}$**
	LUMO	**-2.6321**	**N4-C6*(B*2)$^{36.7}$; C9-C11*(B*2)$^{25.8}$; C5-N7(B2)$^{19.7}$; C9-C11(B2)$^{17.7}$**
	LUMO+1	-1.9795	C5-N7*(B*2)$^{34.7}$; C9-C11*(B*2)$^{21.8}$; N4-C6(B2)$^{16.8}$; C9-C11(B2)$^{14.8}$; S8(LP)$^{11.8}$
1B	**MOs**	**Energy**	**% Atom Contributions**
	HOMO-4	-8.1983	Cl2(LP)$^{48.8}$; Cl3(LP)$^{13.2}$; Pt(LP)$^{38.1}$
	HOMO-3	-8.1527	Pt(LP)$^{59.6}$; Cl3(LP)$^{10.5}$; Cl2(LP)$^{19.1}$; Pt-Cl3(B1)$^{10.7}$
	HOMO-2	-7.9006	Pt(LP)$^{44.1}$; Cl3(LP)$^{16.8}$; Cl2(LP)$^{38.0}$
	HOMO-1	-7.7417	Cl3(LP)$^{73.2}$; Pt(LP)$^{26.8}$
	HOMO	**-7.5062**	**Cl3(LP)$^{46.7}$; Pt(LP)$^{31.4}$; Cl2(LP)$^{21.9}$**
	LUMO	**-1.3139**	**N4-C6*(B*2)$^{36.4}$; C9-C11*(B*2)$^{26.5}$; C5-N7(B2)$^{19.7}$; C9-C11(B2)$^{17.4}$**
	LUMO+1	-0.6601	C5-N7*(B*2)$^{38.8}$; C9-C11*(B*2)$^{25.3}$; N4-C6(B2)$^{19.0}$; C9-C11(B2)$^{16.9}$
1C	**MOs**	**Energy**	**% Atom Contributions**
	HOMO-4	-5.9185	Cl2(LP)$^{55.6}$; Cl3(LP)$^{25.7}$; Pt(LP)$^{18.7}$
	HOMO-3	-5.6215	Pt(LP)$^{100.0}$
	HOMO-2	-5.4798	Cl2(LP)$^{39.7}$; Pt(LP)$^{60.3}$
	HOMO-1	-5.4329	Cl3(LP)$^{68.8}$; Pt(LP)$^{31.2}$
	HOMO	**-5.2051**	**Cl3(LP)$^{44.5}$; Pt(LP)$^{38.0}$; Cl2(LP)$^{17.5}$**
	LUMO	**-3.3856**	**N4-C6*(B*2)$^{37.2}$; C9-C11*(B*2)$^{24.9}$; C5-N7(B2)$^{19.5}$; C9-C11(B2)$^{18.4}$**
	LUMO+1	-2.7574	C5-N7*(B*2)$^{34.1}$; C9-C11*(B*2)$^{21.8}$; N4-C6(B2)$^{16.3}$; C9-C11(B2)$^{14.2}$; S8(LP)$^{13.7}$
1D	**MOs**	**Energy**	**% Atom Contributions**
	HOMO-4	-7.0829	Cl2(LP)$^{36.7}$; Cl3(LP)$^{49.2}$; Pt(LP)$^{14.1}$
	HOMO-3	-6.9343	Pt(LP)$^{100.0}$
	HOMO-2	-6.7359	Cl2(LP)$^{35.9}$; Cl3(LP)$^{49.8}$; Pt(LP)$^{14.3}$
	HOMO-1	-6.6343	Cl3(LP)$^{61.7}$; Pt(LP)$^{25.5}$; Cl2(LP)$^{12.7}$
	HOMO	**-6.4114**	**Cl3(LP)$^{45.5}$; Pt(LP)$^{34.4}$ Cl2(LP)$^{20.1}$**
	LUMO	**-2.4867**	**N4-C6*(B*2)$^{36.7}$; C9-C11*(B*2)$^{26.0}$; C5-N7(B2)$^{19.7}$; C9-C11(B2)$^{17.7}$**
	LUMO+1	-1.8302	C5-N7*(B*2)$^{34.6}$; C9-C11*(B*2)$^{22.0}$; N4-C6(B2)$^{116.8}$; C9-C11(B2)$^{14.7}$; S8(LP)$^{11.9}$
1E	**MOs**	**Energy**	**% Atom Contributions**
	HOMO-4	-5.8132	Cl2(LP)$^{54.2}$; Cl3(LP)$^{26.9}$; Pt(LP)$^{18.8}$
	HOMO-3	-5.5230	Pt(LP)$^{100.0}$
	HOMO-2	-5.3565	Cl2(LP)$^{39.6}$; Pt(LP)$^{60.4}$
	HOMO-1	-5.3152	Cl3(LP)$^{63.7}$; Pt(LP)$^{36.3}$
	HOMO	**-5.0625**	**Cl3(LP)$^{37.3}$; Pt(LP)$^{38.1}$ Cl2(LP)$^{17.5}$**
	LUMO	**-3.2604**	**N4-C6*(B*2)$^{36.7}$; C9-C11*(B*2)$^{24.8}$; C5-N7(B2)$^{19.5}$; C9-C11(B2)$^{18.4}$**
	LUMO+1	-2.6565	C20-O24*(B*2)$^{28.5}$; C5-N7*(B*2)$^{28.2}$; C9-C11*(B*2)$^{17.9}$; N4-C6(B2)$^{13.8}$; C9-C11(B2)$^{11.6}$
1F	**MOs**	**Energy**	**% Atom Contributions**
	HOMO-4	-5.7804	Cl2(LP)$^{54.3}$; Cl3(LP)$^{27.6}$; Pt(LP)$^{18.0}$
	HOMO-3	-5.4665	Pt(LP)$^{100.0}$
	HOMO-2	-5.3303	Cl2(LP)$^{39.3}$; Pt(LP)$^{60.7}$
	HOMO-1	-5.3031	Cl3(LP)$^{63.4}$; Pt(LP)$^{36.6}$
	HOMO	**-5.0460**	**Cl3(LP)$^{44.7}$; Pt(LP)$^{37.4}$ Cl2(LP)$^{18.0}$**
	LUMO	**-3.1621**	**N4-C6*(B*2)$^{37.2}$; C9-C11*(B*2)$^{25.0}$; C5-N7(B2)$^{19.5}$; C9-C11(B2)$^{18.3}$**
	LUMO+1	-2.5335	C20-O24*(B*2)$^{21.1}$; C5-N7*(B*2)$^{31.3}$; C9-C11*(B*219.5; N4-C6(B2)$^{15.2}$; C9-C11(B2)$^{12.9}$

Table 2.2.2.4.4.1. (Continued)

	MOs	Energy	% Atom Contributions
2A	**HOMO-4**	-6.6376	$Pt(LP)^{72.0}$; $N20(LP)^{28.0}$
	HOMO-3	-6.5993	$Cl2(LP)^{48.4}$; $Cl3(LP)^{36.6}$; $N20(LP)^{15.0}$
	HOMO-2	-6.4755	$Cl2(LP)^{24.9}$; $Cl3(LP)^{34.5}$; $Pt(LP)^{40.6}$
	HOMO-1	-6.4222	$Cl2(LP)^{21.4}$; $Cl3(LP)^{46.2}$; $Pt(LP)^{32.4}$
	HOMO	**-6.2153**	**$Cl3(LP)^{29.5}$; $Pt(LP)^{42.4}$; $Cl2(LP)^{28.1}$**
	LUMO	**-2.6213**	**$N7\text{-}C11*(B*2)^{32.1}$; $N4\text{-}C5*(B*2)^{19.7}$; $C6\text{-}C9*(B*2)^{15.6}$; $C6\text{-}C9(B2)^{19.4}$; $N4\text{-}C5(B2)^{13.2}$**
	LUMO+2	-1.9409	$C6\text{-}C9*(B*2)^{26.9}$ $N4\text{-}C5*(B*2)^{26.2}$; $N7\text{-}C11(B2)^{16.6}$; $Pt\text{-}Cl3*(B*2)^{16.5}$; $Pt\text{-}Cl2*(B*2)^{13.8}$
2B	**MOs**	**Energy**	**% Atom Contributions**
	HOMO-4	-8.1372	$N20(LP)^{45.3}$; $Pt(LP)^{35.5}$; $Cl3(LP)^{19.2}$
	HOMO-3	-7.9832	$Cl2(LP)^{48.4}$; $Cl3(LP)^{52.1}$;$Pt(LP)^{14.3}$
	HOMO-2	-7.9746	$Cl2(LP)^{34.0}$; $Cl3(LP)^{15.0}$; $Pt(LP)^{37.7}$; $N20(LP)^{13.3}$
	HOMO-1	-7.8755	$Cl2(LP)^{28.5}$; $Cl3(LP)^{45.5}$; $Pt(LP)^{26.0}$
	HOMO	**-7.6472**	**$Cl3(LP)^{35.0}$; $Pt(LP)^{34.4}$; $Cl2(LP)^{30.6}$**
	LUMO	**-1.3696**	**$N7\text{-}C11*(B*2)^{32.2}$; $N4\text{-}C5*(B*2)^{19.9}$; $C6\text{-}C9*(B*2)^{15.5}$; $C6\text{-}C9(B2)^{19.5}$; $N4\text{-}C5(B2)^{12.8}$**
	LUMO+1	-0.6664	$C6\text{-}C9*(B*2)^{35.0}$ $N4\text{-}C5*(B*2)^{31.4}$; $N7\text{-}C11(B2)^{20.7}$; $S8(LP)^{12.9}$
2C	**MOs**	**Energy**	**% Atom Contributions**
	HOMO-4	-5.7355	$Cl2(LP)^{28.0}$; $Cl3(LP)^{26.6}$; $Pt(LP)^{31.6}$; $N20(LP)^{13.8}$
	HOMO-3	-5.6580	$N20(LP)^{35.0}$; $Pt(LP)^{51.3}$; $O23(LP)^{13.7}$
	HOMO-2	-5.5407	$Cl2(LP)^{24.2}$; $Cl3(LP)^{40.7}$; $Pt(LP)^{35.1}$
	HOMO-1	-5.5039	$Cl2(LP)^{25.9}$; $Cl3(LP)^{36.6}$; $Pt(LP)^{37.5}$
	HOMO	**-5.3150**	**$Cl3(LP)^{33.6}$; $Pt(LP)^{41.6}$; $Cl2(LP)^{24.8}$**
	LUMO	**-3.3899**	**$N7\text{-}C11*(B*2)^{32.1}$; $N4\text{-}C5*(B*2)^{18.8}$; $C6\text{-}C9*(B*2)^{16.3}$; $C6\text{-}C9(B2)^{19.2}$; $N4\text{-}C5(B2)^{13.7}$**
	LUMO+2	-2.7412	$C6\text{-}C9*(B*2)^{32.5}$ $N4\text{-}C5*(B*2)^{32.1}$; $N7\text{-}C11(B2)^{20.4}$; $S8(LP)^{15.0}$
2D	**MOs**	**Energy**	**% Atom Contributions**
	HOMO-4	-6.9727	$Pt(LP)^{74.1}$; $N20(LP)^{25.9}$
	HOMO-3	-6.9120	$Cl2(LP)^{47.4}$; $Cl3(LP)^{32.1}$; $N20(LP)^{20.6}$
	HOMO-2	-6.8029	$Cl2(LP)^{34.5}$; $Cl3(LP)^{24.7}$; $Pt(LP)^{40.9}$
	HOMO-1	-6.7254	$Cl2(LP)^{21.9}$; $Cl3(LP)^{43.5}$; $Pt(LP)^{34.6}$
	HOMO	**-6.5230**	**$Cl3(LP)^{30.8}$; $Pt(LP)^{41.6}$; $Cl2(LP)^{27.6}$**
	LUMO	**-2.4765**	**$N7\text{-}C11*(B*2)^{32.1}$; $N4\text{-}C5*(B*2)^{19.5}$; $C6\text{-}C9*(B*2)^{15.8}$; $C6\text{-}C9(B2)^{19.4}$; $N4\text{-}C5(B2)^{13.2}$**
	LUMO+1	-1.8128	$C6\text{-}C9*(B*2)^{34.2}$ $N4\text{-}C5*(B*2)^{31.5}$; $N7\text{-}C11(B2)^{20.6}$; $S8(LP)^{13.7}$
2E	**MOs**	**Energy**	**% Atom Contributions**
	HOMO-4	-5.5128	$Cl2(LP)^{31.9}$; $Cl3(LP)^{14.1}$; $Pt(LP)^{40.2}$; $N20(LP)^{13.8}$
	HOMO-3	-5.4504	$Cl2(LP)^{14.1}$; $Pt(LP)^{44.8}$; $N20(LP)^{41.2}$
	HOMO-2	-5.3486	$Cl2(LP)^{21.9}$; $Cl3(LP)^{32.3}$; $Pt(LP)^{45.8}$
	HOMO-1	-5.2835	$Cl2(LP)^{21.5}$; $Cl3(LP)^{26.4}$; $Pt(LP)^{35.6}$; $N20(LP)^{16.5}$
	HOMO	**-5.0923**	**$Cl3(LP)^{32.6}$; $Pt(LP)^{50.7}$; $Cl2(LP)^{16.7}$**
	LUMO	**-3.1830**	**$N7\text{-}C11*(B*2)^{32.1}$; $N4\text{-}C5*(B*2)^{18.6}$; $C6\text{-}C9*(B*2)^{16.3}$; $C6\text{-}C9(B2)^{19.2}$; $N4\text{-}C5(B2)^{13.8}$**
	LUMO+1	-2.5760	$C6\text{-}C9*(B*2)^{21.5}$ $N4\text{-}C5*(B*2)^{20.1}$; $N7\text{-}C11(B2)^{113.3}$; $S15(LP)^{11.2}$ $Pt\text{-}Cl3*(B*2)^{18.7}$; $Pt\text{-}Cl2*(B*2)^{15.2}$
2F	**MOs**	**Energy**	**% Atom Contributions**
	HOMO-4	-5.5498	$Cl2(LP)^{16.7}$; $Cl3(LP)^{29.3}$; $Pt(LP)^{35.2}$; $N20(LP)^{18.8}$
	HOMO-3	-5.4809	$Pt(LP)^{61.5}$; $N20(LP)^{38.5}$
	HOMO-2	-5.3937	$Cl2(LP)^{22.2}$; $Cl3(LP)^{30.8}$; $Pt(LP)^{47.0}$
	HOMO-1	-5.3458	$Cl2(LP)^{23.5}$; $Cl3(LP)^{29.6}$; $Pt(LP)^{36.6}$; $N20(LP)^{10.2}$
	HOMO	**-5.1441**	**$Cl3(LP)^{28.0}$; $Pt(LP)^{44.2}$; $Cl2(LP)^{27.3}$**
	LUMO	**-3.1263**	**$N7\text{-}C11*(B*2)^{28.1}$; $N4\text{-}C5*(B*2)^{18.9}$; $C6\text{-}C9*(B*2)^{16.2}$; $C6\text{-}C9(B2)^{19.3}$; $N4\text{-}C5(B2)^{13.7}$**
	LUMO+1	-2.5760	$C6\text{-}C9*(B*2)^{32.4}$ $N4\text{-}C5*(B*2)^{32.4}$; $N7\text{-}C11(B2)^{20.5}$; $S8(LP)^{14.6}$

Detailed properties of molecular orbital analysis showed In **Table 2.2.4.4.1.**. Both complex 1 and 2 was investigated as sum of lone pair, bonding and anti-bonding contributions with their orbital energies for all DFT functions. According to In **Table 2.2.4.4.1.**, **1B** in complex 1 and **2B** in complex 2 have lower values than others in terms of orbital energies. Generally, complexes are classified as HOMO-4, HOMO-3, HOMO-2, HOMO-1, HOMO, LUMO, LUMO+1 and have about same bonding percentange contributions. For example, **2B** compound for complex 2 has %45.3 (N20; lone pair), %36.5 (Pt; lone pair), and %19.2 (Cl3; lone pair) for HOMO-4 orbital. From **Table 2.2.4.4.1.**, ocuppied orbitals have generally lone pairs (as Pt, Cl2, Cl3, and N20) expect ligand (2-mercaptopyrimidine and L-cysteine). But, orbitals of LUMO and LUMO+ have generally bonding and anti-bonding and sometimes lone pairs of ligand parts of complex 1 and 2. For **2B,** HOMO orbital forms distributions of %35.0 (Cl3; lone pair), %34.4 (Pt; lone pair), and %30.6 (Cl2; lone pair). In here, percentanges of lone pair have about closely values. Again, LUMO orbital has %32.2 (N7-C11; π anti-bonding), %19.9 (N4-C5; π anti-bonding), %19.5 (C6-C9; π bonding), %15.5 (C6-C9; π anti-bonding), and %12.8 (N4-C5; π bonding). From these values, percentanges of lone pair have about closely.

Molecular orbitals pictures of **1B** and **2B** showed in **Figure 2.2.4.4.1.** Energy values were seen from HOMO-4 to LUMO+1 as energy diagram. Red electron density of red and green colour are positive and negative, respectively.

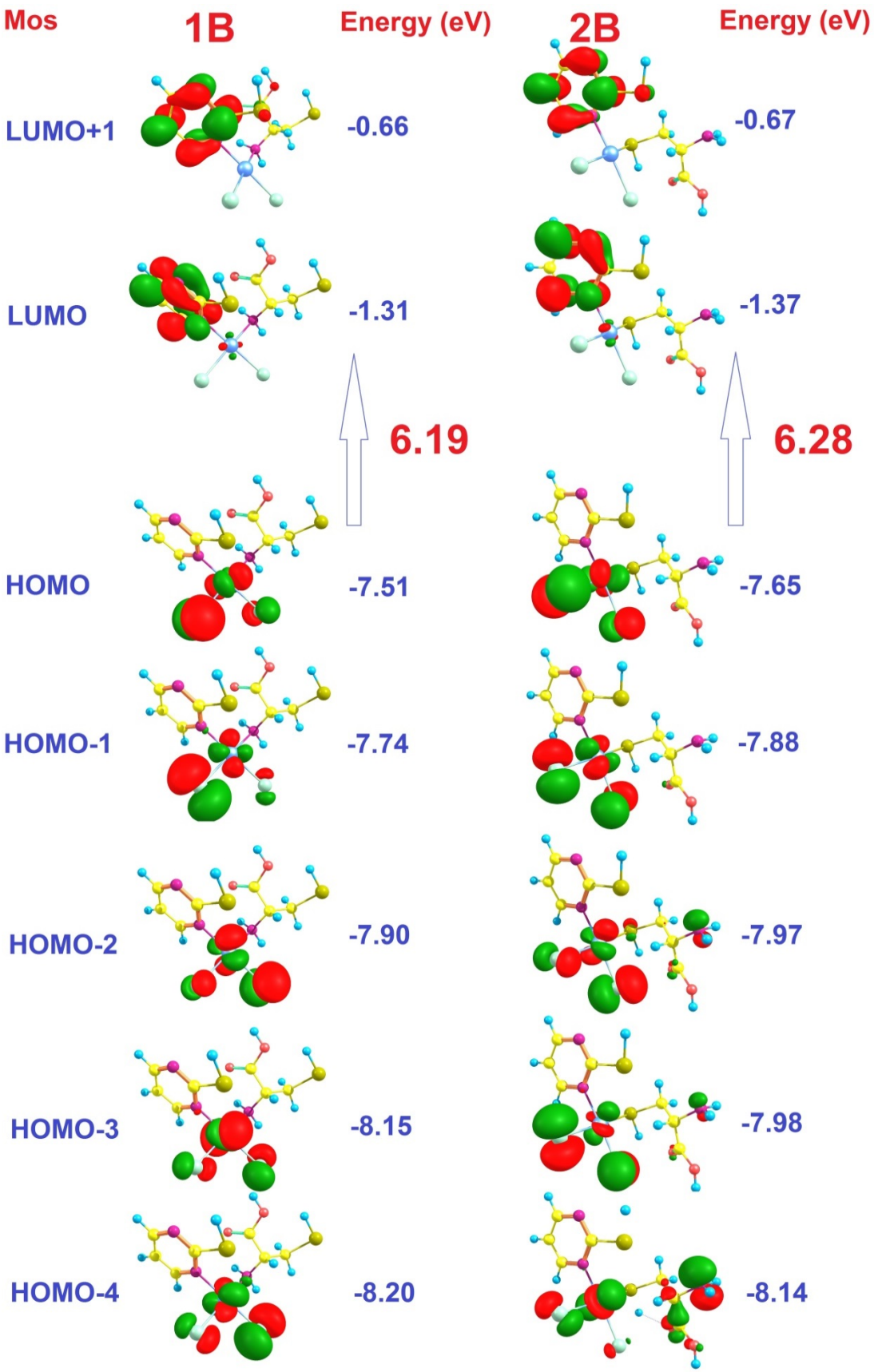

Figure 2.2.4.4.1. Molecular orbitals pictures of 1B and 2B with energies.

2.2.5. Vibrational Spectroscopic Analysis

In **Table 2.2.5.1a.** and **Table 2.2.5.1b.** the FT-IR wavenumbers of **1B** in complex above 700 cm^{-1} bands and **2B** in complex 2 above 400 cm^{-1} bands are illustrated in ligands of 2-mercaptopyrimidine and L-cysteine of complexes are added this table. In **Table 2.2.5.2a.** and **2.2.5.2b.** lists the wavenumbers of the bands observed in the region below 700 cm^{-1} and 400 cm^{-1} in 1B and 2B as theoretical frequencies, respectively. (the frequencies calculated with only the most function of BHANDH are listed, for comparison). PED column of Tables shows the calculated potential energy distribution (PED). PED analysis have been done with VEDA software. Generally, the modes has many mixing of different vibrations.

2.2.5.1. L-cysteine Ligand

In **1B** complex, the modes of 4, 7, 15, 21-23, 26, 28, 30, 34, 36, 38-41, 45-47, 49, 51, 52, 55, 57-60, and 64-66 are listed in **Table 2.2.5.1a.** and In **2B** complex, the modes of 4, 13, 16-20, 22-25, 29, 31, 35, 38-41, 44, 46-49, 54-56, 58-60, 64-66 are listed in **Table 2.2.5.1b.**. The streching vibration wavenumbers of OH are seen in mode 66 (3778.66 cm^{-1}) of **1B**, while in mode 65 in **2B** (3814.32 cm^{-1}). The angular vibration wavenumbers of OH are found in modes of 41 (%26), 38 (%46), 23 (%13), 19 (%16) and 18 (%60) of **1B,** in contrast in modes of 49 (%24), 39 (%51), 20 (%48), and 18 (%32) of **2B**. The $v(NH_2)$ of **1B** and **2B** is 3607.66 and 3814.32 as asymmertric

vibration. The symmetric streching vibration of v(NH_2) is 3490.97 and 3685.50 cm^{-1} in **1B** and **2B**, respectively. These vibration values of **2B** values higher than **1B** because of platin is bounded to N15 atom in **1B**. The angular vibration modes of NH_2 is found several modes of both **1B** and **2B**. For example, mode 52 in **1B** and mode 54 in **2B** have this vibration kind of 1690.12 and 1743.43 cm^{-1}, respectively. Next, two kind vibration kind is formed as CH and CH_2 in L-cystein ligand. So, different bands is determined from vibrational PED analysis. The modes 58 and 60 have streching vibration of CH_2 (3228.79 cm^{-1}; asymmetric, 3156.86 cm^{-1}; symmetric) in **1B**. Similarly, the modes 58 and 60 have streching vibration of CH_2 (3288.26 cm^{-1}; asymmetric, 3188.89 cm^{-1}; symmetric) in **2B**. The CH streching vibration has one band of mode 59 in **1B** and mode 58 in **2B**. Many angular vibration modes can be classified in the tables as both CH and CH_2. The S-H streching vibration in L-cystein is mode 57 in **1B** (2605.81 cm^{-1}) and mode 56 in **2B** (2479.72 cm^{-1})**.** The S-H streching vibration of **2B** compound has the lowest wavenumber value because of bonding between S atom in L-cystein and platin. The angular SH vibration is found in different modes below 1100 cm^{-1}. The streching vibrations of C=O bond in both **1B** and **2B** are investigated as mode 55 (1853.64, cm^{-1} and 1835.58 cm^{-1}, respectively). The C-O bond streching vibrations of **1B** and **2B** are 1421.72 in mode 47 and 1513.79 cm^{-1} in mode 49. This bond has out of plane vibrations below 800 cm^{-1},aiso it is attended many modes as angular vibrations. For example, it is found in mode 16 of **2B** complex how has rate of %57 PED and the angular vibration values in both **1B** and **2B** are below 700 cm^{-1} for CO bonds. Finally,

S-C streching vibrations have found below 900 cm^{-1}. The best values for this vibration type are for **1B** in mode 26 and for **2B** in mode 25.

Table 2.2.5.1a. Theoretical frequencies of ligands (cm^{-1}) of 1B complex.

NO	1B With BHANDH In Molecule 1		
	PED(%)[a]	Ligand[b]	IR
66	ν(OH) (100)	L-cys	3778.66
65	ν(NH_2) (-100), Asym	L-cys	3607.30
64	ν(NH_2) (100), Sym	L-cys	3490.97
63	ν(C9,C6-H) (91), Sym	2-mpym	3351.95
62	ν(C9,C6-H) (-86), Asym	2-mpym	3336.34
61	ν(C9,C6-H) (10) & ν(C11-H) (87)	2-mpym	3320.13
60	ν(CH_2) (-96), Asym	L-cys	3228.79
59	ν(CH) (93)	L-cys	3181.16
58	ν(CH_2) (93), Sym	L-cys	3156.86
57	ν(S23-H) (100)	L-cys	2605.81
56	ν(S8-H) (100)	2-mpym	2590.81
55	ν(C=O) (81)	L-cys	1853.64
54	ν(C-C) (77)	2-mpym	1731.20
53	ν(C=C) (-58) & δ(CN) (-28)	2-mpym	1695.45
52	δ(NH_2) (72)	L-cys	1690.12
51	ν(C-C) (13) & δ(CH_2) (30)	L-cys	1552.04
50	ν(N=C) (39) & δ(CH) (43)	2-mpym	1533.46
49	δ(CH) (75)	L-cys	1528.51
48	ν(C-C) (13) & δ(N-C) (-24) & δ(CH) (43)	2-mpym	1520.25
47	ν(C-O) (33) & δ(NH) (28)	L-cys	1421.72
46	δ(CC) (27) & δ(CS23) (-10) & τ(CH) (30)	L-cys	1393.59
45	δ(NH_2) (-10) & δ(CH_2) (19) & τ(CH) (36)	L-cys	1370.24
44	ν(N=C) (49) & δ(CH) (39)	2-mpym	1359.39
43	ν(N=C) (-59) & δ(CH) (-16)	2-mpym	1338.99
42	δ(CN) (-28) & ν(S8-C) (15) & δ(CH) (37)	2-mpym	1302.86
41	δ(OH) (26) & δ(CH) (10) & δ(NH_2) (35)	L-cys	1287.67
40	δ(NH_2) (12) & δ(CH) (20) & τ(CH_2) (-47)	L-cys	1281.90
39	δ(NH_2) (15) & δ(CH) (32) & τ(CH_2) (28)	L-cys	1241.96
38	ν(C-O) (-22) & δ(OH) (46)	L-cys	1212.63
37	δ(CH) (72)	2-mpym	1200.53
36	ν(coor) (88)	L-cys	1167.20
35	δ(CH) (84)	2-mpym	1157.17
34	δ(C-C) (53) & δ(NH_2) (19)	L-cys	1118.27

Table 2.2.5.1a. (Contiuned)

33	ν(N=C) (31) & δ(Ring) (55)	2-mpym	1110.69
32	τ(CH) (88)	2-mpym	1091.85
31	τ(CH) (-84)	2-mpym	1063.30
30	δ(S23H) (-23) & τ(CH_2) (-28)	L-cys	1055.72
29	δ(S8-H) (92)	2-mpym	934.89
28	δ(C-C) (-17) & & δ(S23H) (-28) & τ(NH_2) (-11)	L-cys	927.93
27	τ(CH) (65)	2-mpym	882.13
26	ν(C-S23) (39)	L-cys	844.35
25	τ(Ring) (-81)	2-mpym	841.59
24	ν(C-S8) (18) & δ(Ring) (69)	2-mpym	817.77
23	ν(C-C) (17) & δ(OH) (13) & τ(NH_2) (-41)	L-cys	804.45
22	δ(S23H) (30) & τ(CH_2) (-19) & γ(CO) (-11)	L-cys	781.52
21	δ(S23H) (25) & γ(CO) (-50)	L-cys	746.44
20	δ(Ring) (78)	2-mpym	706.82

Table 2.2.5.1b. Theoretical frequencies of ligands (cm^{-1}) of 2B complex.

NO	**2B With BHANDH In Molecule 2**		
	PED(%)[a]	**Ligand[b]**	**IR**
66	ν(NH_2) (-98), Asym	L-cys	3814.32
65	ν(OH) (100)	L-cys	3794.49
64	ν(NH_2)(-98), Sym	L-cys	3685.50
63	ν(C9,C6-H) (96), Sym	2-mpym	3353.06
62	ν(C9,C6-H) (-86), Asym	2-mpym	3337.90
61	ν(C9,C6-H) (-10) & ν(C11-H) (-82)	2-mpym	3320.88
60	ν(CH_2) (-100), Asym	L-cys	3288.26
59	ν(CH_2) (99), Sym	L-cys	3188.89
58	ν(CH) (98)	L-cys	3129.11
57	ν(S8-H) (100)	2-mpym	2600.01
56	ν(S15-H) (100)	L-cys	2479.72
55	ν(C=O) (83)	L-cys	1835.58
54	δ(NH_2) (87)	L-cys	1743.43
53	ν(C=C) (-54) & δ(CN) (-30)	2-mpym	1728.74
52	ν(C-C) (-24) & ν(N=C) (24) & δ(CN) (20)	2-mpym	1691.65
51	ν(C-N) (21) & δ(CH) (58)	2-mpym	1530.97
50	ν(C=N) (23) & δ(CH) (58)	2-mpym	1521.10

Table 2.2.5.1b. (Contiuned)

49	ν(C-C) (-25) & ν(C-O) (-25) & δ(OH) (24)	L-cys	1513.79
48	δ(CH_2) (75)	L-cys	1508.11
47	δ(NH) (-18) & δ(CH) (30) & τ(NH) (30)	L-cys	1457.14
46	δ(NH) (30) & δ(CH) (30) & τ(CH) (-12)	L-cys	1389.90
45	ν(Ring) (55) + δ(CH) (37)	2-mpym	1357.29
44	δ(CH_2) (35) & τ(CH) (-40)	L-cys	1352.54
43	ν(C=N) (63) & δ(CH) (-17)	2-mpym	1338.46
42	δ(CN) (40) & ν(C-S8) (14) & δ(CH) (30)	2-mpym	1301.62
41	ν(C-C) (16) & δ(CH) (36) & τ(CH_2) (11)	L-cys	1293.67
40	ν(C-N) (63)	L-cys	1240.58
39	ν(C-O) (-21) & δ(OH) (51)	L-cys	1212.58
38	ν(coor) (88)	L-cys	1200.85
37	δ(CH) (65)	2-mpym	1199.74
36	δ(CH) (78)	2-mpym	1156.66
35	ν(C-C) (37) & δ(NH_2) (13)	L-cys	1114.76
34	ν(C=N) (15) & δ(Ring) (85)	2-mpym	1109.17
33	τ(CH) (-71)	2-mpym	1091.67
32	τ(CH) (-74)	2-mpym	1063.52
31	δ(S15H) (-13) & δ(NH_2) (13) & τ(CH_2) (20)	L-cys	1024.31
30	δ(S8-H) (93)	2-mpym	933.14
29	δ(C-C) (-17) & & δ(S15H) (-34) & τ(NH_2) (-11)	L-cys	889.39
28	τ(CH) (-74)	2-mpym	882.04
27	τ(Ring) (-86)	2-mpym	841.36
26	ν(C-S8) (18) & δ(Ring) (65)	2-mpym	817.63
25	ν(C-S15) (-25) & ν(C-C) (14) & δ(S23H) (-14)	L-cys	803.47
24	δ(S23H) (14) & τ(S23H) (-25) & γ(CO) (-14)	L-cys	772.42
23	ν(C-S15) (18) & τ(S23H) (-27) & γ(CO) (16)	L-cys	733.60
22	ν(C-S15) (-14) & τ(S23H) (-52)	L-cys	715.83
21	δ(Ring) (-57)	2-mpym	705.04
20	δ(CO) (14) & τ(OH) (48) & δ(NH_2) (24)	L-cys	653.19
19	τ(NH_2) (53)	L-cys	618.27
18	δ(CO) (-30) & τ(OH) (32)	L-cys	584.43
17	τ(coor) (-84)	L-cys	534.38
16	δ(CO) (-57)	L-cys	523.34
15	τ(Ring) (-81)	2-mpym	500.77
14	ν(C-S8) (54) & δ(CN) (-17)	2-mpym	476.18
13	ν(C-S15) (26) & δ(CN) (34)	L-cys	404.62

[a] The (+) sign corresponds to a simultaneous elongation (or simultaneous contraction of the bonds), or to the clockwise bending motion, or to the in phase out-of-plane bending motion of the A–B bonds. The (-) sign has the opposite meaning.
[b] Modes are found in ligands.

2.2.5.2. 2-mercaptopyrimidine Ligand

In **1B** complex, the modes of 9, 10, 13, 14, 16, 20, 24, 25, 27, 29, 31-33, 35, 37, 42-44, 48, 50, 53, 54, 56, and 61-63 are listed in **Table 2.2.5.1a.** and In **2B** complex, the modes of 9, 10, 14, 15, 21, 26-28, 30, 32-34, 36, 37, 42, 43, 45, 50-53, 57, 61-63 are listed in **Table 2.2.5.1b.**. Three ring C-H streching vibration bands form according to known stations in modes 61, 62, and 63 for both **1B** and **2B**. The mode 61 has vibrations for three ring C-H bonds. Angular CH vibrations attend into many mixing main vibrations like mode 43 and 44 in **1B**. In addition it has forced modes own as mode 35 both **1B** and **2B**. The S-H streching vibration in 2mpym is mode 56 in **1B** (2590.81 cm^{-1}) and mode 57 in **2B** (2600.01 cm^{-1})**.** The S-H streching vibration of **2B** complex has the lowest wavenumber value. The angular SH vibration are found in different modes below 1000 cm^{-1}. The best ring SH angular vibration values are for **1B**; 934.89 cm^{-1} and for **2B**; 933.14 cm^{-1}. Ring C=C bond streching vibration is seen in mode 53 for **1B** (1695.45 cm^{-1}) as % 58 PED rate and **2B (**1728.74 cm^{-1}) as % 54 PED rate. The N=C vibration band is found in mode 50 for **1B** and **2B**. The mode 50 consists angular CH vibration as %43 in **1B** and % 58 in **2B**. The CS bond only give band as an angular vibration in the mode 9 for **1B** and in the mode 10 for **2B** also has below

400 cm^{-1} wavenumber. Specially, ring angular vibration is seen in the modes of 16, 20, 25 and 33 for **1B** and the modes of 7, 15, 21, 26, and 34 for **2B**. The modes of 25 in **1B** and 27 in **2B** have the best potential energy distribution (PED).

2.2.5.3. Platinum-Ligand

Platinum is bounded to nitrogen atom in L-cysteine ligand and three Pt-N15 streching vibrations form from known vibration bands in **1B** as 666.93 cm^{-1} (%10), 636.62 cm^{-1} (%15), and 592.56 cm^{-1} (%22) and is bounded to

Table 2.2.5.2a. Theoretical frequencies of Pt-Ligands (cm^{-1}) of 1B complex**.**

NO	1B With BHANDH In Molecule 1		
	PED(%)[a]	Ligand[b]	IR
19	ν(C-S23) (-13) & ν(Pt-N15) (10) & δ(CO) (56) & τ(OH) (16)	Mix	666.93
18	ν(Pt-N15) (-15) & τ(OH) (60)	Mix	636.62
17	ν(Pt-N15) (22) & δ(CO) (55)	Mix	592.56
16	τ(Ring) (-81)	2-mpym	534.84
15	δ(CN) (-11) & δ(CO) (-40)	L-cys	508.42
14	τ(CN) (-64)	2-mpym	501.78
13	ν(S8-C5) (53) & δ(CN) (-20)	2-mpym	476.09
12	ν(Pt-Cl3) (82) & ν(Pt-Cl2) (15), Sym	Mix	380.83
11	ν(Pt-Cl3) (-14) & ν(Pt-Cl2) (64), Asym	Mix	373.60
10	τ(S8H) (95)	2-mpym	369.36
9	δ(CS8) (68)	2-mpym	363.43
8	ν(Pt-N15) (-12) & τ(coor) (-64)	Mix	291.37
7	τ(S23H) (-75)	L-cys	275.53
6	δ(N4-Pt-N15) (11) & τ(CC) (49) & & τ(S23H) (25)	Mix	269.45
5	ν(PtN4) (49)	Mix	243.69
4	δ(CC) (-35) & δ(CN) (-35)	L-cys	200.82
3	δ(Cl2PtCl3) (23) & γ(Cl3NNPt) (10) & γ(ClN15ClPt) (10)	Mix	181.20
2	δ(PtN4) (38) & γ(Cl3NNPt) (-26)	Mix	167.90
1	δ(Cl2PtCl3) (67)	Mix	146.36

sulphur atom in L-cysteine ligand and one Pt-N15 streching vibration forms from given vibration band in **2B** as 330.81 cm^{-1} (%68). Pt is done bond with 2-mercaptopyrimidine ligand from nitrogen position and one vibration band forms as 243.69 cm-1 (%49) in **1B** and 243.79 cm-1 (%49) in **2B**. In addition, there are two strong Pt-Cl bond streching vibration in the mode 11 (373.60 cm^{-1}; asymmetric) and mode 12 (380.83 cm^{-1}; symmetric) for **1B** and mode 11 (371.03 cm^{-1}; asymmetric) and mode 12 (378.24 cm^{-1}; symmetric) for **2B**. Again, in-plane bending, out of-plane bending and torsion motions form vibration of bonding of Pt with ligands and Cl atoms specially below 300cm^{-1}.

Table 2.2.5.2b. Theoretical frequencies of Pt-Ligands (cm^{-1}) of 2B complex.

NO	2B With BHANDH In Molecule 2		
	PED(%)[a]	Ligand[b]	IR
12	ν(Pt-Cl3) (71) & ν(Pt-Cl2) (15), Sym	Mix	378.24
11	ν(Pt-Cl3) (-15) & ν(Pt-Cl2) (60), Asym	Mix	371.03
10	δ(CS8) (64)	2-mpym	364.20
9	τ(S8H) (94)	2-mpym	355.79
8	ν(Pt-S15) (68)	Mix	330.81
7	δ(N4-Pt-S15) (18) & τ(Ring) (56)	Mix	267.49
6	ν(PtS15) (10) & δ(CC) (49) & & τ(NH_2) (32)	Mix	259.45
5	ν(PtN4) (49)	Mix	243.79
4	δ(CC) (-24) & δ(CN) (-24)	L-cys	224.25
3	δ(PtS15) (-33) & γ(ClS15ClPt) (10)	Mix	201.81
2	δ(Cl2PtCl3) (62) γ(ClSClPt) (14)	Mix	171.22
1	δ(Cl2PtCl3) (12) & δ(PtN4) 31) & γ(Cl3SNPt) (-18)	Mix	151.43

2.2.6. Energy Comparisons Between 1B and 2B

Detailed energy analysis have been done to find the most stable complex structure using different basis sets at the comparison of **1B** and **2B**

Table 2.2.6.1. Theoretical energy analysis between 1B and 2B attached BSSE and ZPVE correction with different basis sets. The columns of 3, 4, and 5 have Hartrees unit and also 6,7, and 8 have kcal/mol unit.

Basis Set	Molecule	Complex Energy	BSSE Corrected Energy	ZPVE & BSSE Corr. Energy	E1-E2 (Compleex)	E1-E2 (BSSE Corr.)	E1-E2 (ZPVE + BSSE Corr.)
6-311G	**1**	-2415.61461	-2415.59116	-2415.39275	-10.53	-6.88	-5.83
	2	-2415.59784	-2415.58020	-2415.38346			
6-311G(d)	**1**	-2415.89865	-2415.88026	-2415.68108	-6.67	-3.45	-1.95
	2	-2415.88803	-2415.87477	-2415.67797			
6-311+G(d)	**1**	-2415.91297	-2415.89909	-2415.70026	-4.99	-3.08	-1.60
	2	-2415.90502	-2415.89419	-2415.69771			
6-311G(d,p)	**1**	-2415.92763	-2415.91010	-2415.71169	-5.85	-2.89	-1.44
	2	-2415.91831	-2415.90549	-2415.70939			
6-311G(2d)	**1**	-2415.92957	-2415.91472	-2415.71697	-5.58	-3.13	-1.56
	2	-2415.92068	-2415.90974	-2415.71449			
6-311+G(d,p)	**1**	-2415.94097	-2415.92864	-2415.73045	-3.84	-2.49	-1.07
	2	-2415.93485	-2415.92467	-2415.72874			
6-311+G(2d)	**1**	-2415.94168	-2415.93206	-2415.73452	-3.56	-2.61	-1.07
	2	-2415.93600	-2415.92790	-2415.73281			
6-311G(2d,p)	**1**	-2415.95709	-2415.94265	-2415.74481	-4.92	-2.50	-0.99
	2	-2415.94926	-2415.93866	-2415.74324			
6-311G(2df)	**1**	-2415.96471	-2415.95033	-2415.75259	-4.49	-2.19	-0.73
	2	-2415.95755	-2415.94685	-2415.75142			
6-311+G(2d,p)	**1**	-2415.96837	-2415.95977	-2415.76208	-2.60	-1.94	-0.48
	2	-2415.96423	-2415.95668	-2415.76131			
6-311+G(2df)	**1**	-2415.97705	-2415.96796	-2415.76878	-2.59	-1.67	0.77
	2	-2415.97293	-2415.96530	-2415.77001			

in this **table 2.2.6.1.** In this energy analysis, 6-311G basis set have been used with its functions of polarise (d, 2d, f, etc.) and diffuse (+). Corrections of basis set superposition (BSSE) and zero point vibrational energy (ZPVE) have been added to this anlysis improving the accuracy. In this table, the basis set size increases, the gap between the energies of **1B** and **2B** decreases. The rightmost column of table indicates the analysis results. **2B** complex is the lower energy value and more stable structure than **1B** complex in the **6-311+G(2df)** basis set after all corrections. The energy of **2B** is more energtic than **1B** with the value of 0.77 kcal/mol.

CHAPTER 3

CONCLUSION

In the first part of this work, hydrogen bonding interactions between 2-mercaptopyrimidine and L-cysteine was investigated. The Cys-2mpym complexes have been studied at B3LYP/6-311G level. The nature of H-bonds was analyzed through structures, energies, frequencies, and electron density topological analysis. More than 20 kinds of H-bonds including intra- and inter-molecular H-bonds have been found in complexes. Most of inter-molecular H-bonds involve O or (N) atom as H-acceptor. Although **CON2, CON3, CON15, CON16, CON24, CON25,** and **CON26** involve the strongest H-bonds, **CON5** and **CON26** have higher preperation energy and are not the most stable complexes because of the serious deformations. Especially, **CON2**, **CON24**, and **CON25** are the most stable complexes because of lower preparation, better energies of binding and interaction. These have less deformation. Therefore, both strength of H-bonds and structural deformation are important factors for the stability of complexes. Some important relationships between structural parameters (Δ**R** and **δR**), frequency shift (Δ**v**), and electron density topological parameters ($\boldsymbol{\rho_b}$ and $\boldsymbol{\nabla^2_{\rho b}}$) have been found. This work can have some medical implication, because L-cysteine is a

precursor to the formation of certain antioxidants. Stabilized and highly interacting systems of Cys-2mpym complexes could interfere with the biological role of L-cysteine by limiting its availability in these processes.

In second part of this work, the design of novel potential cisplatin complexes with 2-mercaptopyrimidine and L-cysteine compounds was aimed. Because a quarter of a century of clinical research on platinum coordination compounds has yielded remarkable anticancer agents. Cisplatin, the parent compound of the whole class, has exerted a broad spectrum of antitumour activity in solid tumours, and curative effects in germ cell cancer. Carboplatin has successfully been developed as a second generation compound with reduced organ toxicity and, when dosed appropriately, produces antitumour efficacy comparable to cisplatin. The search for a platinum agent with increased activity still remains an elusive goal. It is hoped that progress will be brought about by new agents which might expand upon the utilisation of the platinum compounds in new tumour types (such as oesophageal, colorectal, or prostate cancer) or through innovative approaches (such as radiosensitisation, loco-regional, or oral administration) to their utilisation.

In the part 2, a novel cisplatin derivatives of forming biological active ligands planned using detailed quantum chemical calculations with DFT functions. complex has thought having two differnet bonding position on L-cysteine ligand. Minimum geometries of all functions, natural bond orbital

analysis, many special enegy parameters, reactiviities, vibrational frequencies and HOMO-LUMO have been calculated and comparisons have done related to scientific truths. **1B** in complex 1 and **2B** in complex 2 with BHANDH function have the most stable geometry and energy values versus other DFT functions. **2B** complex has the most stable strucure after the detailed energy analysis in the different basis sets and corrections.

As a result, from all these with using calculation parmeters, more important informations can get in future works to find new active compounds.

REFERENCES

[1] Knight, R. D.; Freeland, S. J.; Landweber, L. F. Trends Biochem Sci 1999, 24, 241.

[2] Lacey, J. C.; Mullins, D. W. Orig Life Evol Biosph 1983, 13.

[3] Lacey, J. C., Jr.; Wickramasinghe, N. S.; Cook, G. W. Orig Life Evol Biosph 1992, 22, 243.

[4] Hoffman, M. M.; Khrapov, M. A.; Cox, J. C.; Yao, J.; Tong,L.; Ellington, A. D. Nucleic Acids Res 2004, 32, D174.

[5] Rodin, S.; Rodin, A.; Ohno, S. Proc Natl Acad Sci USA 1996, 93, 4537.

[6] Dabkowska, I.; Gutowski, M.; Rak, J. Pol J Chem 2002, 76, 1243.

[7] Dabkowska, I.; Rak, J.; Gutowski, M.; Nilles, J. M.; Stokes, S. T.; Radisic, D.; Bowen, K. H. Phys Chem Chem Phys 2004, 6, 4351.

[8] Gutowski, M.; Dabkowska, I.; Rak, J.; Xu, S.; Nilles, J. M.; Radisic, D.; Bowen, K. H. Eur Phys J 2002, D20, 431.

[9] Zhao, Y.; Zhou, L. Theor Chem Acc 2005, 113, 249.

[10] Galetich, I.; Stapanian, S. G.; Shelkovsky, V.; Kosevich, M.;Adamowicz, L. Mol Phys 2002, 100, 3649.

[11] Dabkowska, I.; Gutowski, M.; Rak, J. J Am Chem Soc 2005, 127, 2238.

[12] Dabkowska, I.; Rak, J.; Gutowski, M.; Nilles, J. M.; Stokes, S. T.; Bowen, K. H. J Chem Phys 2004, 120, 6064.

[13] Dabkowska, I.; Rak, J.; Gutowski, M. J Phys Chem A 2002, 106, 7423.

[14] Troitino, D.; Bailey, L.; Peral, F. J Mol Struct Theochem 2006, 767, 131.

[15] Pichierri, F.; Aida, M.; Gromiha, M.; Sarai, A. J Am Chem Soc 1999, 121, 6152.

[16] Kitagawa, Y.; Shoji, M.; Saito, T.; Nakanishi, Y.; Koizumi, K.; Kawakami, T.; Okumura, M.; Yamaguchi, K. Int JQuantum Chem 2008, 108, 2881.

[17] Maul, R.; Ortmann, F.; Preuss, M.; Hannewald, K.; Bech-stedt, F. J Comput Chem 2007, 28, 1817.

[18] Rozas, I.; Alkorta, I.; Elguero, J. Struct Chem 2008, 19, 923.

[19] Bader, R. F. W. Atoms in Molecules: A Quantum Theory; Oxford University Press: Oxford, UK, 1990.

[20] Popelier, P. L. A. Atoms in Molecules: An Introduction; Prentice Hall: London, 2000.

[21] Matta, C. F.; Boyd, R. J. The Quantum Theory of Atoms in Molecules: From Solid State to DNA and Drug Design; WILEY-VCH Verlag GmbH & Co. KGaA: Weinheim, 2007.

[22] Koch, U.; Popelier, P. L. A. J Phys Chem 1995, 99, 9747.

[23] Reed, A.E.; Curtiss, L. A.; Weinhold, F. Chem Rev 1988, 88, 899.

[24] Rosenberg, B.; Van Camp, L.; Krigas, T. *Nature* 1965, *205*, 698.

[25] Rosenberg, B.; Van Camp, L.; Grimley, E. B.; Thomson, A. J. *J.Biol. Chem.* 1967, *242*, 1347.

[26] Rosenberg, B., *Plat. Met. Rev.* 1971, *15*, 42.

[27] Rosenberg, B.; Renshaw, E.; Van Camp, L.; Hartwick, J.; Drobnik, J. *J. Bacteriol.* 1967, *93*, 716.

[28] Rosenberg, B.; Van Camp, L.; Trosko, J. E.; Mansour, H. V.*Nature* 1969, *222*, 385.

[29] Rosenberg, B.; Van Camp, L. *Cancer Res.* 1970, *30*, 1799.

[30] Kociba, R. J.; Sleight, S. D.; Rosenberg, B. *Cancer Chemother. Rep.* 1970, (Part I 54), 325.

[31] Higby, D. J.; Wallace, H. J.; Albert, D. J.; Holland, J. F. *Cancer* 1974, *33*, 1219.

[32] Weiss, R. B.; Christian, M. C. *Drugs* 1993, *46*, 360.

[33] Gordon, M.; Hollander, S. *J. Med.* 1993, 209.

[34] Reedijk, J. *Chem. Commun.* 1996, 801.

[35] Smith, D. B.; Newlands, E. S.; Rustin, G. J. S.; Begent, R. H. J.; Howells, N.; McQuade, B.; Bagshawe, K. D. *Lancet* 1991, *338*, 487.

[36] Jones, A. L.; Hill, A. S.; Soukop, M.; Hutcheon, A. W.; Cassidy, J. Kaye, S. B.; Sikora, K.; Carney, D. N.; Cunningham, D. *Lancet* 1991, *338*, 483.

[37] Marty, M.; Pouillart, P.; Scholl, S.; Droz, J. P.; Azab, M.; Brion, N.; Pujade-Lauraine, E.; Paule, B.; Paes, D.; Bons, J. *New Engl. J. Med.* 1990, *322*, 816.

[38] Cubeddu, L. Z.; Horrman, I. S.; Fuenmayor, N. T.; Finn, A. L. *New Engl. J. Med.* 1990, *322*, 810.

[39] Treskes, M.; W van der Vijgh,. J. F. *Cancer Chemother. Pharmacol.* 1993, *33*, 93.

[40] Korst, A. E. C.; Eeltink, C. M.; Vermorken, J. B.; van der Vijgh, W. J. F. *Eur. J. Cancer* 1997, *33*, 1425.

[41] Reedijk, J. *Chem. Rev.* 1999, *99*, 2499.

[42] Lebwohl, D.; Canetta, R. *Eur. J. Cancer* 1998, *34*, 1522.

[43] Cleare, M. J.; Hoeschele, J. D. *Plat. Met. Rev.* 1973, *17*,3.

[44] Cleare, M. J.; Hoeschele, J. D*. Bioinorg. Chem.* 1973, *2*, 187.

[45] Reedijk, J. *Pure Appl. Chem.* 1987, *59*, 181.

[46] Farrell, N. *Transition Metal Complexes as Drugs and Chemo-therapeutic Agents*; Kluwer Academic Publishers: Boston, 1989.

[47] Sundquist, W. I.; Lippard, S. J. *Coord. Chem. Rev.* 1990, *100*, 293.

[48] *Platinum and Other Metal Coordination Compounds in Cancer Chemotherapy*; Howell S. B., Ed.; Plenum Press: New York, 1991.

[49] Lempers, E. L. M.; Reedijk, J. *Adv. Inorg. Chem.* 1991, *37*, 175.

[50] Reedijk, J. In Handbook of Metal-Ligand Interactions in Biological Fluids. *Bioinorganic Chemistry*; Berthon, G., Ed.; Marcel Dekker Inc.: New York, 1995; Vol. 2, p 967.

[51] Chaney, S. G. *Int. J. Oncol.* 1995, *6*, 1291.

[52] *Platinum and Other Metal Coordination Compounds in Cancer Chemotherapy 2*; Pinedo, H. M., Schornagel, J. H., Eds.; Plenum Press: New York, 1996.

[53] Hambley, T. W. *Coord. Chem. Rev.* 1997, 166, 181.

[54] Sadler, P. J.; Guo, Z. *Pure Appl. Chem.* 1998, *70*, 863.

[55] Jamieson, E. R.; Lippard, S. J. *Chem. Rev.* 1999, *99*, 2467.

[56] Christian, M. C. *Semin. Oncol.* 1992, *19*, 720.

[57] Reedijk, J.; Teuben, J. M. In *Cisplatin: Chemistry and Biochemistry of a Leading Anticancer Drug*, Lippert, B. Ed.; Wiley-VCH:Weinheim, Germany, 1999; pp. 339-362.

[58] Guo, Z. J.; Sadler, P. J. *Adv. Inorg. Chem.* 2000, *49*, 183.

[59] Zhao, Z.; Tepperman, K.; Dorsey, J. G.; Elder, R. C. *J. Chromatogr. Biomed. Appl.* 1993, *615*, 83.

[60] Norman, R. E.; Ranford, J. D.; Sadler, P. J. *Inorg*. *Chem*. 1992, *31*, 877.

[61] Bernareggi, A.; Torti, L.; Facino, R. M.; Carini, M.; Depta, G.; Casetta, B.; Farrell, N.; Spadacini, S.; Ceserani, R.; Tognella, S. *J. Chromatogr*. *B*. 1995, *609*, 247.

[62] Korst, A. E. C.; Eeltink, C. M.; Vermorken, J. B.; van der Vijgh, W. J. F. *Eur. J. Cancer* 1997, *33*, 1425.

[63] Hausheer, F. H.; Kanter, P.; Cao, S.; Haridas, K.; Seetharamulu, P.; Reddy, D.; Petluru, P.; Zhao, M.; Murali, D.; Saxe, J. D.; Yao, S.; Martinez, N.; Zukowski, A.; Rustum, Y. M. *Semin. Oncol.* 1998, *25*, 584.

[64] Jakupec, M. A.; Galanski, M.; Keppler, B. K. In *Metal ions in biological systems,* Sigel, A.; Sigel, H. Eds.; Marcel Dekker, Inc.: New York, 2004; *Vol. 42*, pp. 179-208.

[65] Lippert B., Cisplatin, Chemistry and Biochemistry of Leading Antitumor Drugs,Wiley-VCH, Zuruch, 1999.

[66] Lippert B., *Coordination Chemistry Reviews*. 1999, Vol. 182, pp. 263-295,

[67] Reedijk J.,*Chemical Reviews*. 1999, Vol. 99, pp. 2499-2510.

[68] Fuertes M. A.; Alonso C. & Perez J. M., *Chemical Reviews*, 2003, Vol. 103, pp. 645-662.

[69] Jakupec M. A.; Galanski M. & Keppler B. K., *Reviews of Physiology, Biochemistry and Pharmacology,* 2003, Vol. 146, pp. 1-53.

[70] Kozelka J.; Legendre F.; Reeder F. & Chottard J. C., *Coordination Chemistry Reviews*, 1999, Vol. 190-192.

[71] Reedijk J., *European Journal of Inorganic Chemistry*, 2009, No. 10, pp. 1303-1312.

[72] Soldatovic T. & Bugarcic Z. D., *Journal of Inorganic Biochemistry*, 2005, Vol. 99, pp. 1472-1479.

[73] Harris A.; Qu Y. & Farell N., *Inorganic Chemistry,* 2005, Vol. 44, pp. 1196 1198.

[74] Mambanda A.; Jaganyi D.; Hochreuther S. & van Eldik R., *Dalton Transactions*, 2010, Vol. 39, 3595-3608.

[75] Berners-Price S. J.; Davies M. S.; Cox J. W.; Thomas D. S. & Farrell N., *Chemistry--A European Journal,* 2003, Vol. 9, pp. 713-725.

[76] Lakomska I.; Kooijman H.; Spek A. L.; Shen W. & Reedijk J., *Dalton Transactions*, 2009, Vol. 48, pp. 10736-10741.

[77] Ali M. S.; Khan S. R. A.; Ojima H.; Guzman I. Y.; Whitmire K. H.; Siddik Z. H. & Khokhar A. R., *Journal of Inorganic Biochemistry*, 2005, Vol. 99, pp. 795-804.

[78] Talman E. G.; Bruning W.; Reedijk J.; Spek A. L. & Veldman N., *Inorganic Chemistry*, 1997, Vol. 36, pp. 854-861.

[79] Lemma K.; Shi T. & Elding L. I., *Inorganic chemistry*, 2000, Vol. 39, pp. 1728-1734.

[80] Lemma K.; Sargeson A. M. & Elding L. I., *Dalton Transaction*, 2000, No. 7, pp. 1167-1172.

[81] Jolley J. N.; Yanovsky A. I.; Kelland L. R. & Nolan K. B., *Journal of Inorganic Biochemistry*, 2001, Vol.83, pp.91-100.

[82] Natile G. & Coluccia M., *Coordination Chemistry Reviews*, 2001, Vol. 216-217, pp. 383-410.

[83] Jansen B. A. J.; Brouwer J. & Reedijk J., *Journal of Inorganic Biochemistry*, 2002, Vol.89, pp. 197-202.

[84] Mock C.; Puscasu I.; Rauterkus M. J.; Tallen G.; Wolff J. E. A. & Krebs B., *Inorganica Chimica Acta*, 2001, Vol. 319, pp. 109-116.

[85] Becke, A. D. Phys Rev A 1988, 38, 3098.

[86] Lee, C.; Yang, W.; Parr, R. G. Phys Rev B 1988, 37, 785.

[87] Krishnan, R.; Binkley, J. S.; Seeger, R.; Pople, J. A. J. ChemPhys 1980, 72, 650.

[88] McLean, A. D.; Chandler, G. S. J. Chem Phys 1980, 72,5639.

[89] Boys, S. F.; Bernardi, F. Mol Phys 1970, 19, 553.

[90] Dobrowolski, J. C.; Jamroz, M. H.; Kolos, R.; Rode, J. E.; Sadlej, J. Chem Phys Chem 2007, 8, 1085.

[91] Dobrowolski, J. C.; Rode, J. E.; Sadlej, J. J Mol Struct 2007, 810, 129.

[92] Fernandez-Ramos, A.; Cabaleiro-Lago, E.; Hermida-Ramon, J. M.; Martinez-Nunez, E.; Pena-Gallego, A. J Mol Struct 2000, 498, 191.

[93] Pecul, M. Chem Phys Lett 2006, 418, 1.

[94] Popelier, P. L. A. J Phys Chem A 1998, 102, 1873.

[95] Galvez, O.; Gomez, P. C.; Pacios, L. F. J. Chem Phys 2003,118, 4878.

[96] Tian, S. X. J Phys Chem B 2004, 108, 20388.

[97] Bondi, A. J Phys Chem 1964, 68, 441.

[98] Arnold, W. D.; Oldfield, E. J. Am Chem Soc 2000, 122,12835.

[99] Pacios, L. F. J. Phys Chem A 2004, 108, 1177.

[100] Reed, A. E.; Weinhold, F.; Curtiss, L. A.; Pochatko, D. J. J.Chem Phys 1986, 84, 5687.

[101] A. D. Becke, J. Chem. Phys. 1993, 98, 1372 –1377.

[102] M. P. Waller, A. Robertazzi, J. A. Platts, D. E. Hibbs, P. A. Williams, J. Comput. Chem. 2006, 27, 491 –504.

[103] F. A. Hamprecht, A. Cohen, D. J. Tozer, and N. C. Handy, “Development and assessment of new exchange-correlation functionals,” J. Chem. Phys., 109 (1998) 6264-71.

[104] A. D. Boese, N. L. Doltsinis, N. C. Handy, and M. Sprik, “New generalized gradient approximation functionals,” J. Chem. Phys.,112 (2000) 1670-78.

[105] A. D. Boese and N. C. Handy, “A new parametrization of exchange-correlation generalized gradient approximation functionals,” J. Chem. Phys., 114 (2001) 5497-503.

[106] C. Adamo and V. Barone, “Exchange functionals with improved long-range behavior and adiabatic connection methods without adjustable parameters: The mPW and mPW1PW models,” J. Chem. Phys., 108 (1998) 664-75.

[107] J. P. Perdew, K. Burke, and M. Ernzerhof, “Generalized gradient approximation made simple,” Phys. Rev. Lett., 77 (1996) 3865-68.

[108] J. P. Perdew, K. Burke, and M. Ernzerhof, “Errata: Generalized gradient approximation made simple,” Phys. Rev. Lett., 78 (1997) 1396.

[109] C. Adamo and V. Barone, “Toward reliable density functional methods without adjustable parameters: The PBE0 model,” J. Chem.Phys., 110 (1999) 6158-69.

[110] Tao, J.; Perdew, J. P.; Staroverov, V. N.; Scuseria, G. E. Phys.ReV. Lett. 2003, 91, 146401.

[111] Toulouse, T.; Savin, A.; Adamo, C. J. Chem. Phys. 2002, 117, 10465.

[112] D. Andrae, U. Haussermann, M. Dolg, H. Stoll, H. Preuss, Theor. Chim. Acta 1990, 77, 123 –141.

[113] G. A. Petersson, A. Bennett, T. G. Tensfeldt, M. A. Al-Laham, W. A. Shirley, and J. Mantzaris, “A complete basis set model chemistry. I. The total energies of closed-shell atoms and hydrides of the first-row atoms,” J. Chem. Phys., 89 (1988) 2193-218.

[114] G. A. Petersson and M. A. Al-Laham, “A complete basis set model chemistry. II. Open-shell systems and the total energies of the first-row atoms,” J. Chem. Phys., 94 (1991) 6081-90.

[115] Chattaraj P. K. and Maiti B., 2003 J. Am. Chem. Soc. 125-2705.

[116] Pearson R. G., 1973 Hard and soft acids and bases, Stroudsberg, PA: Dowden, Hutchinson & Ross.

[117] Hill, A. F., 2002, Organotransition Metal Chemistry.

[118] Pearson R.G., 1993 Acc. Chem. Res., 26-250.

[119] Pearson R. G., 1997 Chemical hardness: Application from molecules to solid, Weinheim: Wiley-VCH.

[120] Sen K. D., and Mingos D. M. P., 1993 Chemical hardness: Structure and bonding, Berlin: Springer.

[121] Parr R .G. ,and Yang W., 1989 Density functional theory of atoms and molecules, Oxford: Oxford University Press.

[122] Parr P. G., and Pearson R. G., 1983 J. Am. Chem. Soc. 105-7512.

[123] Vektariene A., Vektaris G., and Svoboda J., 2009 ARKIVOC, 7-311.

[124] Parr R. G., Szentpaly L., and Liu S., 1999 J. Am. Chem. Soc., 121-1922.

[125] Koopmans T., 1933 Physica 1-104.

[126] Liu S., 2005 J. Chem. Sci., 117-477.

[127] Parthasarathi R., Elango M., Subramanian V., and Chattaraj P. K., 2005 Theor. Chem. Acc. 113-257.

[128] Chattaraj P. K., Sarkar U., and Roy D. R., 2006 Chem. Rev., 106-2065.

[129] Pearson R. G., 1987 J. Chem. Ed., 64-561

[130] Parr R. G., and Chattaraj P. K ., 1991 J. Am. Chem. Soc., 113-1854.

[131] Pearson R .G., 1985 J. Am. Chem. Soc., 107-6801.

[132] J. P. Foster and F. Weinhold, J. Am. Chem. Soc. 102, 7211-7218 (1980).

[133] A. E. Reed and F. Weinhold, J. Chem. Phys. 78, 4066-4073 (1983).

[134] A. E. Reed, R. B. Weinstock, and F. Weinhold, J. Chem. Phys. 83, 735-746 (1985).

[135] A. E. Reed and F. Weinhold, J. Chem. Phys. 83, 1736-1740 (1985).

[136] J. E. Carpenter and F. Weinhold, J. Molec. Struct. (Theochem) 169, 41-62 (1988).

[137] A. E. Reed, L. A. Curtiss, and F. Weinhold, Chem. Rev. 88, 899-926 (1988).

[138] F. Weinhold, “Natural Bond Orbital Methods,” In, Encyclopedia of Computational Chemistry P. v.R. Schleyer, N. L. Allinger, T. Clark, J. Gasteiger, P. A. Kollman, H. F. Schaefer III, P. R. Schreiner (Eds.), (John Wiley & Sons, Chichester, UK, 1998), Vol. 3, pp. 1792-1811.

[139] E. D. Glendening, C. R. Landis and F. Weinhold, “Natural Bond Orbital Methods,” WIREs Comp. Mol. Sci. 2, 1-42 (2012).

[140] F. Weinhold, “Natural bond orbital analysis: A critical overview of relationships to alternative bonding perspectives,” J. Comput. Chem. (2012).

[141] F. Weinhold and C. R. Landis, Valency and Bonding: A Natural Bond Orbital Donor-Acceptor Perspective (Cambridge U. Press, London, 2005), Secs 3.E, 4.F.

[142] C. Pimentel, J. Chem. Phys. 19, 446 (1951).

[143] R. E. Rundle, J. Chem. Phys. 17, 671 (1941).

[144] C. A. Coulson, J. Chem. Soc. 1964, 1442 (1964).